UNIVERSITÀ DEL PIEMONTE ORIENTALE

UNIVERSITÀ DEGLI STUDI DEL PIEMONTE ORIENTALE

"AMEDEO AVOGADRO"

Dipartimento di Scienze del Farmaco

Dottorato di Ricerca in Chemistry & Biology

XXXIII CICLO

"Tumor Associated Macrophages (TAMs) a pivotal orchestrator in cancer-related inflammation and a new important target in cancer-therapy"

Drug discovery and Development (MED 04)

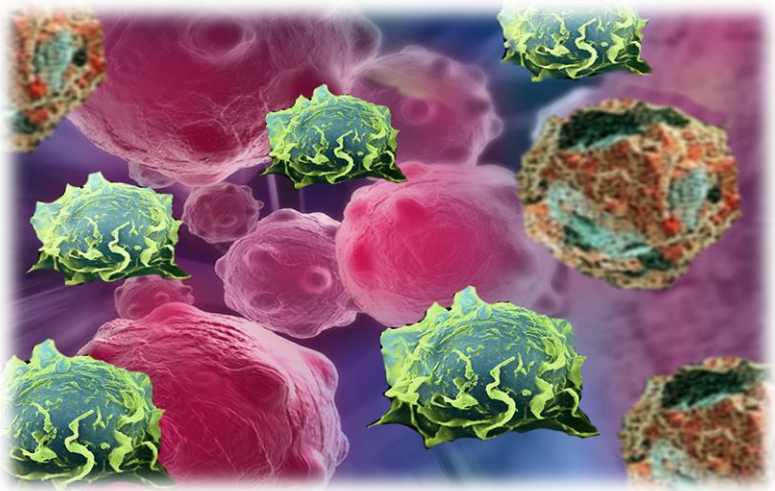

Dottorando: **Silvia MOLA**

Coordinatore: **Prof. Gian Cesare TRON**

Tutor: **Chiara PORTA, PhD**

INTRODUCTION

INFLAMMATION AND CANCER

In the 19th century, for the first time Rudolf Virchow hypothesized the existence of a causal link between inflammation and cancer[1]. This idea came up when he observed that tumor biopsies were highly infiltrated by leukocytes and that sites of chronic inflammation frequently represented the setting of tumor growth and development[2].

Virchow's hypothesis was neglected until the last decades, when the growing number of experimental, epidemiological and clinical evidence has demonstrated that inflammation fuels tumor onset, growth, and progression. Consistently, the chronic use of non-steroidal anti-inflammatory drugs (NSAIDs, e.g. aspirin), reduces incidence and mortality of many cancers[3,4] and inhibition of specific inflammatory cytokines, such as interleukin 1β (IL-1β), significantly lowers the risk of lung cancer development, as demonstrated by the Canakinumab Anti-inflammatory Thrombosis Outcomes Study (CANTOS)[5].

The existence of a functional link between inflammation and cancer is widely recognized, however, the molecular mechanisms underlying the tumor promoting functions of inflammation are still largely unknown. Therefore, dissecting these mechanisms, represents a fundamental step towards the development of new strategies for cancer prevention and treatment[6].

Tissue damages, due to physical or ischemic injury, exposure to toxins, exogenous or endogenous infections, trigger the inflammatory process, which involves a well-coordinated reaction of the innate and adaptive immune system, that promotes damage repair allowing for full or at least partial reconstitution of tissue integrity and functions[7]. The first line of defense is represented by the innate immune cells, including neutrophils, macrophages, mast cells, dendritic cells and natural killer cells, that initiate the inflammatory response by releasing cytokines, chemokines, matrix-remodeling proteases and reactive oxygen and nitrogen species[2,6]. Acute inflammation is usually a self-limiting process, whereas, chronic inflammation, due to a failure of mechanisms required for resolving the inflammatory response, generates a permissive microenvironment that facilitates and contributes to cancer development and progression[1].

Although in established tumors inflammation and cancer are two coexisting processes, in the initial phases of tumor onset, the link between inflammation and cancer can emerge through the contribution of two different pathways: the intrinsic pathway, driven by genetic alterations that lead to both neoplastic transformation and inflammation, and the extrinsic pathway is triggered by infection or irritant agents that initially cause chronic inflammation, and subsequently

neoplastic transformation[6]. Both pathways, converge and promote the activation of transcription factors, principally nuclear factor-κB (NF-κB), signal transducer of transcription (STAT3) and hypoxia-inducible factor (HIF1α), that induce the expression of genes encoding cytokines, chemokines, anti-apoptotic molecules and cyclins, promoting inflammation as well as survival and proliferation of neoplastic cells[2] (*Fig.1*).

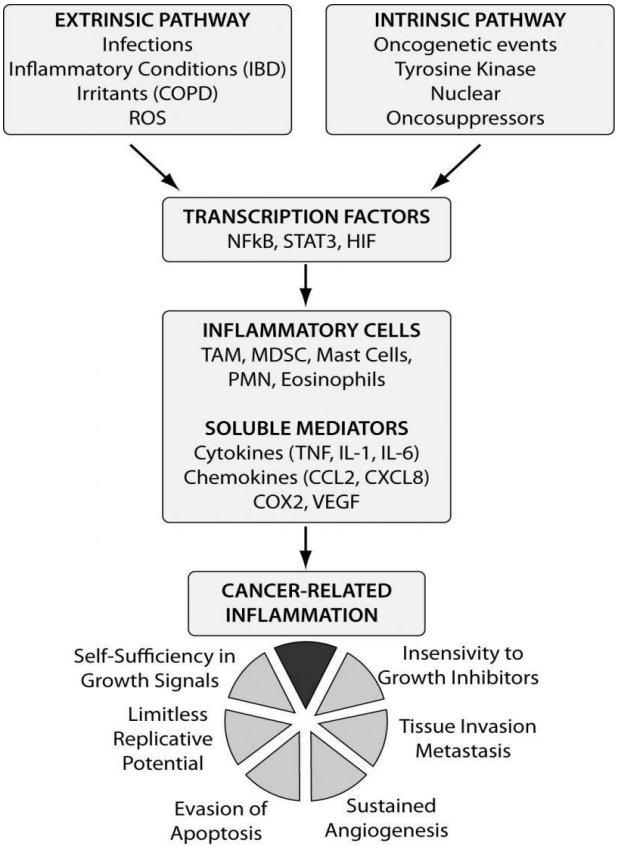

Figure 1. The Extrinsic and Intrinsic Pathways drive the inflammatory process[8]. There are two pathways correlated with inflammation and cancer: the extrinsic and intrinsic pathways. The first one is related to genetic events (e.g. oncogenes), whereas the second one, the chronic inflammation is due to infections or irritants. Both pathways converge in a single way, able to sustain cancer promotion and development.

1.1.1.1 The Intrinsic Pathways of cancer-related Inflammation.

Genetic alterations of different tumor-suppressor genes (e.g. p53, VHL, TGFβ, Apc) and oncogenes (e.g. RET, RAS and MYC) have been found associated with both neoplastic transformation and the activation of the inflammatory response[9].

For example, p53 is the most important tumor suppressors factor, that in response to various cellular stresses, (e.g. DNA damage, hypoxia, and nutrient deprivation) and modulates the expression of genes regulating the cell cycle, apoptosis, and DNA repair[10–12]. Additionally, p53 acts as an antagonist for the nuclear factor-kB (NF-kB)[13,14], therefore limiting inflammation, guaranteeing cellular homeostasis and avoiding cell transformation. Instead of, in the context of chronic inflammation, the constitutive activation of NF-kB induces the production of inflammatory cytokines that impair p53 activity, increasing the risk of cancer development[15–17].

On the other hand, both *in vitro* and *in vivo* studies have reported that expression of various p53 mutants correlated with increased NF-kB expression[18–20].

Different *in vitro* experiments have reported that, tumor cells harboring mutant p53 promote inflammatory responses through different mechanisms, including: enhancement of NF-kB transcriptional activity in response to the cytokine Tumor necrosis factor (TNF-α)[20], repression of secreted interleukin-1 receptor antagonist (sIL-1Ra)[21], promotion of NF-kB-dependent chemokines (e.g. CXCL5, CXCL8, and CXCL12)[22] and increased of cytokine and chemokine expression in response to TLR3 (Toll-like-receptor 3)ligands[23]. Accordingly, *in vivo*, in a chemical model of colorectal cancer (CRC), loss of p53 in intestinal epithelial cells (IEC) results in increased NF-kB-dependent inflammatory microenvironment supporting epithelial-mesenchymal transition (EMT) and colonic tumor progression[24].

Overall, these studies indicate that p53 mutants heighten the response of tumor cells to microenvironmental cues, thereby supporting cancer-related inflammation.

Moreover, these observations have been confirmed in human premalignant and malignant lesions[25], (e.g. in head and neck and in non–small cell lung cancers), where in many cases, p53 mutants correlate with constitutive activation of NF-kB and a reduced apoptosis[26].

In conclusion, loss of tumor suppressor p53 inhibits proper DNA repair and accelerate DNA damage, that in turn fuels inflammation[27], establishing a feed-forward loop that enhances tumor development[28,29].

Moreover, activation of different oncogenes increases the production of many inflammatory mediators that support the recruitment of myeloid cells[30]. For example, K-Ras oncogenic

signaling regulates the expression of different cytokines (IL-8, IL-1a and IL-1β) and chemokines (e.g. CCL2, CXCL1, CXCL3)[31], that drive the accumulation of inflammatory cells[35] leading to the construction of a chronic and "smoldering" state of inflammation that promotes neoangiogenesis and tumor growth[32].

1.1.1.2 The extrinsic pathway of cancer-related inflammation.

It has been estimated that up to 25% of cancers are sustained by chronic inflammation[6] and infections.

Panel 1: **Some associations between inflammation and cancer risk**

Malignancy	Inflammatory stimulus/condition
Bladder	Schistosomiasis
Cervical	Papillomavirus
Ovarian	Pelvic inflammatory disease/talc/tissue remodelling
Gastric	*H pylori* induced gastritis
MALT lymphoma	*H pylori*
Oesophageal	Barrett's metaplasia
Colorectal	Inflammatory bowel disease
Hepatocellular	Hepatitis virus (B and C)
Bronchial	Silica, asbestos, cigarette smoke
Mesothelioma	Asbestos
Kaposi's sarcoma	Human herpesvirus type 8

In fact, different pathogens including virus (e.g. human papilloma virus, Hepatitis B and C virus), bacteria (*Helicobacter pylori*) and parasites (e.g. *Schistosoma haematobium Clonorchis sinensis and Opisthorchis viverrini*) are causally linked to cancers, that selectively arise in chronically infected organs (*Panel 1*)[33].

Beyond pathogens, commensal microbial species could exert different pro-tumoral activities. Indeed, in different types of cancer, (e.g. colon cancer[34], pancreatic cancer [35], hepatocellular carcinoma[36], lung cancer[37,38]), it has been reported that commensal microorganisms, by translocation through the protective tissue barrier (e.g. intestinal epithelial barrier), adherence to cancer cells and release of metabolites, are able to promote inflammation and sustain tumor growth. At the same time, when travelling with tumors cells to the distant metastatic sites, they participate in the sustenance of the inflammatory process and metastasis diffusion[30].

In CRC, different studies have suggested the pro-tumorigenic role of *Fusobacterium*, indeed, it promotes the initial phase of CRC development producing bacteria-derived virulence factors (e.g. FadA, Fap2, RaD), that impair colonic epithelial cell junctions, favoring its translocation, and the recruitment and activation of inflammatory cells, building up an inflammatory microenvironment, that fosters neoplastic transformation[39]. Further important pro-tumorigenic species enriched in CRC in tumor bearers, are represented by *Streptococcus gallolyticus, Bacteroides fragilis, Escherichia coli, and Enterococcus faecalis*[34].

In liver cancer, gut microbial components reach the liver via the portal circulation and enhance inflammation, fibrosis, and carcinogenesis. However, translocation of intestinal bacteria, triggers inflammatory responses through Toll-like receptors, contributing to liver fibrosis and

cirrhosis, that are responsible for the high rate of HCC development[36]. Whereas, in lung cancer, Jin and colleagues have discovered that exists a crosstalk between microbiota and immune cells, able to regulate tumor development. Local microbiota promotes inflammation and tumor cell proliferation by stimulating Myd88-dependent IL-1β and IL-23 production and by inducing proliferation and activation of inflammatory γδ T cells[37].

Cancer can be also associated with chronic inflammatory conditions due to autoimmune disorders and exposure to different physical (radiation), mechanical and chemical harmful environmental cues. It has been recognized that patients suffering of inflammatory bowel diseases (IBDs), both ulcerative colitis and Crohn's disease have approximately, a 3 fold higher risk of developing CRC than general population. Of note, risk increases according to the length and severity of the disease. For ulcerative colitis the percentage of patients that develop cancer range from 2% after 10 years to 18% after 30 years. For Crohn disease, around 8% of patients develop cancer after 30 years[40–42].

Lung exposure of chemical irritants, such as tobacco-derived products and asbestos fibers fuel chronic inflammation and increase the risk of lung cancer and malignant mesothelioma, respectively[43,44].

The persistent accumulation and activation of inflammatory cells promote cancer development, trough the production of inflammatory mediators, that augment mutation rates and favor the proliferation and the survival of mutated cells.

In addition, Reactive Oxygen Species (ROS) and Nitrogen Species (RNS) are crucial factors able to induce DNA damage and genomic instability. Elevated ROS levels accompanied with down-regulation of cellular antioxidant enzyme systems, are essential to maintain tumorigenic cell signaling, sustaining tumor cell proliferation, survival, autophagy, and metastasis[45], through the activation of transcriptional factors (NF-KB, STAT-3)[8,46].

1.1.1.3 The molecular mediators of cancer-related inflammation

The intrinsic and extrinsic pathways share many crucial molecular players including transcription factors (NF-κB, HIF1α and STAT3), cytokines (e.g. IL1β, IL6, TNF, IL-23), chemokines (CCL2, CXCL8) and pro-angiogenic factors (VEGF)[8].

NF-κB represents a crucial molecular lynchpin that connects inflammation to tumorigenesis, indeed this transcription factor is a master regulator of the expression of inflammatory cytokines, as well as genes that regulate cell proliferation, survival, adhesion and angiogenesis[1,6,47].

Inflammation is usually associated with hypoxia in different pathological conditions, in particular inflammatory diseases, since numerous studies reported an extensive crosstalk between NF-κB (inflammation) and HIF (hypoxia)[48]. HIF-1α is an essential transcriptional factor in the hypoxic tumor environment. In this setting, HIF regulates changes in glycolysis, nutrient uptake, angiogenesis, apoptosis, and cell migration, contributing to tumor survival and metastasis. Several studies have demonstrated that HIF-1 expression is elevated in different types of solid tumor (e.g. colon, lung and breast cancers) and correlated with a poor prognosis [49,50]. Constitutive activation of the transcriptional factor STAT3 promotes tumor cells proliferation, survival, angiogenesis and invasion, by activating both inflammatory pro-oncogenic pathways and immune suppressive programs[51–53].

(Cytokines also contribute to cancer-related inflammation, by favoring leukocyte recruitment, neo-angiogenesis, tumor cell proliferation, invasion and metastatization (*Panel 2*)[1,54]. As well know, IL-6 exterts both a direct effect on tumor cells, (e.g. affecting proliferation and survival, activating genes ancoding for antiapoptotic and proliferative proteins) and on myeloid cells, promoting their differentiation toward a suppressor phenotype[45]. In addition, IL-6 induces VEGF expression that consequently promotes tumor angiogenesis [6] and also it heightens cancer cell stemness thereby contributing to resistance of a chemo- and radiotherapy[30].

Panel 2: **Actions of cytokines and chemokines which may facilitate cancer growth, invasion and metastasis**

DNA damage via reactive oxygen
Inhibition of DNA repair via reactive oxygen
Functional inactivation of tumour suppressor genes
Autocrine/paracrine growth and survival factors for malignant cells
Induction of vascular permeability and extravasation of fibrin/fibronectin
Tissue remodelling via induction/activation of matrix metalloproteinases
Control of tumour-cell migration, direct and indirect
Control of leucocyte infiltrate
Modulation of cell:cell adhesion molecules
Subversion of host immune responses
Stimulation of angiogenesis and angiogenic factor production
Resistance to cytotoxic drugs
Loss of androgen responsiveness

IL-1β is another important cytokine that is often overexpressed in variuos types of cancer, (such as colon, lung, breast, head cancers) and that negatively correlate with patients' prognosis[8]. Mechanistically, IL-1β increases the expression of pro-inflammatory, pro-angiogenic and pro-metastatic genes, (e.g. IL-6, IL-8, VEGF, TGFβ and MMPs), promoting tumor progression and resistence to therapy[45].

Tumor initiation and progression is also sustained by chemokines (CCL2, CCL5, CCL17, CLL22, CXCL12, CXCL8), soluble molecules released by both tumor and stromal cells that orchestrate immune cells recruitment, promoting, angiogenesis, tumor growth and invasion[45].

Tumor-Associated Macrophages (TAMs)

Undoubtedly, Tumor-Associated Macrophages (TAMs) are the major population of inflammatory cells that accumulate in solid tumors where they can reach up to 50% of the tumor mass[55]. Despite their potential cytotoxic activities, in many cases TAMs cooperate with tumors to promote their own development, growth and malignant progression. Understanding the mechanisms driving TAMs accumulation and functional activation pave the way for the development of new strategies that alone or in association with conventional radio/chemio-therapy and/or immunotherapy open promises for cancer patients[56–58].

1.1.2 Origin of TAMs

Although the recruitment of cells of the monocyte-macrophage lineage represents one of the hallmarks of cancer-related inflammation[55], over the last years, the discovery that many tissue resident macrophages (TRM) are a self-maintaining population of embryonic origin has brought into question of TAMs' ontogeny and its functional relevance.

Nowadays, several preclinical studies have pointed out the dual origin of TAMs (*Fig.2*) but, to what extent the developmental diversity might integrate with the functional activity is still under debate. TAMs are a heterogeneous population of cells that originate from both newly recruited monocytes and TRM.

In many cancer types, the most of TAMs derive from circulating monocytes ($Ly6C^+$ $CCR2^+$); that are generated from adult bone marrow hematopoietic stem cells. These inflammatory monocytes are recruited to the tumor tissue, by chemokines (e.g. CCL2, CXCL12, CCL18, CCL20), cytokines, complement components and CSF-1. Along with these chemoattractants, the activation of the integrins α4β1 and αLβ2, drives the extravasation of monocytes in tumor tissue where they undergo Notch-dependent differentiation in $Ly6C^-$ $CD11c^+MHCII^+CD11b^{lo}Vcam1^+$ TAMs[58–61] . This population of monocytes-derived TAMs variable coexist with a population of TRM that in some organs, such as liver, brain, epidermis, lungs peritoneum and heart, mainly derive from embryonic progenitors[62–65]. So far, different markers have been exploited to distinguish TRM ($CX3CR1^{hi}$, MERTK, CD64, Siglec1, F4/80) from bone-marrow-derived macrophages (instead of Integrin α4, L-selectin, Ly6c, and Nr4a1)[58] and to explore their relative impact on disease progression

For example, in a mouse model of lung cancer, it has been demonstrated that both TRMs and monocytes-derived TAMs participate in tumor promotion, however tissue-resident interstitial macrophages specifically support tumor growth, while monocyte-derived TAMs contribute to

tumor remodeling and spreading[66]. In contrast in a genetic murine model of breast cancer, only monocytes derived TAMs appear to express tumor promoting activities. Indeed, inhibition of monocytes-derived TAM accumulation resulted in T cells activation and decreased tumor growth, whereas TRM depletion was inconsequential[67]. In glioblastoma monocytes-derived TAMs constituted approximately 85% of the total population, with TRM accounting for the approximately 15% remaining[68].

At the opposite, recent studies have indicated that TRM (CD163+ Tim4+) from omentum are the key driver in the invasive progression of metastatic ovarian cancer[69]

Overall these studies suggest that the contribution of TRM and monocytes-derived TAMs depend on tumor origin. Certainly, dissecting the cross-talk between developmental origin and functional heterogeneity is an outstanding issue that the advent of single-cell based approaches will likely help to figure out.

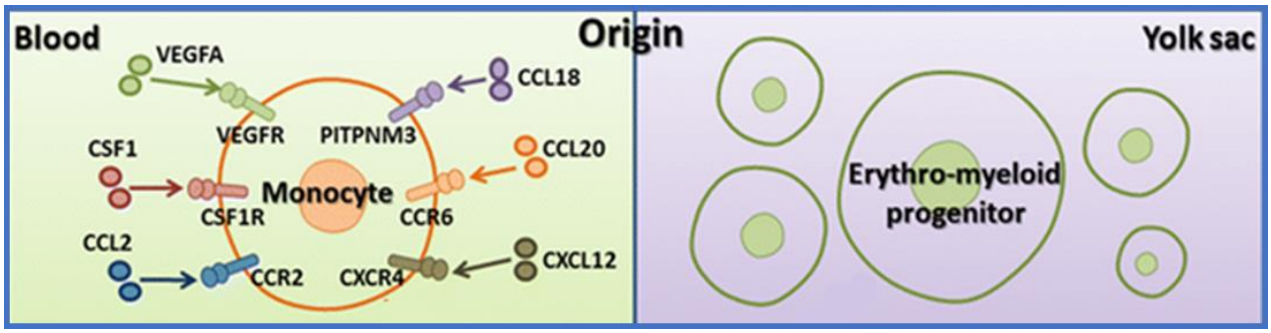

Figure 2. The dual origin of TAMs: from the circulating monocytes in the blood or for tissue resident macrophages[70].

1.1.3 Functional states of TAMs

Several experimental studies suggest that, the transition from early neoplastic events (elimination phase) towards advanced tumor stages (escape phase) is associated with a functional switch of TAMs' polarized activation[71]

At the first phase of tumor development, TAMs express an antitumor-(M1-like) phenotype, therefore they produce high level of inflammatory cytokines (e.g. TNF α) and effector molecules (e.g. ROS and RNS) capable to kill tumor cells both directly and through tissue destructive reactions, centered on the vessel wall (hemorrhagic necrosis)[55,70,72].

M1-like-TAMs also support the activation of anti-tumor T cell responses. Indeed, they are powerful antigen presenting cells through the expression of high levels of major histocompatibility complex class II (MHCII) and B7 molecules and the production of inflammatory cytokines, such as IL-12. They also produce chemokines, such as CXCL9, CXCL10, CXCL11, that drive the recruitment and activation of T-cells[55,70,72].

Unfortunately, during tumor progression, different TME changes, including hypoxia, excessive production of cellular metabolites (e.g. lactate) and immunosuppressive conditions, promote an alternatively activated or M2-like phenotype[73]. Various cytokines and signals expressed by different cell types (tumor cells, fibroblast, eosinophils, basophils, Th2 T cells and B cells) drive M2-like TAM activation[55,72–74]. Among these, IL10, prostaglandin E2 (PGE2), TGFβ, IL6, CCL2, MCSF and migration-stimulating factor (MSF) were reported to induce M2-like polarization[74].

Owing to their M2-skewed phenotype, TAMs exert several pro-tumoral functions, inducing cell proliferation and survival, (through the production of EGF, FGF, PDGF), promoting immune suppression, (by releasing immune-suppressive molecules, such as IL-0 and TGFβ), enhancing angiogenesis, tumor cell migration and metastatization[64] (*Fig.3*).

In 80% of human cancer studies, high number of TAMs that largely express an M2-skewed phenotype are associated with poor prognosis, especially in glioblastoma and lymphoma, renal cell carcinoma and breast, pancreatic, head and neck cancers[58].

As demonstrated by *in vivo* studies and clinical evidence, blockade of M2 phenotype and enhanced activation of M1 macrophages could be a promising anti-cancer therapy[75,76].

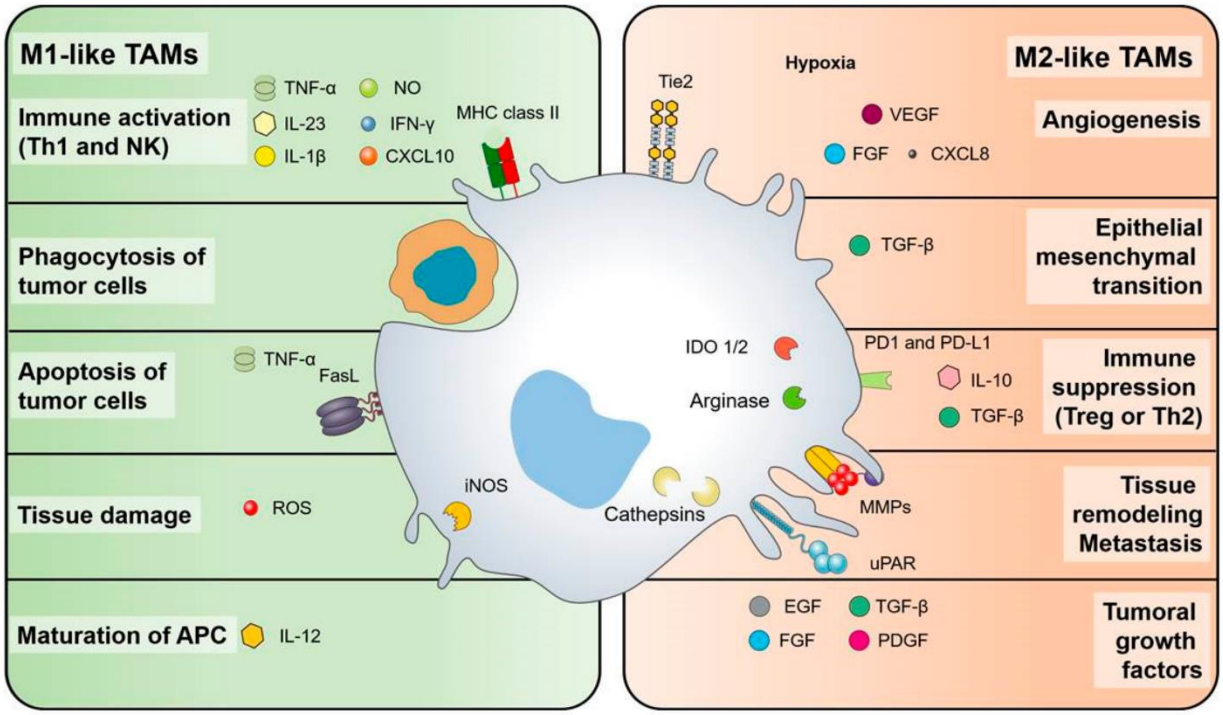

Figure 3. Different states of TAMs polarization[55]**.** A gradual switch of macrophages polarization, from M1-like phenotype to M2-like phenotype takes place during tumor progression. During tumor elimination phase M1-like TAMs exert cytotoxic and anti-tumoral activities, while in next phase M2-like TAMs sustain tumor growth and development.

1.1.3.1 Epigenetic Modifications control macrophages activation

The regulation of macrophage activation status is highly controlled by epigenetic modifications, that include DNA methylation and histone modifications[77].

DNA methylation mediates gene silencing by adding a methyl group to the 5'-carbon of the cytosine in promoter-associated CpG islands[78]. DNA methyltransferases (e.g. DMT1 and DNMT3b) are implicated in M1 polarization; in detail, DMT1 increases the levels of TNFα and IL-6, through the silencing of SOCs1[79], whereas DNMT3b downregulates the expression of ARG1 and CD206[80]. Although their impact on macrophages polarization is clear, the role of DNA methyltransferases in TAMs remains poorly understood[77].

Histone modifications include different types of post-translational modifications, but methylation and acetylation are the most important modifications that occur in macrophages [77]. Histone acetylation, mediated by histone acetyltransferases (HAT), is associated with the activation of transcription, whereas histone deacetylation, mediated by and histone deacetylases (HDACs), is associated with transcriptional repression[77].

HDACs have an ambivalent effect in TAMs, studies have demonstrated that, in prostate cancer, Pan HDAC inhibits M2-functions in TAMs; blocking the secretion of VEGF and IL-10 it's able to prevent EMT process [81]. In contrast, murine models of breast, lung and pancreatic cancer have showed that, HDAC activity promotes tumor growth by increase TAMs NO production [82], and its inhibition is able to restore TAM phagocytic activity, promoting the reduction of tumor burden and the metastasis diffusion[83].

On the other hand, histone methyltransferases (HMT) and histone demethylases (HDM), that respectively catalyze histone methylation and demethylation, are involved in the regulation of macrophages polarization, in particular, DNMT3B and DMMT1 promote M1 phenotype, preventing M2 markers expression[79], whereas PRMT1, HMT, SMYD3 positively regulate M2 polarization[78].

Although in macrophages, the effect of histone modifications was studied, on TAMs it is yet to be clarified.

1.1.4 Function of TAMs in the Tumor Microenvironment (TME)

TAMs can promote tumor progression and dissemination by numerous ways: producing growth factors for tumor cells, secreting immunosuppressive mediators, promoting angiogenesis and release proteases that remodel the extracellular matrix in favor of cancer dissemination (*Fig.4*).

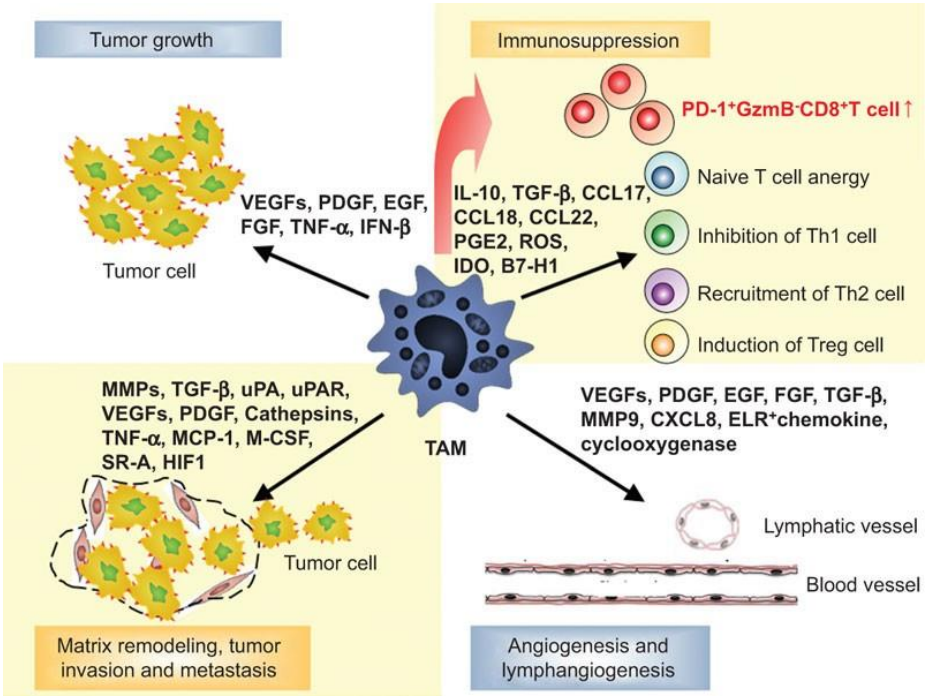

Figure 4. Pro-tumoral activities of Tumor Associated Macrophages (TAMs)[60]. TAMs represent the major population of myeloid cells recruited in tumor site. They promote and sustain tumor cells by producing growth factor (e.g. PDGF, EGF, VEGF) and creating an immunosuppressive tumor microenvironment (TME). Furthermore, TAMs promote angiogenesis and lymphangiogenesis that favor cells invasion and metastasis.

1.1.4.1 TAMs favor Immunosuppression

In tumor, TAMs contribute to the establishment of an immunosuppressive environment, which is in turn associated with cancer immune escape (*Fig.4*).

M2-likeTAMs present a secretory profile characterized by low levels of inflammatory and immunostimulatory cytokines (e.g. IL-12, IL18, IL-1β, TNFα and IFNγ) and high expression of pro-restorative and immunosuppressive cytokines (e.g. IL10, TGFβ and PGE2), that inhibit cytotoxic and adaptive immune responses. In detail, TGF-β reduces dendritic cells migration and maturation, downregulates MHC-II surface expression on macrophages, triggers exhausted NK-cell phenotype inhibiting their cytolytic activity and suppresses Th1 differentiation in favor

of Treg expansion[84,85]. In the same time, the release of PGE_2 inhibits IFNγ production and compromises NK cells functions[86].

Furthermore, the release of chemokines, such as CCL17, CCL18 and CCL22, contributes to drive the selective recruitment of T-cell subsets lacking cytotoxic activity[56,72], and CCL2 production enhances the migration to the tumor site of $CCR2^+$monocytes, where they acquire an M2-like phenotype.

In addition, TAMs express immune checkpoint ligands, such as programmed cell death ligand 1 (PD-L1), PD-L2, B7H4 and CTLA4 ligands B7-1, B7-2, which upon binding to the immune-checkpoint receptors, they trigger T cell cycle arrest, anergy, and apoptosis[56,72]. Several studies showed that, PD-L1, PD-L2 and B7-H4 are overexpressed on TAMs in hepatocellular carcinoma, glioblastoma and pancreatic cancer, ovarian carcinoma[72,87].

In the same time, the expression of major histocompatibility complex in TAMs results completely deregulated, on one side, TAMs express low MHC class II and on the other, the expression of MHC class I molecules is completely unbalanced.

The non-classical MHC-I molecules, HLA-G and -E co-operate to induce anergy in the TME, indeed HLA-E on the surface of the TAMs binds the inhibitory receptor CD94/NKG2A expressed by NK cells and cytotoxic T lymphocytes, inhibiting their activity and protecting TAMs from the cytolysis. Whereas HLA-G inhibits IFNγ secretion, NK and CD8T cells cytotoxicity and induces tolerogenic dendritic cells, enable to promote T cells activation [88,89].

Another mechanism, by which TAMs directly inhibit T cell cytotoxicity is through the enzyme indoleamine 2,3 dioxygenase (IDO), that induces a significant depletion of the amino-acid tryptophan (Trp), that is essential for T cells proliferation, differentiation and activation [90,91]. In addition, TAMs lead to T cells suppression, by locally depleting L-arginine, thought the activation the enzyme Arginase 1 (ARG1)[73,92].

If in the primary tumor, TAMs induce T cells apoptosis, through the release of NO[93], in the metastatic niches, metastasis-associated macrophage precursors (MAMPCs) suppress the cytotoxic activity of $CD8^+$ T cells through a ROS–mediated mechanism[94].

The role of TAMs in immunomodulation also includes their capacity to inhibit phagocytosis, indeed, they can promote tumor immune evasion through expression of signal regulatory protein α (SIRPα). SIRPα is a cell-surface protein, mainly expressed on myeloid cells, (including macrophages and dendritic cells), that is the receptor for CD47, a cell surface protein, that typically protects normal cells from phagocytosis. The overexpressed CD47 receptors on tumor cells interact with SIRPα and deliver the “do not eat me” signals to TAMs, hence, playing a crucial role in the instauration of a phagocytosis resistance mechanism and in the promotion

of tumor escape. Blockade of the CD47-SIRPα signal has been shown to stimulate phagocytosis, leading to tumor cell elimination [95–97].

Besides, another interesting pathway involved in the resistance of phagocytosis is the leukocyte immunoglobulin-like receptor B (LILRB: 1 and 2), negative regulators of myeloid cell activation. Cancer cells express MHC-I molecules on their surface, that interact with LILRBs on macrophage and inhibit phagocytosis clearance [95,97]. Especially, studies have demonstrated that LILRB1 expression is particularly abundant on TAMs and blocking the MHC class I–LILRB1 signaling axis might sensitize tumors to macrophage attack, making these cells more vulnerable to phagocytic clearance[98]. Furthermore, LILRB2 inhibition markedly downregulates multiple gene targets involved in M2-like phenotype, enhancing pro-inflammatory responses in TAMs and restoring antitumor immunity[99].

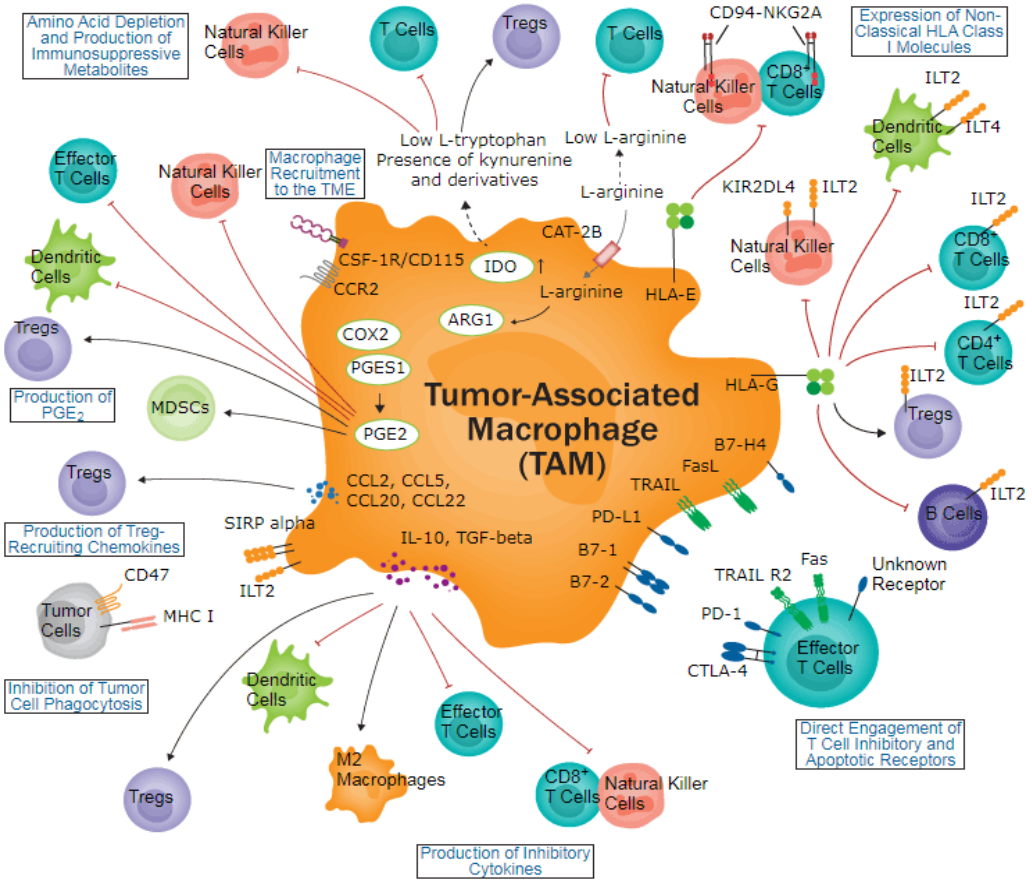

Figure 4. Different pathways involved in TAMs immunosuppressive activity[100]. TAMs have a key role in immunosuppression, producing cytokines, chemokines and immunosuppressive metabolites, expressing inhibitory receptor for T cells, inhibiting their phagocytic activity.

1.1.4.2 TAMs induce Angiogenesis and Lymphangiogenesis

In solid tumors many areas of hypoxia are present, neoangiogenesis facilitates oxygenation and nutrients delivery to neoplastic cells, contributing to tumor growth[101]. Hypoxia-inducible-factors are the principal transcription factors activated by low oxygen tension. In particular, HIF1α, which is expressed in TAMs, drives the expression of a variety of pro-angiogenic genes. TAMs, preferentially accumulate in hypoxic regions, are involved in the production and release of potent proangiogenic cytokines (VEGF, TNFa, IL8), growth factors (platelet-derived growth factor (PDGF), basic fibroblast growth factor (bFGF), macrophage colony– stimulating factor, (CSF-1/M-CSF), MMPs (MMP2, MMP9, MMP12) and other molecules, able to potentiate tumor invasiveness, through the initiation of new blood or lymphatic vessels[102,103].

This correlation between TAMs and the formation of a new tumor vasculature is clearly demonstrated in different types of human cancers, (such as melanoma, B-cell non-Hodgkin's lymphoma, mucoepidermoid carcinoma of salivary glands, pulmonary adenocarcinoma, glioma, and leiomyosarcoma and breast and gastric cancer)[104], and in experimental mouse tumor models, the genetic or pharmacological depletion of macrophages has undoubtedly confirmed that TAMs are the principal inducers of the ‘‘angiogenic switch’’[70].

In particular, both in mice and in human, a specific subpopulation of TAMs ($Tie2^+$) is able to interact with mural pericytes and regulate the vascular structure [105]. $Tie2^+$ TAMs are attracted into the tumors by endothelial cell-derived cytokines angiopoietin-2 (ANG-2), which interacts with their TIE receptors, and CXCL12 that respectively was linked by their CXCR4 receptors. $Tie2^+$ TAMs are essential to increase the vascular density and favor metastasis dissemination [106,107], through the release of high levels of MMP9, VEGF-A, COX-2, and Wnt5a[106]. Several studies have demonstrated that, a genetic deletion of TIE2 blocks ANGPT2- TIE2 signaling pathway in TAMs, decreasing angiogenic interaction[107].

TAMs not only can regulate metastasis dissemination by angiogenesis, but also promote lymphangiogenesis. Since in human breast cancer, higher numbers of TAM are associated with lymphatic microvessel density, lymph node metastasis or lymph vessel invasion. TAMs support tumor lymphangiogenesis, by secreting high levels of VEGF and MMPs, promoting tumor dissemination and progression[107] (*Fig.* 5).

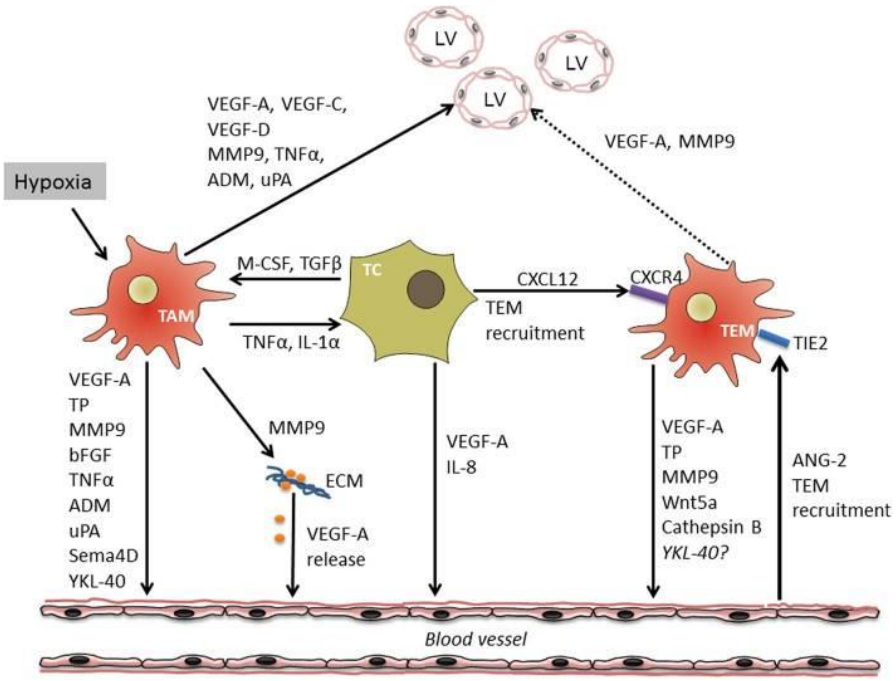

Figure 5. Molecular pathways involved in TAMs promoting angiogenesis[55].

1.1.4.3 TAMs promote tumor cells invasion and metastasis

Cancer is a systemic disease, indeed during their progression, neoplastic cells acquire distinctive ability to leave the primary tumor site and reach distant sites where they settle down and grow[103], and the metastatic process represents the most critical phase of the disease, leading up to 90% of cancer deaths[108]. This process is driven not only by the intrinsic alterations in tumor cells, but also by the implicated cross-talk between cancer cells and their altered TME components, especially TAMs, that contribute to tumor invasiveness and worse prognosis[1]. The metastatic process is a multistep sequence that includes invasion of the basement membrane and cell migration, intravasation into the vasculature or lymphatic system, survival in the circulatory system, extravasation and adaption and growth in the metastatic sites[109] and TAMs are crucially implicated in all the different steps of this process (*Fig.6*).

TAMs favor the first step of tumor invasion by releasing cytokines, such as TGFβ, IL1β, IL8, TNFα, that trigger epithelial-mesenchymal transition (EMT), a process in which epithelial cancer cells shift to gain a mesenchymal phenotype: cells acquire fibroblast properties by augmenting their motility and their ability to penetrate surrounded matrix[110]. *In vitro* and *in vivo* studies have revealed an abundance of TAM infiltrate in the EMT hotspots in tumor site[111], where they participate to enhance the expression of mesenchymal markers like vimentin, snail and N-cadherin and repress E-cadherin levels in tumor cells[97,111,112].

Moreover, TAMs participate in extracellular matrix (ECM) degradation and cell-ECM interaction, focal events in metastasis dissemination[97]. They release numerous proteolytic enzymes, including matrix metalloproteases (MMP-2, MMP-9), plasmin, urokinase-type plasminogen activator (uPA), osteonectin, and cathepsins, thus permitting the degradation of the basal membrane and surrounding connective tissues, to facilitate tumor cell invasion and migration[97,113].

Cell migration is sustained by cells-ECM interaction and it is guarantee by TAM-derived secreted protein acidic and rich in cysteine (SPARC), a matricellular protein that favors the interactions between tumor cells-fibronectin and vitronectin, promoting rapid transolcation into blood vessels[114,115].

Next, macrophages assist the entry of tumor cells into the blood and lymphatic vessels[116],where they acquire the capacity to survive and disseminate in the body[117]. TAMs not only promote the entrance of tumor cells into the circulation by a positive feedback loop, consisting of tumor cell-produced CSF-1 and TAM-produced EGF[118], but also protect them by NK cytotoxic activity[119].

Finally, in the later phase, TAMs both assist tumor cells extravasation and prepare sites for tumor cells growth in the pre-metastatic niches (PMNs). TAMs are accumulated in selected distant tissues in response to tumor-derived factors (such as CCL2, CSF-1, VEGF, PLGF, TNF-α, TGF-β, tissue inhibitor of metallopeptidase (TIMP)-1, and exosomes), where they facilitate the homing of circulating tumor cells (CTCs) and generate a permissive TME, for cancer cell seeding[120].

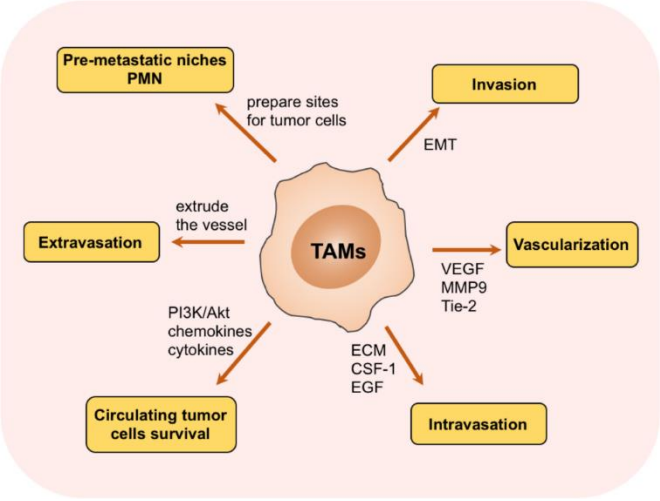

Figure 6. **TAMs favor metastatic process**[97]. TAMs assist in all steps of metastasis instauration, starting from tumor cells invasion, to generate a permissive pre-metastatic niches (PMN).

1.1.5 TAMs as a therapeutic target

Owing to the importance of TAM activities for tumor development and progression, new therapeutic strategies targeting TAMs are widely investigated[121]. Different approaches are under evaluation, such as reduction of the number of TAMs on tumor site by their selective killing, inhibition of their recruitment and TAM re-education, in order to restore their tumoricidal activity[55,70,121] (*Fig.7-8*).

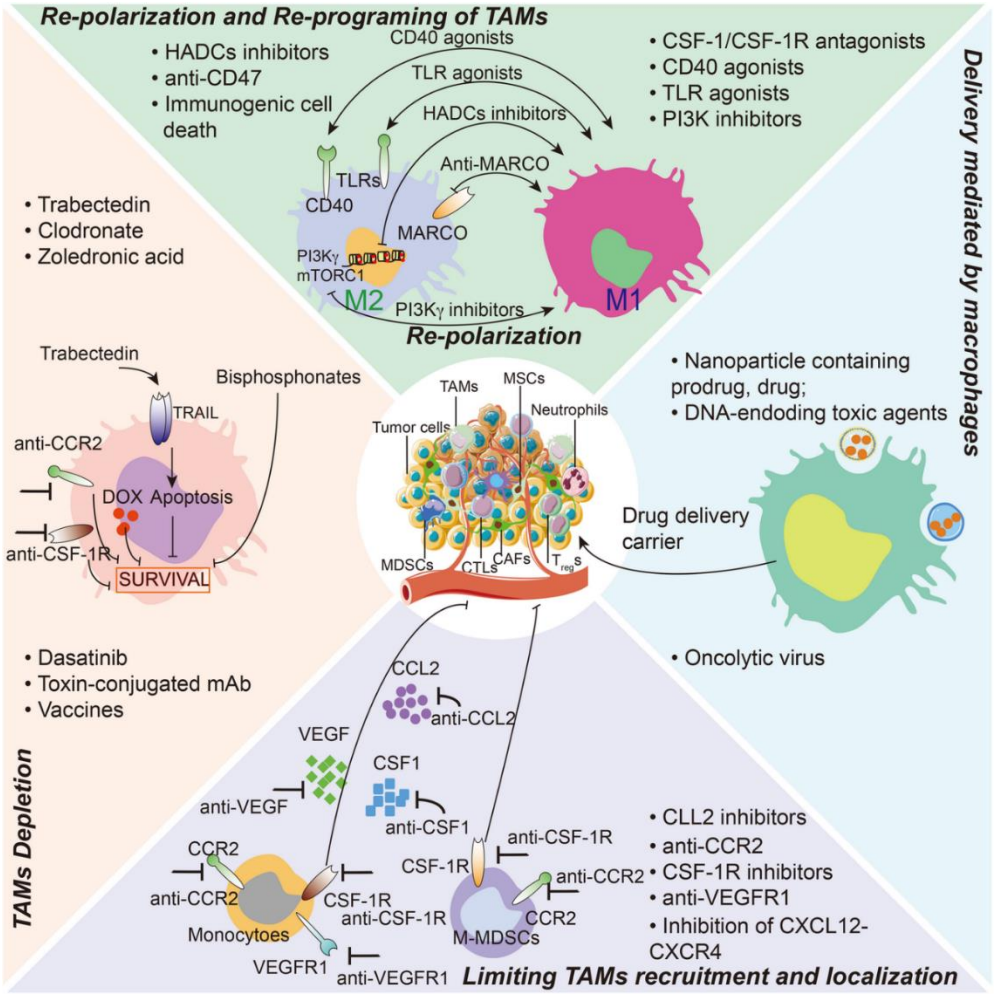

Figure 7. Different strategies to target TAMs[70]. TAMs targeted approaches include inhibition of TAM recruitment and localization, re-polarization /re-programing (either or) of their phenotype, TAM depletion induce their elimination or exploiting TAMs as a delivery system for antitumor drugs.

1.1.5.1 Inhibition of monocytes recruitment into the tumor and TAMs neutralization.

The accumulation of macrophages in tumors is due to the continuous recruitment of monocytes from the circulation, in response to chemo-attractants produced by tumor cells. The pivotal orchestrators of monocytes migration are the tumor-derived factors (TDFs): CCL2, CXCL12 and CSF-1[55].

Studied have shown that high levels of CCL2 in tumor, as well in serum, are associated with poor prognosis in different types of tumors[122].

In several preclinical model (e.g. melanoma, prostate, breast, lung and liver cancers) neutralization of CCL2/CCR2 axis, using anti-CCL2 antibodies or CCR2 inhibitors, has demonstrated a suppression in TAM accumulation and a consequent reduction of tumor growth and metastasis[122–124]. Moreover, in a mouse model of ovarian cancer, CCL2 inhibition has improved the effect of paclitaxel and carboplatin therapies[125].

On this basis, several CCL2-neutralising antibodies are now in clinical trial, and in particular, preliminary clinical studies in solid tumors have shown that carlumab (a human immunoglobin G1κ antibody, that binds to CCL2), causes efficient deflection of macrophages and delay in tumor regrowth after chemotherapy[126].

Currently, CCR2 antagonists are in clinical trials as monotherapy in patients with metastatic cancers, or in combination with chemotherapy (FOLFIRINOX) in advanced pancreatic adenocarcinomas. Patients treated with only chemotherapy did not show an objective response, in contrast, in combination therapy group, half of patients had an objective tumor response, and the majority of those patients achieved local tumor control[127].

Moreover, accumulating evidence has demonstrated the essential role of CXCL12-CCR4 axis in tumor progression, in fact, CXCL12 mediates recruitment and retention of $CXCR4^+$ bone marrow–derived cells to the neoangiogenic niches, supporting vascularization and tumor growth[128].

Nowadays, Mozobil® (also known as plerixafor, and AMD3100) is emerging as CXCR4 receptor antagonist, that disrupts the CXCL12-CXCR4 axis, mobilizing hematopoietic stem cells to the peripheral blood and preventing their accumulation in the tumor site. Since, it is under evaluation in different trials (NCT02179970, NCT03277209) in patients with solid tumors and patients with acute myeloid leukemia[55].

CSF-1 is abundantly produced in several tumors and is essential for macrophages differentiation. Its neutralization through monoclonal antibodies, antisense oligonucleotides, or kinase inhibitors gave promising results in different preclinical studies, including acute myeloid

leukemia, melanoma mammary carcinoma, and glioblastoma [129–131]; therefore, blocking CSF-1R is under evaluation in phase I/II clinical trials with different types of advanced solid tumors[132].

In murine model of breast, prostate and cervical tumors, anti-CSF-1R dependent TAM depletion correlate with an expansion of tumor infiltrating cytotoxic CD8 T cells and an improved therapeutic response[55]

An interesting example is represented by CSF-1R targeting anti-body, RG7155, that has demonstrated an important clinical activity in diffuse-type giant-cell tumor patients, due to an important reduction of TAMs and a consequent increase of CD8+/CD4+ T cells ratio[133]. Another interesting example is represented by the compound PLX3397, in different types of human cancer in combination with radiotherapy or chemotherapy or ICBs, it is able to enhance the efficacy of the treatment[134–136].

Another druggable target on TAMs is represented by the scavenging receptor CD163. In a melanoma mouse model, the researchers have conjugated CD163 antibody with a lipid carrier loaded with doxorubicin to target the selective depletion of $CD163^+$ TAMs, obtaining a significant tumor regression[137]

Prior to these innovative treatments, bisphosphonates have represented a wide used approach for TAM depletion[138], due their ability to inhibit proliferation, migration of macrophages and induce their apoptosis[139].

In experimental models, the encapsulation of clorodronate in liposomes (Clodrolip) positively reduced macrophages tumor infiltration in bone metastasis from lung cancer and lung metastasis from breast cancer limiting metastasis diffusion[140]. Furthermore, different studies have demonstrated the activity of another bisphosphonate, the Zoledronic acid, which is able to reduce tumor burden in a mouse model of bone metastases from breast cancer[55].

Although bisphosphonates had promising results *in vivo*, the high toxicity and the inconsistent results in patients have limited their use in therapy[141].

Trabectedin is another important antineoplastic agent, that not only it is able to target tumor cells but also TAMs, mediating their apoptosis, through the activation of caspase 8 by TNF-related apoptosis-inducing ligand (TRAIL)[141].

1.1.5.2 Reprogramming of TAMs toward an M1 phenotype

Given the high plasticity of TAMs, rewiring their activation towards the M1 phenotype has emerged as an interesting therapeutic strategy[142].

Studying the molecular basis of TAMs, our group has demonstrated, that nuclear accumulation of p50 NF-κB inhibitor homodimers drives the expression of an M2 transcriptional program associated with tumor growth and progression. Since, in preclinical models of fibrosarcoma and melanoma, ablation of p50 restores M1 inflammatory responses and antitumor resistance, suggesting p50 as a potential target for TAM reprogramming[143].

Nowadays, several approaches, based on the re-education of TAMs in anti-tumor cells, have shown beneficial activities both in preclinical and in clinical studies.

An interesting target for macrophage repolarization is represented by Toll-like receptors (TLRs), the innate immunity pattern recognition receptors, that upon engagement by their ligands, mediate the activation of M1-like functional polarization of macrophages.

In this context, the endosomal TLRs (TLR3, TLR7, TLR8 and TLR9) represented interesting druggable targets for synthetic ligands.

The activation of TLR3 by poly I:C is able to restore the cytotoxic activities of macrophages in a mouse model of colon cancer, increasing the production of the inflammatory cytokines IL6, IL12, TNFα, iNOS, enhancing the antigen uptake and improving T cell priming. Currently, the antitumor effect of Poly I:C is investigated in clinical trials, alone or in combination of ICBs therapy in different types of cancer[144,145].

TLR7/TLR8 activation is another attractive target for TAM repolarization. Indeed, Imiquimod, TLR7/TLR8 agonist, induces strong M1 activation, showing an antitumoral activity in different preclinical models, including basal cell carcinoma, melanoma and breast cancer skin metastases[122]. Furthermore, another imiquimob analogue represents a promising drug for TAM reprogramming, since intra-tumor injection of a TLR7/8 agonist 3M-052, induces macrophage repolarization and consequently tumor regression in a mouse model of subcutaneous melanoma[146]

Currently, clinical trials on solid tumor are evaluating the combination of TLR7/8 agonists and chemotherapy or immune checkpoints.

Furthermore, the therapeutic efficacy of the TLR9 agonist, Cytosine phosphate guanin (CpG) oligodeoxinucleotides, was reported by different preclinical studies, Guiducci and colleagues have demonstrated that the combination Cpg-ODN and IL10 antagonist promptly switched M2 cells to an M1 phenotype, sustaining their cytotoxic activities[147].

An attractive target to repolarize macrophages is the activating receptor CD40, expressed on the surface of APC cells, such as dendritic cells, monocytes, macrophages and B lymphocytes. Its activation mediates the expression of MHC molecules, the production of pro-inflammatory cytokines and promotion of T cell activation[55].

In various mouse model of cancer, agonistic anti-CD40 antibodies have shown to favor cytotoxic functions of TAMs, for example, in colon and breast cancer model their combination with ICBs led to a complete tumor rejection in about half of treated mice. Moreover, in murine model of colon, sarcoma and breast cancer, the combination of anti-CD40 plus anti-CSF-1R antibodies resulted in M1 macrophages repolarization, CD8 T cells activation and a significant anti-tumor effect[148].

Currently, different CD40 agonists are under evaluation in several clinical trials for solid tumors, either as a single agent, or in combination with conventional chemotherapy or immunotherapy[55].

In pancreatic cancer, the combination of CD40 agonist antibodies with gemcitabine resulted in tumor regression and in an increase of survival, due to the restoration of antitumor macrophages effect, in fact, they sustained antigen-presentation reestablishing immune surveillance[149]

Another promising target to repolarize TAMs, is PI3Kγ, a kinase expressed primarily in myeloid cells, that controls the switch between immune stimulation to suppression[76]. PI3Kγ inhibition enhanced proinflammatory cytokines expression, cytotoxic T cells recruitment into tumor and consequently lead to tumor regression[76]. *In vitro,* inhibition of PI3Kγ, with Ibrutinib or with TG100-115, induces TAM expression of IL12 and a downregulation of TFGβ and ARG1. Moreover, the inhibition of PI3Kγ signaling in different mouse models, (e.g. head and neck SCC, lung, breast and PDAC), has suppressed tumor growth and enhanced anti-tumor immunity[150].

The macrophage receptor with collagenous structure (MARCO) is another attracting target. It is a scavenger receptor, mainly expressed by a subpopulation of TAMs with an M2-like immunosuppressive gene signature, both in murine tumor models and in human cancer.

Anti-TAM antibodies directed against the scavenger receptor MARCO induce suppression of tumor growth and metastatic dissemination both in 4T1 mammary carcinoma model and B16 melanoma mouse model[122,151]. Furthermore, MARCO represents a potential new immune target for anti-TAM treatment in a subset of NSCLC patients[152].

The CD47 (on tumor cells)–SIRPα (on phagocytic cells) axis is involved in the regulation of phagocytosis. In the context of tumor, the overexpression of CD47 represents a phagocytosis resistance mechanism[96]. At the moment, there are two anti-CD47 mAbs (Hu5F9-G4 and

CC-90002) and one soluble recombinant SIRPα–crystallizable fragment (Fc) fusion protein (TTI-621). The pharmacological inhibition of CD47-SIRPα pathway, using a monoclonal antibody or soluble SIRPα-Fc construct can restore phagocytosis and killing of tumor cells by macrophages in various preclinical cancer models; at the moment, these pharmacological treatments are being tested in phase I clinical trials[122,153].

Another possibility to reprogram TAMs is represented by the class IIA HDAC inhibitors, that can selectively reprogram monocytes and macrophages in the tumor, enhancing their inflammatory properties as described in luminal B-type breast cancer model, where intraperitoneal injection of HDAC inhibitor TMP195 not only has increased monocytes infiltration, but also stimulated the differentiation into antitumoral macrophages[154].

1.1.5.3 TAMs as a delivery of therapeutics agents

An emerging strategy to treat tumors, is to consider TAMs as a drug delivery system, taking advantage of their ability to target and migrate to the tumor sites, creating a live cell-mediated drug delivery system[155,156].

Macrophages loaded with drugs ex vivo, could be reintroduced into the circulation, where thanks to their tumor-homing capacity they unload the drug directly at tumor site, minimizing adverse effects[157]. Different studies have demonstrated that macrophages could be interesting carriers to improve antitumor efficacy, by conveying drug-containing nanoparticles (e.g. doxorubicin) or pro-drugs, toxic agents or oncolytic virus[158–160].

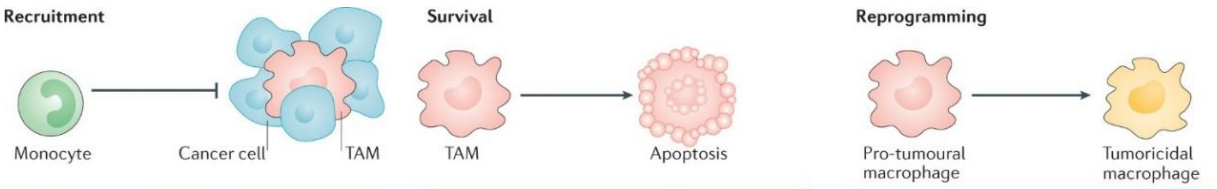

Drug name	Target	Inhibitor type
Carlumab	CCL2	mAb
PF04136309	CCR2	Small molecule
PLX3397	CSF1R	Small molecule
PLX7486	CSF1R	Small molecule
JNJ-40346527	CSF1R	Small molecule
ARRY-382	CSF1R	Small molecule
BLZ945	CSF1R	Small molecule
IMC-CS4	CSF1R	mAb
R05509554	CSF1R	mAb
RG7155	CSF1R	mAb
FPA008	CSF1R	mAb

Drug name	Target	Inhibitor type
Clodronate	NA	Small molecule
Zoledronic acid	NA	Small molecule
Trabectedin	Caspase 8	Small molecule
PLX7486	CSF1R	Small molecule
JNJ-40346527	CSF1R	Small molecule
ARRY-382	CSF1R	Small molecule
BLZ945	CSF1R	Small molecule
IMC-CS4	CSF1R	mAb
R05509554	CSF1R	mAb
RG7155	CSF1R	mAb
FPA008	CSF1R	mAb

Drug name	Target	Inhibitor type
Hu5F9-G4	CD47	mAb
CC-90002	CD47	mAb
TTI-621	SIRPα	Fusion protein
CP-870,893	CD40	Agonistic antibody
RO7009789	CD40	Agonistic antibody
Imiquimod	TLR7	Small molecule
852A	TLR7	Small molecule
IMO-2055	TLR9	Small molecule
BLZ945	CSF1R	Small molecule

Figure8. Different approaches to target TAMs[122].

Bibliography

1. Balkwill, F. & Mantovani, A. Inflammation and cancer: back to Virchow? *The Lancet* **357**, 539-45, (2001).

2. Mantovani, A., Garlanda, C. & Allavena, P. Molecular pathways and targets in cancer-related inflammation. *Annals of Medicine* vol. 42 161–170 (2010).

3. Rothwell, P. M. *et al.* Effect of daily aspirin on long-term risk of death due to cancer: analysis of individual patient data from randomised trials. *The Lancet* **377**, 31-41, (2011).

4. Rothwell, P. M. *et al.* Effect of daily aspirin on risk of cancer metastasis: a study of incident cancers during randomised controlled trials. *The Lancet* **379**,1591-601, (2012).

5. Ridker, P. M. *et al.* Effect of interleukin-1β inhibition with canakinumab on incident lung cancer in patients with atherosclerosis: exploratory results from a randomised, double-blind, placebo-controlled trial. *The Lancet* **390**, 1833-42, (2017).

6. Mantovani, A., Allavena, P., Sica, A. & Balkwill, F. Cancer-related inflammation. *Nature* vol. 454 436–444 (2008).

7. Greten, F. R. & Grivennikov, S. I. Inflammation and Cancer: Triggers, Mechanisms, and Consequences. *Immunity* vol. 51 27–41 (2019).

8. Del Prete, A. *et al.* Molecular pathways in cancer-related inflammation. *Biochemia Medica*, **21**, 264-75, (2011).

9. Ancrile, B., Lim, K.-H. & Counter, C. M. Oncogenic Ras-induced secretion of IL6 is required for tumorigenesis. *Genes & Development* **21**, 1714-19, (2007).

10. Lowe, S. W., Cepero, E. & Evan, G. Intrinsic tumour suppression. *Nature* **432**, 307-15, (2004).

11. Vogelstein, B., Lane, D. & Levine, A. J. Surfing the p53 network. *Nature* **408**, 307-10, (2000).

12. Oren, M. Decision making by p53: life, death and cancer. *Cell Death & Differentiation* **10**, 431-42, (2003).

13. Komarova, E. A. *et al.* p53 is a suppressor of inflammatory response in mice. *The FASEB Journal* **19**, 1030-2, (2005).

14. Schwitalla, S. *et al.* Loss of p53 in Enterocytes Generates an Inflammatory Microenvironment Enabling Invasion and Lymph Node Metastasis of Carcinogen-Induced Colorectal Tumors. *Cancer Cell* **23**, 93-106, (2013).

15. Ikeda, A. *et al.* p300/CBP-Dependent and -Independent Transcriptional Interference between NF-κB RelA and p53. *Biochemical and Biophysical Research Communications* **272**, (2000).

16. Wadgaonkar, R. *et al.* CREB-binding Protein Is a Nuclear Integrator of Nuclear Factor-κB and p53 Signaling. *Journal of Biological Chemistry* **274**, 1879-82, (1999).

17. Webster, G. A. & Perkins, N. D. Transcriptional Cross Talk between NF-κB and p53. *Molecular and Cellular Biology* **19**, 3485-95, (1999).

18. Scian, M. J. *et al.* Tumor-Derived p53 Mutants Induce NF-κB2 Gene Expression. *Molecular and Cellular Biology* **25**, 10097-110, (2005).

19. Gulati, A. P. *et al.* Mutant human tumor suppressor p53 modulates the activation of mitogen-activated protein kinase and nuclear factor-κB, but not c-Jun N-terminal kinase and activated protein-1. *Molecular Carcinogenesis* **45**, 26-37, (2006).

20. Weisz, L. *et al.* Mutant p53 Enhances Nuclear Factor B Activation by Tumor Necrosis Factor in Cancer Cells. *Cancer Research* **67**, 2396-401, (2007).

21. Ubertini, V. *et al.* Mutant p53 gains new function in promoting inflammatory signals by repression of the secreted interleukin-1 receptor antagonist. *Oncogene* **34**, 2493-504, (2015).

22. Vaughan, C. A. *et al.* p53 mutants induce transcription of NF-κB2 in H1299 cells through CBP and STAT binding on the NF-κB2 promoter and gain of function activity. *Archives of Biochemistry and Biophysics* **518**, 79-88, (2012).

23. Menendez, D., Lowe, J. M., Snipe, J. & Resnick, M. A. Ligand dependent restoration of human TLR3 signaling and death in p53 mutant cells. *Oncotarget* **7**, 61630-42, (2016).

24. Schwitalla, S. *et al.* Loss of p53 in Enterocytes Generates an Inflammatory Microenvironment Enabling Invasion and Lymph Node Metastasis of Carcinogen-Induced Colorectal Tumors. *Cancer Cell* **23**, 93–106 (2013).

25. Cooks, T., Harris, C. C. & Oren, M. Caught in the crossfire: p53 in inflammation. *Carcinogenesis* **35**, 1680-90, (2014).

26. Weisz, L. *et al.* Mutant p53 Enhances Nuclear Factor B Activation by Tumor Necrosis Factor in Cancer Cells. *Cancer Research* **67**, (2007).

27. Andriani, G. A. *et al.* Whole Chromosome Instability induces senescence and promotes SASP. *Scientific Reports* **6**, (2016).

28. Vermeulen, L. *et al.* Defining Stem Cell Dynamics in Models of Intestinal Tumor Initiation. *Science* **342**, 995-8, (2013).

29. Henry, C. J. *et al.* Aging-associated inflammation promotes selection for adaptive oncogenic events in B cell progenitors. *Journal of Clinical Investigation* **125**, 4666-80, (2015).

30. Greten, F. R. & Grivennikov, S. I. Inflammation and Cancer: Triggers, Mechanisms, and Consequences. *Immunity* vol. 51 27–41 (2019).

31. Liao, W. *et al.* KRAS-IRF2 Axis Drives Immune Suppression and Immune Therapy Resistance in Colorectal Cancer. *Cancer Cell* **35**, 559-72, (2019).

32. Sparmann, A. & Bar-Sagi, D. Ras-induced interleukin-8 expression plays a critical role in tumor growth and angiogenesis. *Cancer Cell* **6**, 447-58, (2004).

33. Porta, C. , E. R. and A. S. Mechanisms linking pathogens-associated inflammation and cancer. *Cancer Lett* **305(2)**, 250–262 (2011).

34. Mola, S., Pandolfo, C., Sica, A. & Porta, C. The Macrophages-Microbiota Interplay in Colorectal Cancer (CRC)-Related Inflammation: Prognostic and Therapeutic Significance. *International Journal of Molecular Sciences* **21**, 1-30, (2020).

35. McAllister, F. *et al.* Oncogenic kras activates a hematopoietic-to-epithelial IL-17 signaling axis in preinvasive pancreatic neoplasia. *Cancer Cell* **25**, 621–637 (2014).

36. Dapito, D. H. *et al.* Promotion of Hepatocellular Carcinoma by the Intestinal Microbiota and TLR4. *Cancer Cell* **21**, 504–516 (2012).

37. Jin, C. *et al.* Commensal Microbiota Promote Lung Cancer Development via γδ T Cells. *Cell* **176**, 998-1013, (2019).

38. Greathouse, K. L. *et al.* Interaction between the microbiome and TP53 in human lung cancer. *Genome Biology* **19**:123, (2018).

39. Wu, J., Li, Q. & Fu, X. Fusobacterium nucleatum Contributes to the Carcinogenesis of Colorectal Cancer by Inducing Inflammation and Suppressing Host Immunity. *Translational Oncology* **12**, 846-51, (2019).

40. Erreni, M., Mantovani, A. & Allavena, P. Tumor-associated Macrophages (TAM) and Inflammation in Colorectal Cancer. *Cancer Microenvironment* **4**, 141-54, (2011).

41. Van der Kraak, L. Colitis-associated colon cancer: Is it in your genes? *World Journal of Gastroenterology* **21**, 11688-99, (2015).

42. Wang, K. & Karin, M. Tumor-Elicited Inflammation and Colorectal Cancer, *Adv Cancer Res,* **128**, 173-96, (2015).

43. Kadariya, Y. *et al.* Inflammation-related IL1β/IL1R signaling promotes the development of asbestos-induced malignant mesothelioma. *Cancer Prevention Research* **9**, 406–414 (2016).

44. Takahashi, H., Ogata, H., Nishigaki, R., Broide, D. H. & Karin, M. Tobacco Smoke Promotes Lung Tumorigenesis by Triggering IKKβ- and JNK1-Dependent Inflammation. *Cancer Cell* **17**, 89–97 (2010).

45. Atretkhany, K.-S. N., Drutskaya, M. S., Nedospasov, S. A., Grivennikov, S. I. & Kuprash, D. V. Chemokines, cytokines and exosomes help tumors to shape inflammatory microenvironment. *Pharmacology & Therapeutics* **168**, 98-112, (2016).

46. Aggarwal, V. *et al.* Role of reactive oxygen species in cancer progression: Molecular mechanisms and recent advancements. *Biomolecules* vol. 9 735 (2019).

47. Allavena, P., Germano, G., Marchesi, F. & Mantovani, A. Chemokines in cancer related inflammation. *Experimental Cell Research* vol. 317 664–673 (2011).

48. D'Ignazio, L., Bandarra, D. & Rocha, S. NF-κB and HIF crosstalk in immune responses. *FEBS Journal* vol. 283 413–424 (2016).

49. Palazon, A., Goldrath, A. W., Nizet, V. & Johnson, R. S. HIF Transcription Factors, Inflammation, and Immunity. *Immunity* vol. 41 518–528 (2014).

50. Talks, K. L. *et al.* The Expression and Distribution of the Hypoxia-Inducible Factors HIF-1α and HIF-2α in Normal Human Tissues, Cancers, and Tumor-Associated Macrophages. *The American Journal of Pathology* **157**, 411-21, (2000).

51. Bromberg, J. & Darnell, J. E. The role of STATs in transcriptional control and their impact on cellular function. *Oncogene* **19**, 2468-73, (2000).

52. Yu, H., Pardoll, D. & Jove, R. STATs in cancer inflammation and immunity: a leading role for STAT3. *Nature Reviews Cancer* **9**, 798-809, (2009).

53. Zhang, H.-F. & Lai, R. STAT3 in Cancer—Friend or Foe? *Cancers* **6**, 1408-40, (2014).

54. Mantovani, A. & Allavena, P. The interaction of anticancer therapies with tumor-associated macrophages. *Journal of Experimental Medicine* vol. 212 435–445 (2015).

55. Anfray, Ummarino, Andón & Allavena. Current Strategies to Target Tumor-Associated-Macrophages to Improve Anti-Tumor Immune Responses. *Cells* **9**:46, (2019).

56. Condeelis, J. & Pollard, J. W. Macrophages: Obligate Partners for Tumor Cell Migration, Invasion, and Metastasis. *Cell* **124**, 263-6, (2006).

57. Mantovani, A. & Locati, M. Tumor-Associated Macrophages as a Paradigm of Macrophage Plasticity, Diversity, and Polarization. *Arteriosclerosis, Thrombosis, and Vascular Biology* **33**, 1478-83, (2013).

58. Pathria, P., Louis, T. L. & Varner, J. A. Targeting Tumor-Associated Macrophages in Cancer. *Trends in Immunology* **40**, 310-27, (2019).

59. Cortez-Retamozo, V. *et al.* Origins of tumor-associated macrophages and neutrophils. *Proceedings of the National Academy of Sciences* **109**, 2491-6, (2012).

60. Liu, Y. & Cao, X. The origin and function of tumor-associated macrophages. *Cellular & Molecular Immunology* **12**, 1-4, (2015).

61. Movahedi, K. & van Ginderachter, J. A. The Ontogeny and Microenvironmental Regulation of Tumor-Associated Macrophages. *Antioxidants & Redox Signaling* **25**, 775-91, (2016).

62. Epelman, S., Lavine, K. J. & Randolph, G. J. Origin and Functions of Tissue Macrophages. *Immunity* **41**, 21-35, (2014).

63. Gomez Perdiguero, E. *et al.* Tissue-resident macrophages originate from yolk-sac-derived erythro-myeloid progenitors. *Nature* **518**, 547-51, (2015).

64. Hashimoto, D. *et al.* Tissue-Resident Macrophages Self-Maintain Locally throughout Adult Life with Minimal Contribution from Circulating Monocytes. *Immunity* **38**, 792-804, (2013).

65. Yona, S. *et al.* Fate Mapping Reveals Origins and Dynamics of Monocytes and Tissue Macrophages under Homeostasis. *Immunity* **38**, 79-91, (2013).

66. Loyher, P.-L. *et al.* Macrophages of distinct origins contribute to tumor development in the lung. *Journal of Experimental Medicine* **215**, 2536-53, (2018).

67. Franklin, R. A. *et al.* The cellular and molecular origin of tumor-associated macrophages. *Science* **344**, 921–925 (2014).

68. Chen, Z. *et al.* Cellular and Molecular Identity of Tumor-Associated Macrophages in Glioblastoma. *Cancer Research* **77**, 2266-78, (2017).

69. Etzerodt, A. *et al.* Tissue-resident macrophages in omentum promote metastatic spread of ovarian cancer. *Journal of Experimental Medicine* **217**, (2020).

70. Yang, L. & Zhang, Y. Tumor-associated macrophages: from basic research to clinical application. *Journal of Hematology & Oncology* **10**, (2017).

71. Mantovani, A. & Sica, A. Macrophages, innate immunity and cancer: balance, tolerance, and diversity. *Current Opinion in Immunology* **22**, 231-7, (2010).

72. Mantovani, A., Marchesi, F., Malesci, A., Laghi, L. & Allavena, P. Tumour-associated macrophages as treatment targets in oncology. *Nature Reviews Clinical Oncology* **14**, 399-416, (2017).

73. Caux, C., Ramos, R. N., Prendergast, G. C., Bendriss-Vermare, N. & Ménétrier-Caux, C. A Milestone Review on How Macrophages Affect Tumor Growth. *Cancer Research* **76**, 6439-42, (2016).

74. Sica, A. & Mantovani, A. Macrophage plasticity and polarization: in vivo veritas. *Journal of Clinical Investigation* **122**, 787-95, (2012).

75. Genard, G., Lucas, S. & Michiels, C. Reprogramming of Tumor-Associated Macrophages with Anticancer Therapies: Radiotherapy versus Chemo- and Immunotherapies. *Frontiers in Immunology* **8**:828, (2017).

76. Kaneda, M. M. *et al.* PI3Kγ 3 is a molecular switch that controls immune suppression. *Nature* **539**, 437–442 (2016).

77. Larionova, I., Kazakova, E., Patysheva, M. & Kzhyshkowska, J. Transcriptional, Epigenetic and Metabolic Programming of Tumor-Associated Macrophages. *Cancers* **12**, (2020).

78. de Groot, A. E. & Pienta, K. J. Epigenetic control of macrophage polarization: Implications for targeting tumor-associated macrophages. *Oncotarget* vol. 9 20908–20927 (2018).

79. Cheng, C. *et al.* SOCS1 hypermethylation mediated by DNMT1 is associated with lipopolysaccharide-induced inflammatory cytokines in macrophages. *Toxicology Letters* **225**, 488-97, (2014).

80. Yang, L. & Karin, M. Roles of tumor suppressors in regulating tumor-associated inflammation. *Cell Death and Differentiation* vol. 21 1677–1686 (2014).

81. Groot, A. E. de, Zarif, J. C. & Pienta, K. J. Abstract 4005: HDAC inhibitors regulate M2 tumor-associated macrophage function through histone acetylation. in *Tumor Biology* (American Association for Cancer Research, 2017). doi:10.1158/1538-7445.AM2017-4005.

82. Tran, K. *et al.* The combination of the histone deacetylase inhibitor vorinostat and synthetic triterpenoids reduces tumorigenesis in mouse models of cancer. *Carcinogenesis* **34**, 199–210 (2013).

83. Jambhekar, A., Dhall, A. & Shi, Y. Roles and regulation of histone methylation in animal development. *Nature Reviews Molecular Cell Biology* **20**, 625-41, (2019).

84. Lopez-Yrigoyen, M., Cassetta, L. & Pollard, J. W. Macrophage targeting in cancer. *Annals of the New York Academy of Sciences* nyas.14377 (2020) doi:10.1111/nyas.14377.

85. Malekghasemi, S. *et al.* Tumor-Associated Macrophages: Protumoral Macrophages in Inflammatory Tumor Microenvironment. *Advanced Pharmaceutical Bulletin* **10**, 556-65, (2020).

86. Holt, D., Ma, X., Kundu, N. & Fulton, A. Prostaglandin E 2 (PGE 2) suppresses natural killer cell function primarily through the PGE 2 receptor EP4. *Cancer Immunology, Immunotherapy* **60**, 1577–1586 (2011).

87. Gottlieb, C. E., Mills, A. M., Cross, J. v. & Ring, K. L. Tumor-associated macrophage expression of PD-L1 in implants of high grade serous ovarian carcinoma: A comparison of matched primary and metastatic tumors. *Gynecologic Oncology* **144**, 607–612 (2017).

88. Marchesi, M. *et al.* HLA-dependent tumour development: A role for tumour associate macrophages? *Journal of Translational Medicine* **11**, 247 (2013).

89. Morandi, F. & Pistoia, V. Interactions between HLA-G and HLA-E in physiological and pathological conditions. *Frontiers in Immunology* vol. 5 (2014).

90. Mazzone, M., Menga, A. & Castegna, A. Metabolism and TAM functions-it takes two to tango. *The FEBS Journal* **285**, 700-16, (2018).

91. Noy, R. & Pollard, J. W. Tumor-Associated Macrophages: From Mechanisms to Therapy. *Immunity* vol. 41 49–61 (2014).

92. Arlauckas, S. P. *et al.* Arg1 expression defines immunosuppressive subsets of tumor-associated macrophages. *Theranostics* **8**, 5842–5854 (2018).

93. Saio, M., Radoja, S., Marino, M. & Frey, A. B. Tumor-Infiltrating Macrophages Induce Apoptosis in Activated CD8 + T Cells by a Mechanism Requiring Cell Contact and Mediated by Both the Cell-Associated Form of TNF and Nitric Oxide . *The Journal of Immunology* **167**, 5583–5593 (2001).

94. Kitamura, T. *et al.* Monocytes differentiate to immune suppressive precursors of metastasis-associated macrophages in mouse models of metastatic breast cancer. *Frontiers in Immunology* **8**, (2018).

95. Feng, M. *et al.* Phagocytosis checkpoints as new targets for cancer immunotherapy. *Nature Reviews Cancer* **19**, (2019).

96. Murata, Y., Kotani, T., Ohnishi, H. & Matozaki, T. The CD47-SIRP signalling system: its physiological roles and therapeutic application. *Journal of Biochemistry* **155**, 335–344 (2014).

97. Lin, Y., Xu, J. & Lan, H. Tumor-associated macrophages in tumor metastasis: Biological roles and clinical therapeutic applications. *Journal of Hematology and Oncology* vol. 12 (2019).

98. Barkal, A. A. *et al.* Engagement of MHC class i by the inhibitory receptor LILRB1 suppresses macrophages and is a target of cancer immunotherapy article. *Nature Immunology* **19**, 76–84 (2018).

99. Chen, H. M. *et al.* Blocking immunoinhibitory receptor LILRB2 reprograms tumor-associated myeloid cells and promotes antitumor immunity. *Journal of Clinical Investigation* **128**, 5647–5662 (2018).

100. https://www.rndsystems.com/pathways/tumor-associated-macrophage-tam.

101. Lin, E. Y., Gouon-Evans, V., Nguyen, A. v. & Pollard, J. W. The macrophage growth factor CSF-1 in mammary gland development and tumor progression. *Journal of Mammary Gland Biology and Neoplasia* **7**:76, (2002).

102. Gomes, F. G., Nedel, F., Alves, A. M., Nör, J. E. & Tarquinio, S. B. C. Tumor angiogenesis and lymphangiogenesis: Tumor/endothelial crosstalk and cellular/microenvironmental signaling mechanisms. *Life Sciences* **92**, (2013).

103. Qian, B. Z. & Pollard, J. W. Macrophage Diversity Enhances Tumor Progression and Metastasis. *Cell* vol. 141 39–51 (2010).

104. Gazzaniga, S. *et al.* Targeting tumor-associated macrophages and inhibition of MCP-1 reduce angiogenesis and tumor growth in a human melanoma xenograft. *Journal of Investigative Dermatology* **127**, 2031–2041 (2007).

105. Matsubara, T. *et al.* TIE2-expressing monocytes as a diagnostic marker for hepatocellular carcinoma correlates with angiogenesis. *Hepatology* **57**, 1416-25, (2013).

106. Mazzieri, R. *et al.* Targeting the ANG2/TIE2 Axis Inhibits Tumor Growth and Metastasis by Impairing Angiogenesis and Disabling Rebounds of Proangiogenic Myeloid Cells. *Cancer Cell* **19**, 512–526 (2011).

107. Riabov, V. *et al.* Role of tumor associated macrophages in tumor angiogenesis and lymphangiogenesis, *Front. Physiol.,* **5**:75, (2014).

108. Gupta, G. P. & Massagué, J. Cancer Metastasis: Building a Framework. *Cell* vol. 127 679–695 (2006).

109. Chambers, A. F., Groom, A. C. & MacDonald, I. C. Dissemination and growth of cancer cells in metastatic sites. *Nature Reviews Cancer* vol. 2 563–572 (2002).

110. Wirtz, D., Konstantopoulos, K. & Searson, P. C. The physics of cancer: the role of physical interactions and mechanical forces in metastasis. *Nature Reviews Cancer* **11**, 512-22, (2011).

111. Fu, X. T. *et al.* Macrophage-secreted IL-8 induces epithelial-mesenchymal transition in hepatocellular carcinoma cells by activating the JAK2/STAT3/Snail pathway. *International Journal of Oncology* **46**, 587–596 (2015).

112. Liu, C. Y. *et al.* M2-polarized tumor-associated macrophages promoted epithelial-mesenchymal transition in pancreatic cancer cells, partially through TLR4/IL-10 signaling pathway. *Laboratory Investigation* **93**, 844–854 (2013).

113. Kim, J. & Bae, J.-S. Tumor-Associated Macrophages and Neutrophils in Tumor Microenvironment. *Mediators of Inflammation* **2016**, (2016).

114. Barker, T. H. *et al.* SPARC regulates extracellular matrix organization through its modulation of integrin-linked kinase activity. *Journal of Biological Chemistry* **280**, 36483–36493 (2005).

115. Sangaletti, S. *et al.* Macrophage-derived SPARC bridges tumor cell-extracellular matrix interactions toward metastasis. *Cancer Research* **68**, 9050–9059 (2008).

116. Wyckoff, J. B. *et al.* Direct visualization of macrophage-assisted tumor cell intravasation in mammary tumors. *Cancer Research* **67**, 2649–2656 (2007).

117. Robinson, B. D. *et al.* Tumor microenvironment of metastasis in human breast carcinoma: A potential prognostic marker linked to hematogenous dissemination. *Clinical Cancer Research* **15**, 2433–2441 (2009).

118. Lin, Y., Xu, J. & Lan, H. Tumor-associated macrophages in tumor metastasis: Biological roles and clinical therapeutic applications. *Journal of Hematology and Oncology* vol. 12 1–16 (2019).

119. Gil-Bernabé, A. M. *et al.* Recruitment of monocytes/macrophages by tissue factor-mediated coagulation is essential for metastatic cell survival and premetastatic niche establishment in mice. *Blood* **119**, 3164–3175 (2012).

120. Kaplan, R. N., Psaila, B. & Lyden, D. Bone marrow cells in the 'pre-metastatic niche': within bone and beyond. *Cancer and Metastasis Reviews* **25**, 521-9, (2007).

121. Komohara, Y., Fujiwara, Y., Ohnishi, K. & Takeya, M. Tumor-associated macrophages: Potential therapeutic targets for anti-cancer therapy. *Advanced Drug Delivery Reviews* vol. 99 180–185 (2016).

122. Cassetta, L. & Pollard, J. W. Targeting macrophages: Therapeutic approaches in cancer. *Nature Reviews Drug Discovery* vol. 17 887–904 (2018).

123. Argyle, D. & Kitamura, T. Targeting macrophage-recruiting chemokines as a novel therapeutic strategy to prevent the progression of solid tumors. *Frontiers in Immunology* vol. 9 2629 (2018).

124. Teng, K. Y. *et al.* Blocking the CCL2-CCR2 axis using CCL2-neutralizing antibody is an effective therapy for hepatocellular cancer in a mouse model. *Molecular Cancer Therapeutics* **16**, 312–322 (2017).

125. Moisan, F. *et al.* Enhancement of paclitaxel and carboplatin therapies byCCL2 blockade in ovarian cancers. *Molecular Oncology* **8**, 1231–1239 (2014).

126. Brana, I. *et al.* Carlumab, an anti-C-C chemokine ligand 2 monoclonal antibody, in combination with four chemotherapy regimens for the treatment of patients with solid tumors: an open-label, multicenter phase 1b study. *Targeted Oncology* **10**, 111–123 (2015).

127. Nywening, T. M. *et al.* Targeting tumour-associated macrophages with CCR2 inhibition in combination with FOLFIRINOX in patients with borderline resectable and locally advanced pancreatic cancer: A single-centre, open-label, dose-finding, non-randomised, phase 1b trial. *The Lancet Oncology* **17**, 651–662 (2016).

128. Petit, I., Jin, D. & Rafii, S. The SDF-1-CXCR4 signaling pathway: a molecular hub modulating neo-angiogenesis. *Trends in Immunology* **28**, 299–307 (2007).

129. Goswami, S. *et al.* Macrophages promote the invasion of breast carcinoma cells via a colony-stimulating factor-1/epidermal growth factor paracrine loop. *Cancer Research* **65**, 5278–5283 (2005).

130. Manthey, C. L. *et al.* JNJ-28312141, a novel orally active colony-stimulating factor-1 receptor/FMS-related receptor tyrosine kinase-3 receptor tyrosine kinase inhibitor with potential utility in solid tumors, bone metastases, and acute myeloid leukemia. *Molecular Cancer Therapeutics* **8**, 3151–3161 (2009).

131. Pyonteck, S. M. *et al.* CSF-1R inhibition alters macrophage polarization and blocks glioma progression. *Nature Medicine* **19**, 1264–1272 (2013).

132. Consonni, F. M. *et al.* Myeloid-derived suppressor cells: Ductile targets in disease. *Frontiers in Immunology*, **10**:536, (2019).

133. Ries, C. H. *et al.* Targeting tumor-associated macrophages with anti-CSF-1R antibody reveals a strategy for cancer therapy. *Cancer Cell* **25**, 846–859 (2014).

134. Mok, S. *et al.* Inhibition of colony stimulating factor-1 receptor improves antitumor efficacy of BRAF inhibition. *BMC Cancer* **15**, (2015).

135. Patwardhan, P. P. *et al.* Sustained inhibition of receptor tyrosine kinases and macrophage depletion by PLX3397 and rapamycin as a potential new approach for the treatment of MPNSTs. *Clinical Cancer Research* **20**, 3146–3158 (2014).

136. Zhu, Y. *et al.* CSF1/CSF1R blockade reprograms tumor-infiltrating macrophages and improves response to T-cell checkpoint immunotherapy in pancreatic cancer models. *Cancer Research* **74**, 5057–5069 (2014).

137. Etzerodt, A. *et al.* Specific targeting of CD163+ TAMs mobilizes inflammatory monocytes and promotes T cell-mediated tumor regression. *Journal of Experimental Medicine* **216**, 2394–2411 (2019).

138. Rogers, T. L. & Holen, I. Tumour macrophages as potential targets of bisphosphonates. *Journal of Translational Medicine* vol. 9 177 (2011).

139. Hiraoka, K. *et al.* Inhibition of bone and muscle metastases of lung cancer cells by a decrease in the number of monocytes/macrophages. *Cancer Science* **99**, 1595–1602 (2008).

140. Lahmar, Q. *et al.* Tissue-resident versus monocyte-derived macrophages in the tumor microenvironment. *Biochimica et Biophysica Acta (BBA) - Reviews on Cancer* **1865**, (2016).

141. Germano, G. *et al.* Role of Macrophage Targeting in the Antitumor Activity of Trabectedin. *Cancer Cell* **23**, 249–262 (2013).

142. Rubio, C. *et al.* Macrophage polarization as a novel weapon in conditioning tumor microenvironment for bladder cancer: can we turn demons into gods? *Clinical and Translational Oncology* vol. 21 391–403 (2019).

143. Saccani, A. *et al.* p50 nuclear factor-κB overexpression in tumor-associated macrophages inhibits M1 inflammatory responses and antitumor resistance. *Cancer Research* **66**, 11432–11440 (2006).

144. Vidyarthi, A. *et al.* TLR-3 Stimulation Skews M2 Macrophages to M1 Through IFN-αβ Signaling and Restricts Tumor Progression. *Frontiers in Immunology* **9**, (2018).

145. Zhao, J. *et al.* Anti-tumor macrophages activated by ferumoxytol combined or surface-functionalized with the TLR3 agonist poly (I: C) promote melanoma regression. *Theranostics* **8**, 6307–6321 (2018).

146. Singh, M. *et al.* Effective Innate and Adaptive Antimelanoma Immunity through Localized TLR7/8 Activation. *The Journal of Immunology* **193**, 4722–4731 (2014).

147. Guiducci, C., Vicari, A. P., Sangaletti, S., Trinchieri, G. & Colombo, M. P. Redirecting in vivo elicited tumor infiltrating macrophages and dendritic cells towards tumor rejection. *Cancer Research* **65**, 3437–3446 (2005).

148. Wiehagen, K. R. *et al.* Combination of CD40 agonism and CSF-1R blockade reconditions tumor-associated macrophages and drives potent antitumor immunity. *Cancer Immunology Research* **5**, 1109–1121 (2017).

149. Beatty, G. L. *et al.* CD40 agonists alter tumor stroma and show efficacy against pancreatic carcinoma in mice and humans. *Science* **331**, 1612–1616 (2011).

150. Qiu, X. *et al.* Recent discovery of phosphoinositide 3-kinase γ inhibitors for the treatment of immune diseases and cancers. *Future Medicinal Chemistry* **11**, (2019).

151. Li, X. *et al.* Harnessing tumor-associated macrophages as aids for cancer immunotherapy. *Molecular Cancer* vol. 18 1–16 (2019).

152. la Fleur, L. *et al.* Expression of scavenger receptor <scp>MARCO</scp> defines a targetable tumor-associated macrophage subset in non-small cell lung cancer. *International Journal of Cancer* **143**, 1741–1752 (2018).

153. Gu, S. *et al.* CD47 Blockade Inhibits Tumor Progression through Promoting Phagocytosis of Tumor Cells by M2 Polarized Macrophages in Endometrial Cancer. *Journal of Immunology Research* **2018**, (2018).

154. Guerriero, J. L. *et al.* Class IIa HDAC inhibition reduces breast tumours and metastases through anti-tumour macrophages. *Nature* **543**, (2017).

155. Huang, W.-C. *et al.* Tumortropic monocyte-mediated delivery of echogenic polymer bubbles and therapeutic vesicles for chemotherapy of tumor hypoxia. *Biomaterials* **71**, 71–83 (2015).

156. Choi, M. R. *et al.* A cellular trojan horse for delivery of therapeutic nanoparticles into tumors. *Nano Letters* **7**, 3759–3765 (2007).

157. Pei, Y. & Yeo, Y. Drug delivery to macrophages: Challenges and opportunities. *Journal of Controlled Release* **240**, (2016).

158. Muthana, M. *et al.* Macrophage delivery of an oncolytic virus abolishes tumor regrowth and metastasis after chemotherapy or irradiation. *Cancer Research* **73**, 490–495 (2013).

159. Ovais, M., Guo, M. & Chen, C. Tailoring Nanomaterials for Targeting Tumor-Associated Macrophages. *Advanced Materials* **31**, 1808303 (2019).

160. Si, J., Shao, S., Shen, Y. & Wang, K. Macrophages as Active Nanocarriers for Targeted Early and Adjuvant Cancer Chemotherapy. *Small* **12**, 5108-119, (2016).

Outline of the Thesis

Tumor Associated Macrophages (TAMs) are the major population of leucocytes infiltrating tumors and the master regulators of cancer-related inflammation. Despite, their potential anti-tumor activity, TAMs acquire an M2-skewed phenotype endowed of many tumor-promoting activities, including suppression of adaptive immunity and induction of angiogenesis, tumor cells proliferation, survival and migration. Beyond contributing to tumorigenesis, TAMs can profoundly affect the response to anti-cancer therapies, either impairing or enhancing the efficacy of anti-cancer strategies. Accumulating clinical studies have confirmed TAMs as prognostic indicators of cancer progression and as attractive targets for the development of new therapeutic approaches.

Our study is focused on TAMs with the dual aim: 1) identification of new important molecules driving TAM pro-tumoral functions 2) gathering information regarding the impact of TAMs on anti-tumor activity of EPZ-6438, a new epigenetic modulator that is under clinical evaluation

1) To identify new molecular players of TAM pro-tumoral activities, we analyzed the alterations of the phospho-proteoma of TAMs isolated from murine MN/MCA1 fibrosarcoma, as compared to resting (ctr), M1 (IFNγ/LPS for 30 min) and M2 (IL-4 for 8h) polarized macrophages. We originally found the phosphorylation of Tripartite motif-containing 28 (TRIM28) at Ser473 (TRIM28 S473p) in both M1-polarized PECs and TAMs. TRIM28 is a member of the Kruppel-Associated-Box Proteins that participates in the dynamic organization of chromatin and is involved in multiple cellular activities. To get insights the triggers and the molecular mechanisms driving TRIM28 S473p in macrophages, we analyzed different inflammatory signals, including cytokines (IFNγ, TNFα, IL-1β, IL-6), microbial products (TLR ligands) and selected molecules of their signaling cascades. In the attempt to identify potential tumor-derived signals controlling TRIM28 S473p in TAMs, we also tested immunoregulatory molecules (IL-10, PGE2), that we have found enriched in fibrosarcoma. We next explored in vivo, the functional relevance of myeloid TRIM28 in different contexts of cancer related inflammation. We generated mice lacking the protein TRIM28 in myeloid cells (TRIM28$^{LysM\text{-}Cre}$) and we used these mice to evaluate whether the total absence of TRIM28 could affect TAM activity in both fibrosarcoma model and in colitis-associated cancer (CAC) model. To get insights into the effects of lack of TRIM28 on LPS-induced inflammatory gene expression, we generated mRNA sequencing (mRNA-seq) data sets of WT(TRIM28$^{LysM\text{-}Cre}$) and TRIM28 KO (*TRIM28*$^{flox/flox}$) PECs under both untreated condition (Ctr) and following the treatment with 10ng/ml LPS for 4 hours to induce M1-polarized activation or for 20 hours to induce an LPS-tolerant phenotype.

TRIM28 acts as an oncogenic driver in different cancer types, including colorectal cancer (CRC). So far, phosphorylation of TRIM28 on serine 473 (S473) has been found associated with DNA repair mechanisms and epigenetic stability. Given that, we have found that both TLR ligands and inflammatory cytokines can induced TRIM28 S473p, we explored the impact of inflammation on TRIM28-dependent DNA damage response and consequent susceptibility of intestinal epithelial cells (IECs) to undergo neoplastic transformation. We treated TRIM28$^{Villin\text{-}Cre}$ and TRIM28$^{flox/flox}$ mice with AOM /DSS and we analyzed inflammatory response and tumor development. Next, to dissect the mechanisms whereby TRIM28 in IECs influence inflammation-driven CRC development, we analyzed the transcriptional profile of IECs/tumor cells and lamina propria immune cells by single cell RNAseq approach. This is a state-of-the-art NGS approach that allows to improve the characterization of heterogeneous cell populations and thus the resolution of complex biological systems. We analyzed both the tumor lesions and the colon of AOM/DSS-treated mice 9 days (colitis) after the first DSS administration, when the mutant cells due to AOM treatment likely start the selection operated by immune cells.

2) Malignant Pleural Mesothelioma (MPM) is a highly aggressive cancer with long latency period and dismal prognosis. Recently, EPZ-6438 (tazemetostat) has entered in clinical trials due to the anti-proliferative effects reported on MPM cells. We set up a reliable 3D MPM-monocytes spheroid model to investigate the impact of TAMs on MPM cell responsiveness to EPZ-6438. We initially confirmed the anti-proliferative effects of EZH2 inhibitor in MPM spheroids, then we evaluated both monocytes recruitment into the tumor spheroids and their functional differentiation towards a TAMs-like phenotype (Mo-TAMs). We performed gene expression analysis by RT-PCR and we tested Mo-TAMs activity by evaluating tumor cell proliferation and spreading. Next, we analyzed the effect of prolonged EPZ-6438 treatment on monocytes recruitment into MSTO spheroids as well as on Mo-TAMs gene expression. We analyzed the functional impact of Mo-TAM on the anti-tumor effects due to EZH2 inhibition in MPM cells. Finally, we tested the susceptibility of MPM cells to the cytotoxic activity of M1-polarized monocytes in order to evaluate the potential synergistic effect of EPZ-6438 in combination with therapeutic strategies of TAMs re-programming in M1 effectors.

Graphical Abstract

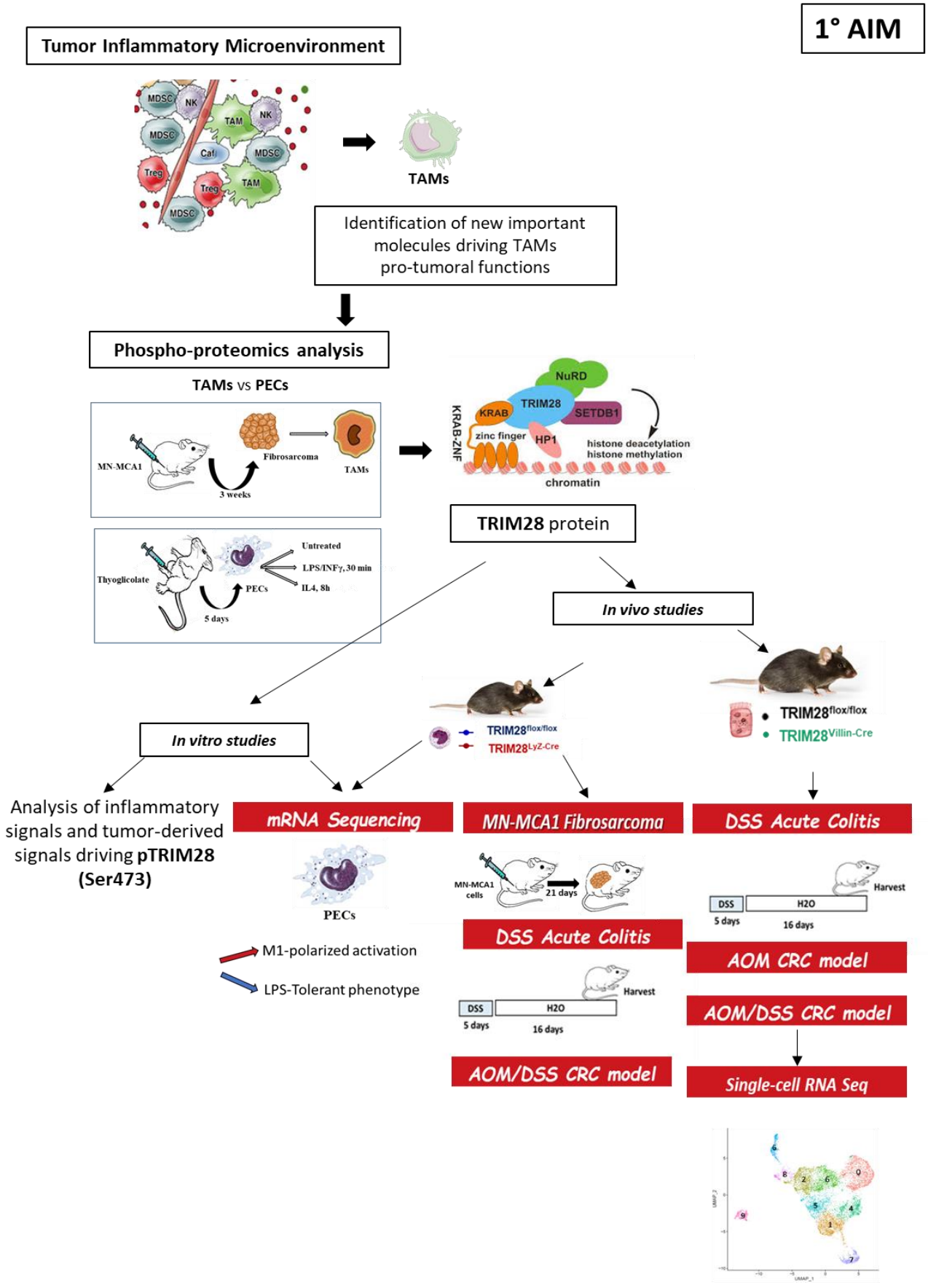

Treatments in Clinical Oncology

2° AIM

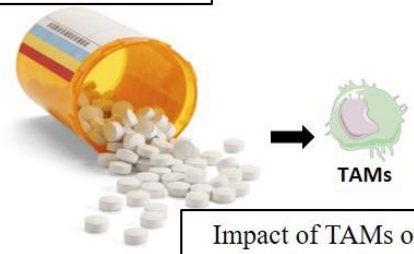

TAMs

Impact of TAMs on Malignant pleural mesothelioma therapy

EPIGENETIC targets

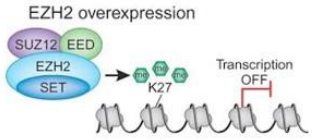

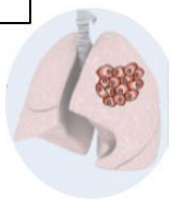

- **EZH2 inhibitors**

EPZ-6438

3D MPM-monocytes spheroid model

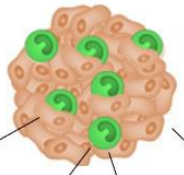

Effect of EPZ-6438 on:
- **tumor cell proliferation**
- **Expression of monocyte chemoattractants**
- **Recruitment of monocytes**

- **Monocyte recruitment**
- **Macrophage differentiation**
- **Functional polarized activation (Mo-TAM)**

Impact of monocytes on tumor cell response to EPZ-6438-treatment

Effect of EPZ-6438 on
- **Monocyte responsiveness to M1 (LPS) and M2 (IL-4, IL-10) polarized signals**
- **Mo-TAM phenotype**

- **Tumor cell proliferation**
- **Tumor cell spreading**

CHAPTER 1

TRIM28 is a novel regulator in cancer-related inflammation.

Silvia Mola[1,2], Valentina Garlatti[1], Alessandro Ippolito[1], Lorenzo Carraro[1], Francesca Maria Consonni[1], Alberto Termanini[3], Giulia Soldà[3], Javier Cibella[3], Gabriela Grigorean[4], Clelia Peano[3], Paolo Kunderfranco[3], Roberta Carriero[3], Chiara Porta[1,2] and Antonio Sica[1,3].

[1]Department of Pharmaceutical Sciences, Università del Piemonte Orientale "Amedeo Avogadro", Novara, Italy.

[2]Center for Translational Research on Autoimmune & Allergic Diseases (CAAD), Università del Piemonte Orientale "Amedeo Avogadro", Novara, Italy

[3]Humanitas Clinical and Research Center – IRCCS -, Rozzano (MI) – Italy

[4] IFOM, Fondazione Istituto FIRC di Oncologia Molecolare, 20139 Milan, Italy.

Unpublished Data

Abstract

Tumor-associated macrophages (TAMs) are key components of the inflammatory tumor microenvironment (TME) supporting tumor development, growth and progression. Over the last years, the therapeutic value of macrophage-targeting approaches has been successfully proven in small cohorts of cancer patients. This evidence supports new studies to gather the molecular pathways underlying the pro-tumoral activities of TAMs.

To identify new molecular players of TAM pro-tumoral activities we analyzed the alterations of the phospho-proteoma of TAMs isolated from murine MN/MCA1 fibrosarcoma, as compared to resting (ctr), M1 (IFNγ/LPS, 30 min) and M2 (IL-4, 8 hours) polarized macrophages. We originally found the phosphorylation of Tripartite motif-containing 28 (TRIM28) at Ser473 (TRIM28 S473p) in both M1-polarized PECs and TAMs. TRIM28 is a member of the Kruppel-Associated-Box Proteins that participates in the dynamic organization of chromatin and is involved in multiple cellular activities.

We found that different pro-inflammatory signals, including cytokines (TNFα, IL-1, IL-6) and microbial products (ligands of TLR4, 2 and 5) induce a transient TRIM28 S473p, via the MyD88-p38 dependent pathway, whereas selected immunomodulatory mediators (IL-10, PGE2) trigger a mild, but long-lasting TRIM28 S473p.

We explored *in vivo*, the functional relevance of myeloid TRIM28 by studying mice the lack the protein in myeloid cells ($TRIM28^{LysM\text{-}Cre}$) and we found that the total absence of TRIM28 in myeloid cells does not affect the pro-tumoral activities of TAMs in fibrosarcoma model nor tumor multiplicity in colitis-associated cancer (CAC) model but exacerbated colitis. Accordingly, RNA-seq analysis indicates that TRIM28 modulates macrophage response to both short and prolonged LPS treatment by affecting the expression of selected gene transcriptional programs associated to activation of adaptive immunity, cell metabolism and oxidative stress response, including DNA damage response. Noteworthy, lack of TRIM28 in intestinal epithelial cells (IECs) confers resistance to CAC, using a single cell RNAseq approach we provide data suggesting that TRIM28 in IEC impact on immune cells composition during the transition from colitis to cancer along with mild effects on the expansion of neoplastic cells with an EMT^{high} gene signature and accumulation of Goblet and Paneth cells under colitis stage. Overall, these results identify TRIM28 as a new molecular target at the crossroads between inflammation and cancer.

Introduction

Although the existence of a functional link between chronic inflammation and cancer has been suggested in the 19th century, the importance of inflammation in the pathogenesis of cancer has only been proven in the last two decades[1–3]. Nowadays, it has been estimated that up to 20% of all human cancers are causally associated with chronic inflammation[4].

Several studies have shed light on the molecular and cellular inflammatory circuits that support tumor development. Myeloid cells are an important source of reactive oxygen species (ROS) and reactive nitrogen intermediates (RNI)-that favor DNA mutations[5]. Several inflammatory cytokines (e.g., IL-6, IL-1, IL-23, IL-17A) can directly promote neoplastic cells survival, proliferation and genomic instability, through the activation of the transcription factors NF-κB and STAT3[6,7], as well as the inhibition of p53 activity[8,9].

Nevertheless, inflammatory response, supported by innate immune cells, is also crucial for the activation of an adaptive immune response (e.g., IL-12, IFNγ) capable to eliminate nascent tumors[2]. Although immune cells continuously recognize and destroy nascent tumor cells, the genetically unstable neoplastic cells are able to evade immune surveillance by selecting new variants of transformed cells, characterized by their loss of antigenicity and immunogenicity, consequently generating an immunosuppressive microenvironment that is fundamental for tumor formation and advancement (*immuno-editing)*[1,3].

Tumor associated macrophages (TAMs) represent the major component of the tumor microenvironment (TME) and the crucial orchestrator of tumor-promoting inflammation[10].

Macrophages are characterized by high heterogeneity and plasticity, namely the capacity to express different programs of polarized activation in response to the dynamic change of microenvironmental signals. Macrophage plasticity, *in vivo*, emerges as a continuum of different functional states of polarized activation, ranging from the pro-inflammatory and anti-tumor M1-phenotype to the immunosuppressive and pro-healing M2- phenotype[11].

Cytokines such as IFN-γ and tumor necrosis factor-α (TNF-α), predominantly secreted by Th1 cells, activate macrophages towards a classic M1 phenotype, instead, Th2 (IL-4) and immunosuppressive (IL-10) cytokines promote the expression of alternative M2-skewed programs[12–14]. Despite their potential cytotoxic activities, in many established cancers, the most of macrophages acquire an M2-skewed phenotype devoid of cytotoxic activity and endowed of immunosuppressive and pro-healing properties[15–17].

Therefore, a growing number of clinical studies have confirmed TAMs as prognostic indicators of cancer progression[17,18] and as promising therapeutic targets[10]. Indeed, over the last years, the

therapeutic value of macrophage-targeting approaches has been successfully proven in small cohorts of cancer patients. This evidence supports new studies to gather the molecular players underlying the pro-tumoral activities of TAMs.

In agreement with previous findings in established tumors[19], we have recently reported that progressive nuclear accumulation of p50 NF-κB in macrophages during intestinal tumor development drives tumor-promoting reprogramming of colorectal cancer–associated inflammation[20]. Here we started by the analysis of the alterations of the phospho-proteoma of TAMs isolated from murine MN/MCA1 fibrosarcoma to find new molecular players of TAMs pro-tumoral activities.

We identified Tripartite motif containing 28 (TRIM28) TRIM28, a pleiotropic protein that participates in the dynamic organization of chromatin and regulates numerous different processes including gene expression, DNA repair, pluripotency, proliferation, differentiation and cell survival. Then, we focused on the role of TRIM28 on both macrophage activation and inflammation-driven cancer.

Materials and Methods

Mice

Wild type mice (C57BL6J) mice were purchase from Charles River Laboratories (Calco, Italy), B6.Cg-Tg(Vil1-cre)997Gum/J (*Villin-Cre*) mice and B6.129P2-Lyz2tm1(cre)Ifo/J (*LysM-Cre*) mice were from Jackson Laboratories (Bar Harbor, Maine, USA), and *TRIM28*$^{flox/flox}$ mice, (on a C57BL6J background strain), were from the laboratory of Professor G. Carl Huber (University of Michigan Medical School, Dept. of Cell & Developmental Biology).

TRIM28 $^{flox/flox}$ mice were crossed with *LysM-Cre* mice or with *Villin-Cre* mice, to generate mice with specific deletion of TRIM28 in macrophages (M$\phi^{\Delta TRIM28}$) or in intestinal epithelial cells (IEC) of the small and large intestines (IEC$^{\Delta TRIM28}$).

Myd88 knock-out mice were from Professor Francesca Granucci, (University of Milano-Bicocca, Milan, Italy).

In all experiments male mice with 8-10 weeks of age were used.

Mice are maintained in transparent cages of plexiglas with a litter of corn cobs de-dusted, to absorb droppings. Standard conditions of temperature (24±2°C), humidity (60±5%) and illumination (12 hours light, 12 hours dark) were applied. During experimental period, mice had free access to water and feed. They were monitored daily, and euthanized when displayed excessive discomfort. The study was designed in compliance with: Italian Governing Law (Legislative Decree 116 of Jan. 27, 1992); EU directives and guidelines (EEC Council Directive 86/609, OJ L 358, 12/12/1986); Legislative Decree September 19, 1994, n. 626 (89/391/CEE, 89/654/CEE, 89/655/CEE, 89/656/CEE, 90/269/CEE, 90/270/CEE, 90/394/CEE, 90/679/CEE); the NIH Guide for the Care and Use of Laboratory Animals (1996 edition); The study was approved by the The Ethics Committee for Animal Experimentation - C.E.S.A.P.O. University of Piemonte Orientale " A. Avogadro " and by Ministry of Health, Italy.

Genotyping of mice was performed by PCR using the following primers, for *LysM-Cre* mice: P1 (common primer) 5′-CCC AGA AAT GCC AGA TTA CG-3′, P2 (mutant primer) 5’-CTT GGG CTG CCA GAA TTT CTC-3’ and P3 (WT primer) 5’-TTA CAG TCG GCC AGG CTG AC-3’. Thermic profile: 94° 3min (1 cycle), 94° 30s, 62° 1min, 72° 1min, 72° 2min (30 cycles) and 10° for the rest of time. Wild type mice give an amplicon of 350 bp, an additional product of 700bp indicates the presence of mutant (*LysM-Cre)* allele.

For *Villin-Cre* mice: IMR1878: 5’-GTG TGG GAC AGA GAA CAA ACC-3’, IMR1879: 5’-ACA TCT TCA GGT TCT GCG GG-3’, IMR8744: 5’-CAA ATG TTG CTT GTC TGG TG-

3' and IMR8745: 5'-GTC AGT CGA GTG CAC AGT TT-3'. Thermic profile: 94° 3min (1 cycle), 94° 30s, 64° 1min, 72° 1,5min, 72° 3min (35 cycles) and 10° for the rest of time. PCR gives rise to an amplicon of 200 bp as internal control and of 1100bp if the transgene (*Villin-Cre*) is present. For *TRIM28*$^{flox/flox}$ mice: YD208 (WT primer) 5'-GGA ATG GTT CAT TGG TG-3', VR211 (Flox primer) 5'-ACC TTG GCC CAT TTA TTG ATA AAG-3' and TV210 (Flox primer): 5'-GCG AGC ACG AAT CAA GGT CAG-3'. Thermic profile: 94° 3min (1 cycle), 94° 30s, 55° 30s, 72° 1 min, 72° 7min (30 cycles) and 10° for the rest of time. A PCR product of 152 bp is representative of WT DNA, while a 180bp amplicon identifies the *TRIM28*$^{flox/flox}$ allele.

Purification of Peritoneal Exudate Macrophages (PECs)

WT C57BL6J, TRIM28$^{LysM-Cre}$ and *TRIM28*$^{flox/flox}$ mice were injected intra-peritoneum (i.p.) with 1ml of 3% (wt/vol) thioglycollate medium. 5 days after injection, mice were sacrificed and PECs were collected by washing the peritoneal cavity with saline solution. PECs were centrifuged at 1200 rpm, 4°, 8 min; the supernatant was discarded and the cells were re-suspended in saline solution. Cells were pelleted again (1000rpm, 4°C, 10 min), resuspended in RPMI 1640 supplemented with 1% L-Glutamine and 1% penicillin-streptomycin (incomplete RPMI) and counted with Turk solution. PECs were seeded in plates ($8x10^6$ cells in 100 mm Petri dish) and incubated at 37°C and 5% of CO_2. After 1h, cells were vigorously washed with saline to eliminate non-adherent cells. Macrophages were cultured in RPMI 1640 supplemented with 1% L-Glutamine and 1% penicillin-streptomycin and 10% of FBS (complete RPMI). After at least 1h of recover, PECs were stimulated as following indicated.

Purification of Tumor Associated Macrophages (TAMs)

TAMs were purified from murine solid tumor fibrosarcoma. Tumor cells were injected intra-muscle (i.m.) at a concentration of 10^5 cell/mice in the left leg, 21 days later tumors reached a volume of about 2 cm^3, mice were euthanized and tumors were harvested. Each tumor was cut in small pieces (avoid necrotic zone and blood vessels) and washed with saline solution. To get a single cell suspension, tumor pieces were put in a bottle containing a PBS solution with 0,125% trypsin endotoxin-free, (20-40 ml/tumor) and incubated at 37°C for 30-40min, in a stirring way. Next, FBS (1/5 of the total volume) was added to inactivate trypsin, cell suspension was filtered with a sterile gauge and centrifuged at 1000 rpm, 10 min. Cells were re-suspended in incomplete RPMI 1640, diluted with 10% Trypan Blue (diluted 1:10, *Sigma*) and counted. Cell suspension was seeded in incomplete RPMI ($20x10^6$ cells in 100 mm Petri dish), and incubated at 37°C, 5% of CO_2, for 1 hour. Then, cells were vigorously washed with

saline, in order to eliminate non-adherent cells, and complete RPMI medium was added. After 1 hour in incubator for recovering, TAMs were treated as following described.

Isolation of Human Monocytes

Monocytes were obtained from buffy coats of healthy donors. Blood was washed once with saline at 1000 rpm to remove plasma and platelets, and then centrifuged on Ficoll (*GE Health Care*) at 2200, RT, 30 min (brake free). Peripheral blood mononuclear cells were collected at the interface. Then, after two washes with saline, monocytes were purified by fractionation on a one-step discontinuous Percoll (*GE Health Care*) gradient. Cells obtained from Ficoll gradient were washed twice in saline and suspended in isoosmotic complete RPMI 1640 medium. The Percoll solution was prepared by mixing 9.25 parts of concentrated Percoll and 0.75 parts of PBS; (the osmolarity of this solution was adjusted to 285 mOsm). Cell suspension was carefully layered on the top of the 46% Percoll solution; tubes were centrifuged at 2000 rpm, RT, 30 min. Monocytes were recovered at the interface, washed twice in saline and resuspended at $5*10^6$ cells/ml in RPMI 1640 medium supplemented with 1% FBS, plated and left 1 hour in incubator, after they were washed with saline and cultured in complete medium until treatment.

Cell culture and reagents

PECs and TAMs were cultured in RPMI 1640 (Lonza), with 10% foetal bovine serum (*Lonza*), L-Glutamine (2mM, *Lonza*), and penicillin-streptomycin (100U/ml, *Lonza*).

Lipopolysaccharide from Salmonella abortus equi S-form (LPS, 10ng/ml), PAM_3CSK_4 (2μg/ml), Flagellin (100ng/ml), Loxoribine (100μM) and Poly I-C (10μg/ml) were purchased from *Enzo Life Sciences*. Oligodeoxynucleotide with CpG_{1826} (1μg/ml) sequence (5'-tccatgagcttcctgagctt-3), was produced by MWG-biotech (*M-Medical s.r.l.*).

Cytokines (IL-1, IL-4, IL-6, IL-10, IFNγ, PGE2 and TNFα, 20ng/ml) were acquired from *Peprotech*.

Wortmannin (100nM), a PI3Ks inhibitor, and p38 MAPK inhibitor (SB202190, 10μM) were purchased from *Sigma-Aldrich.*

PHOSPHOPROTEOMIC ANALYSIS OF TAMs AND POLARIZED PECs

The phospho-proteoma of TAMs isolated from murine fibrosarcoma (MN/MCA1) was analysed in comparison to naïve (untreated), classic (M1) and alternative (M2) polarized macrophages (PECs).

To get M1 polarized PECs, cells were stimulated with LPS (100ng/ml) and IFNγ (200U/ml) for 30 minutes, whereas for M2 activation, PECs were treated with IL-4 (20ng/ml) for 8 hours.

Protein extraction

After the indicated treatments, cells were washed twice with ice-cold PBS 1X, then lysed with 300µL/Petri of Lysis Buffer (25mM Tris-HCl, pH8; 75mM NaCl; 2,5mM EGTA, pH 8; 0,75mM $MgCl_2$; 10% Glycerol [vol/vol]; 1% Tryton X-100 [vol/vol]; 50mM NaF, 10mM NaPP, 10mM Na_3VO_4; 100µg/ml PMSF, Cocktail α-protease 1X). After 20 minutes of incubation on ice the cell lysates were collected in eppendorf and centrifuged (at 4°C, 13000 rpm, 20 min) to eliminate cell debrises. Supernatants (protein extracts) were transferred in new tube and stored at -80°C. Protein extracts were quantified with Comassie brilliant blue assay kit (*Thermo Scientific).* 300µg of each protein extracts were precipitated with 6 volume of acetone, and incubated o.n. at -20°C. After this period, the samples were centrifuged at 13000 rpm, 10 min; the supernatant was discarded and the pellet was air dried for 30 minutes. At the end, samples were stored at -80°C.

Phosphorylation maps

To generate the phosphorylation map of the different samples we took advantage of the iTRAQ technique (Isobaric tags for relative and absolute quantitation). This method was based on the covalent labelling of the N-terminus and sidechain amines of peptides from protein digestions with tags of varying mass. Our reagent, the 4-plex iTRAQ, could be used to label all peptides from 4 different samples/treatments. These samples were then pooled and fractionated by nano liquid chromatography. From all fractions, phosphopeptides were enriched on TiO_2 beads in the presence of 2,5-dihydrobenzoic acid and analyzed by tandem mass spectrometry (MS/MS). The relative abundance (ratio) of the peptides was defined by measuring the low molecular mass reporter ions generated by the fragmentation of the attached tag. Next, fragmentation data were in silico analyzed to identify the labelled phospho-peptides, hence the corresponding proteins. Next, by using the Ingenuity Pathways Analysis (IPA) software maps of protein-protein interaction was created.

Immunostaining and Confocal Microscopy Analysis

Cryostat tumor sections (from murine fibrosarcoma) of 8 μm were fixed in PFA 4% for 15 min. Endogenous peroxidises were blocked with 2-3% H_2O_2 (40%) in H_2O, for 5 minutes. Unspecific binding sites were blocked with BSA 2% + Triton 100X 0,1%, in PBS+/+ Tween20 (0,05%), for 1hour. Immunostaining was carried out with rat anti-mouse CD3 (#A0452, *DAKO*), rat anti-mouse F4/80 (clone CI:A3-1, *AbD Serotec*), rat anti-mouse Ly6G (clone 1A8 BD), rabbit anti-mouse KAP1 (clone: 10484, *Abcam*, 1:500) and rabbit anti-mouse P-KAP1 (clone: EPR5249, *Epitomics*, 1:700), for 1 hour. Goat anti-rat AlexaFluor 488 conjugated and donkey anti-rabbit AlexaFluor 647 conjugated were used as secondary antibodies.

Nuclei were stained with DAPI (4',6-diamidino-2-phenylindole) (#D1306, *Life Technologies*) and then mounted with ProLong Antifade Gold Reagent (P-36931, *Life Technologies*). Slides were analyzed with Olympus Fluoview FV1000 laser scanning confocal microscope with 60X (N.A.0.4).

FACS ANALYSIS

$5x10^5$ and $1x10^6$ cells were used for staining extra- and intra-cellular antigens respectively. Staining was performed in FACS buffer at 4°C for 20 minutes, with the following antibodies: FITC anti-mouse LY6C (clone 1A8, *Miltenyi*), PE anti-mouse Ly6G (clone1G7-10G, *Miltenyi*), APC anti-mouse CD11b (clone M1/70, *Biolegend*), and PerCP-Cy5.5 anti-mouse CD45 (clone 30-F11, *Biolegend*), Alexa488 anti mouse CD8a (clone 53-6.7, *Biolegend*), PE anti-mouse CD4 (clone GK 1.5, *Biolegend*) and APC anti-mouse INF-γ/Isotype (clone XMG 1.2, *Biolegend*) FITC anti-mouse CD11b (clone M1/70, *Pharmigen*), PE anti-mouse F4/80 (clone BM8, *Biolegend*), APC anti-mouse Ki-67 (clone 16A8, *Biolegend*).

For intracellular staining (INF-γ, Ki-67) Cytofix/Cytoperm and PermWash staining kit (*Pharmigen)* were used according to the manufacturer's protocol. Cells were detected using the BD FACS Canto cytofluorimeter and analyzed with Flowjo Software.

Western Blot (WB) Analysis

30 μg total of proteins were separated on 7.5% SDS-PAGE under reducing conditions and transferred onto nitrocellulose membrane. Membrane was incubated at RT, with 5% nonfat dry milk (*Applichem*) or 5%BSA (*Sigma*) in TBST (50mM Tris, 150mM NaCl, 0,1% Tween) to saturate non-specific binding sites. After 1 hour of blocking, membrane was incubated with the primary antibody solution at 4°C, o.n. Next, the membrane was washed with TBST for 10 minutes at RT (three times) and incubated with the HRP-conjugated secondary antibodies solution. After 1 hour at RT, membrane was washed three times for 10 minutes with TBST. Finally,

chemiluminescence substrate (ECL, *Biorad*) was added and signals were detected at trans-illuminator Chemidoc (*Biorad*).

List of primary antibodies and conditions of use: pTRIM28 Ser 473, (Clone: EPR5249, EPITOMICS), dilution 1:50000, 5% BSA, 4°C, o/n; TRIM28 (ab 10484, *Abcam*), diluition 1:1000, 5% milk, 4°C, o/n; p-AKT (*Cell Signaling*), dilution 1:1000, 5% BSA, 4°C, o/n; IKB-α, dilution 1:1000), 5% milk, 4°C, o/n; : p-STAT6 (*Cell Signaling*) dilution 1:1000, in BSA 5%, o/n, 4°C; Actin (*Sigma-Aldrich*), dilution 1:10000, 5% milk, RT, 1 hour.

List secondary antibodies: Goat- α-Rabbit-HRP-coniugated (7074S, *Cell Signaling*) and Goat-α-Mouse-HRP-coniugated (7076S, *Cell Signaling*); dilution 1:5000, RT, 1 hour.

Total RNA extraction

RNA was extracted according to the manufacturer's instructions of *RNeasy Mini Kit* (*Qiagen*). RNA was quantified by using *Nanodrop* spectrophotometer. RNA quality was assessed as 260/280 and 260/230 OD ratio >1.5. 2 μg of RNA was reverse transcribed by the Script Advanced icDNA Synthesis Kit (*Biorad*), and then 4ul of diluted CDNA (ratio 1:5) was used as a template for SYBER Green Master Mix (*Biorad*) and detected by the CFX96 Real-Time System (*BioRad*). All samples were run in triplicate. Expression data were normalized to Actin housekeeping mRNA and were analyzed by the $2^{-(\Delta Ct)}$ method. Results are expressed or as $2^{-(\Delta Ct)}$ or as fold upregulation respect to the control cell population. The sequences of gene-specific were designed by using https://www.ncbi.nlm.nih.gov/tools/primer-blast/. The primers are synthetized by *Sigma-Aldrich* and their list is reported in Supplementary Table S1.

RNAseq

Peritoneal macrophages (PEC) were isolated from TRIM28$^{LysM\text{-}Cre}$ and *TRIM28*$^{flox/flox}$ mice after 5 day of i.p. injection with 1ml of 3% thioglycolate solution (ref). Cells were left untreated, activated by 4 hour of LPS (100ng/ml) (ditta) treatment (LPS) or tolerized by (L/L) by 20 hours of LPS treatment.For each condition, experiments were performed in duplicate, for a total of 12 samples. Total RNA was extracted *RNeasy Mini Kit* (*Qiagen*) according to the manufacturer's instructions RNA quality was assessed on an Agilent 4200 TapeStation, obtaining a mean RNA integrity number (RIN) of 6.4 (max: 7.4, min 4.9). Libraries were prepared starting from 500 ng of total RNA with the SMARTer® Stranded Total RNA Sample Prep Kit - HI Mammalian Clontech-Takara), following the manufacturer's instructions. Libraries were sequenced as 76-bp paired-end reads on a NextSeq550 platform (Illumina). Reads were mapped to the UCSC mm10 reference genome and to the *Mus Musculus* transcriptome [Illumina's iGenomes reference

annotation, *http://support.illumina.com/sequencing/sequencing_software/igenome.html*] with Star v.2.7.1a[21], and gene count tables generated using htseq v.0.11.2[22]. Quality control (QC) was performed on raw data (.fastq files) using FastQC v.0.11.8[23], and on aligned data (.bam files) using RSeQC v.2.6.4[24]. The final QC report was generated with MultiQC v.1.7[25], by aggregating the results and statistics obtained with multiple tools (FastQC, STAR, htseq, RSeQC). Differential gene expression was performed using pairwise comparisons between experimental groups with the DeSeq2 Bioconductor package[26], using a Wald test to assess statistical significance of the observed fold change differences. Differentially expressed (DE) genes were selected using a false discovery rate (FDR) of ≤0.01, and a log2 fold change of ≥1 or ≤ -1. Gene set enrichment analyses were performed using the TopGo Bioconductor package [https://bioconductor.org/packages/release/bioc/html/topGO.html] as well as Metascape [27] with default parameters, independently on upregulated and downregulated genes.

MN/MCA1 Fibrosarcoma

TRIM28$^{LysM\text{-}Cre}$ and *TRIM28*$^{flox/flox}$ were injected intra-muscle in the left hind limb with 10^5 MN/MCA1 cells. Starting from the 14th day, tumor growth was monitored three times a week by measuring tumor volume with a calliper. Since MN/MCA1 fibrosarcoma metastasise to the lungs, when tumor reached a volume of about 2.5 cm (about 21th day), mice were sacrificed, tumors were weighted and lung metastases were counted. To isolate TAMs, tumors were disaggregated as described above. Further, tumors and spleens were analysed for the composition of infiltrated immune cells by Fluorescence-activated cell sorting (FACS) analysis. To this aim, each tumor was disaggregated at 37°C, for 20 minutes in a solution of 0,5mg/ml collagenase, in incomplete RPMI. Next, the collagenase activity was blocked by adding EDTA to a final concentration of 10mM. Tumors pieces were smashed by pipetting up and down with a Pasteur pipette. Next, cell suspension was diluted with 10-20 ml of PBS 1X and filtered through a sterile gauge. Cell suspension was filtered again on a 70µm cell strainer and centrifuged at 1000 rpm, for 10 minutes. Cells were re-suspended in FACS buffer (HBSS with 1% FBS) and counted.

Spleens were smashed on a 70µm cell strainer in complete RPMI, and centrifuge at 1200 rpm, for 8 minutes. To eliminate erythrocytes, cells were resuspended with ACK buffer lysis (*Lonza*) (2ml/spleen) and kept at RT for 5 minutes. Cells were centrifuged (at 1200 rpm, for 8 minutes), re-suspended in FACS buffer and counted. To evaluate the level of INF-γ produced by CD4 and CD8 cells, $1x10^6$ splenocytes were re-suspended in complete RPMI medium and activated with PMA+Ionomycin for 4 hours.

Dextran Sodium Sulphate (DSS) - induced acute colitis

To induce acute colitis, 8- to 10-week-old mice (*TRIM28*$^{LysM\text{-}Cre}$, TRIM28$^{Villin\text{-}Cre}$ and *TRIM28* $^{flox/flox}$ littermates), were treated with1.5% dextran sodium sulphate (DSS, MP Biomedicals, molecular mass: 40 kDa) in drinking water for 5 days, followed by 2 weeks of tap water. To evaluate colitis mice were daily monitored for body weight. Mice were euthanized if they showed signs (visible rectal bleeding or a 25-30% decreased of initial body weight) of excessive discomfort. Mice were sacrificed or at day 8, (acute phase of colitis) or at 18th day, (recovery). Colon were harvested and measured. The extent of colon shortening reflects the degree of inflammation.

Azoxymethane (AOM)/DSS AOM-CRC model

To recapitulate IBD-associated CRC, 10- to 12-week-old mice were injected intra-peritoneal (i.p.) with a single dose (10 mg/kg of body weight) of the mutagenic agent azoxymethane (Sigma). Five days later, mice received water with 1.2-1.5% dextran sodium sulfate for 5 days, separated by 16 days of tap water. This cycle of DSS treatment was repeated two more times. After 3 months of AOM/DSS treatment, mice develop multiple colonic tumors. During DSS treatment, the clinical course of colitis was evaluated by monitoring mice body weight[28].

AOM-CRC model

To reproduce sporadic CRC, mice were i.p. injected with AOM (10mg/kg of body weight), once a week for 6 weeks. After 6 months mice developed multiple visible colonic polyps[29].
At the time of harvest, mice were euthanized, colons were resected, flushed with saline solution, opened longitudinally, and macroscopically evaluated for tumor numbers.

Single-Cell RNA-Seq

Sample preparation

Single-cells RNAseq was performed on 8895 Intestinal Epithelial Cells (IECs, Epcam^{+}-CD45$^{-/+}$) and on 32944 immune cells (Epcam^{-}-CD45^{+}) derived from the entire colon tissues or the tumor lesions of 2 mouse strains (TRIM28^{VillinCre} and *TRIM28*$^{flox/flox}$ mice). For each strain, 2 different conditions were analyzed: the acute phase of colitis (at the 1st DSS cycle) and during tumor development 3 weeks after the last cycle of DSS. For each condition, experiments were performed in duplicate, for a total of 12 samples.
Colon were longitudinally cut and washed with PBS to remove feces and debris. Colon tissues (in 1st analysis) or tumors (in 2nd analysis) were sliced into small fragments roughly 2 mm long. and incubated under rotation (speed 35-40) in HBSS (w/o Ca^{2+}/Mg^{2+}) containing 5% FBS, 10

mmol/L HEPES, 2.5 mmol/L EDTA for 20 minutes at 37°C (twice). Tissues were collected and washed in HBSS medium containing 5mM $CaCl_2$ and then finely minced and incubated under rotation in HBSS containing 5% FBS, 10 mmol/L HEPES, 5mM $CaCl_2$, dispase/collagenase (1 mg/mL; Roche), collagenase IV (250 μg/mL; Serva), and DNAse (40 μg/mL; Roche) for 20 minutes at 37°C.

The single cell suspension was then passed through a through a 100-μm and 70-μm cell strainers and centrifuged 1450rpm, 4°, 6 min.

10 million cells/group were stained in 0.5% FBS, HBSS solution with anti-mouse CD45 (FITC, clone 30-F11, *Biolegend*), anti-Epcam (ApC-eFluor 780, Clone G88, *Invitrogen*), in the presence of LIVE/DEAD (Pacific Blue, *Invitrogen*) to evaluate cell viability. $CD45^+$ cells and $Epcam^+$ cells were collected after sorting (BD FACSAria™ Fusion sorter). Cells were resuspended in 1ml PBS plus 0.04% BSA and washed two times by centrifugation at 450 rcf for 7min. After the second wash cells were resuspended in 30 ul and counted with an automatic cell counter (Countess II, Thermo Fisher) to get a precise estimation of total number of cells recovered.

Afterwards cells, mixed following this ratio 70% $CD45^+$-$Epcam^-$ cells + 30% $Epcam^+$- $CD45^{+/-}$ cells, for each sample were loaded into one channel of the Single Cell Chip A using the Single Cell 3' v2 single cell reagent kit (10X Genomics) for Gel bead Emulsion generation into the Chromium system. Following capture and lysis, cDNA was synthesized and amplified for 14 cycles following the manufacturer's protocol (10X Genomics). 50 ng of the amplified cDNA were then used for each sample to construct Illumina sequencing libraries. Sequencing was performed on the NextSeq500 Illumina sequencing platform following 10x Genomics instruction for reads generation. A sequencing depth of at least ~ 50.000 reads/cell was obtained for each sample.

Data pre-processing and integration

Reads, derived from raw sequencing data, were aligned to the mm10 mouse genome with Cell Ranger v3.0.1[30] and count matrices were loaded with Seurat R package v3.0.1. Ribosomial genes and cells having less than 200 or more than 3000 expressed genes were removed. Data normalization was performed by applying the NormalizeData Seurat function (method = LogNormalize). Then, the "SCT" normalization[31] was performed on each sample, obtaining an integrated dataset consisting of 41,839 cells. A principal component analysis (PCA) was performed on the top variable features and the first 20 principal components (PCs) were selected for downstream analysis. The FindClusters Seurat function was used with different resolution values to identify cell clusters and their stability was assessed with the clustree R package

v.0.4[32]. A final clustering resolution of 0.1 was chosen, giving rise to a total of 11 clusters. Cluster marker genes were obtained using the FindAllMarkers Seurat function (FDR < 0.05). Reclustering of epithelial and immune cells was performed by repeating the same analysis to different subset of the whole dataset. Reclustering of epithelial cells was obtained considering the subsets of cells belonging to clusters number 3, 5, 8 and 10 (8,895 cells) and a clustering resolution of 0.4 was chosen. Reclustering of immune cells was obtained considering the subsets of cells belonging to the remaining clusters (32,944 cells) and a clustering resolution of 1.0 was selected.

To determine the cells frequency shift between experimental conditions the number of cells belonging to each cluster has been divided into the experimental groups, obtaining a table where each column corresponds to an experimental group and each row correspond to a cluster. Cells frequency were then obtained by using the prop.table R function (margin = 2). Both reclustering was considered separately. For epithelial cells, clusters 6, 8 and 9 were excluded from the counting process.

Statistical analysis

Statistical evaluation of the differential analysis was performed by one-way ANOVA and unpaired Student's *t*-test. (GraphPad Prism software). significance level was set at *p < 0.05, **p < 0.01 and ***p < 0.001.

Results

Tripartite motif-containing 28 (TRIM28) protein is new target of the inflammatory kinase signaling shared by TAMs and M1-polarized macrophages

Mass spectrometry-based phosphoproteomics is a powerful methodology for the study of kinase signaling, an essential process for cellular activity[33]. To investigate the molecular pathways underlying the TAMs pro-tumoral activities we analyzed the alterations of the phospho-proteoma of TAMs isolated from murine MN/MCA1 fibrosarcoma, as compared to resting (ctr), M1 (IFNγ/LPS, 30min) and M2 (IL-4, 8 hours) polarized macrophages (*Fig. 1A top*). The protein extracts were labeled with the 4-plex isobaric tags for relative and absolute quantitation (**iTRAQ**), then the combined and dried digests were subjected to phospho-peptide enrichment using Magnetic Titanium Dioxide Phosphopeptide Enrichment Kit and subsequently prepared for liquid chromatography-tandem mass spectrometry (LC-MS/MS) analysis. The relative abundance (ratio) of the peptides was defined by measuring the low molecular mass reporter ions generated by the fragmentation of the attached tag. Next, in silico analysis of the fragmentation data for peptide scoring, protein identification, and quantification were performed using MaxQuant software[34]. The results, representative of two biological replicates, showed a list of 24 proteins with the higher different levels of phosphorylation among the distinct populations of analyzed macrophages.

In particular, Tripartite motif-containing 28 (TRIM28) emerged as the protein with the highest levels of phosphorylation on Ser473 (S473p) in M1-polarized PECs and TAMs (*Fig.1 A down and Supplementary Fig.1 A-C*).

TRIM28, also known as KRAB (Kruppel-associated box)-associated protein (KAP1) or transcription intermediary factor 1β (TIF1β) is a member of the Kruppel-Associated-Box Proteins that participates in the dynamic organization of chromatin and is involved in multiple aspects of cellular physiology, including immunology, cancer biology, virology and embryo development [35,36].

TRIM28 biological activity is mainly regulated by post-translational modifications including sumoylation, ubiquitination and phosphorylation.

Western-blot analysis of a new set of biological samples confirmed high levels of TRIM28 S473p in both M1-polarized PECs and TAMs, along with a similar amount of total TRIM28 protein in all samples (*Fig. 1B*). Taken together, these results indicate that TRIM28 S473p is triggered in both M1-polarized PECs and TAMs, without any significant alteration of the total amount of protein.

To ascertain *in vivo*, the phosphorylation of TRIM28 S473 in TAMs, MN/MCA1 tumor sections were immunostained with anti-F4/80 along with anti-TRIM28 or anti-PhosphoTRIM28(Ser473) antibodies. Confocal microscopy analysis confirmed that almost all TAMs ($F4/80^+$ cells) express TRIM28 in its Ser473 phosphorylated form. Furthermore, we observed a significant amount of TRIM28 S473p in T-cells ($CD3^+$) and proliferating ($Ki67^+$) cells, which largely represent tumor cells. Overall, these results suggest that TRIM28 could play a role in tumor development by modulating both neoplastic cells activities and cancer-related inflammatory microenvironment.

NAME	DESCRIPTION	M1vsCTR	M2vsCTR	TAMvsCTR	M1vsM2	M1vsTAM	M2vsTAM	M2vsM1	TAMvsM1	TAMvsM2
TRIM28	tripartite motif containing 28	25.82		8.40	12.20		-9.26	-13.51		6.04
GPN1	GPN-loop GTPase 1	5.75	3.426			3.88			-5.92	
C16orf54	chromosome 16 open reading frame 54	2.78	2.499							
ARHGEF2	Rho/Rac guanine nucleotide exchange factor (GEF) 2	2.57			4.06			-4.52		
GALNT7	UDP-N-acetyl-alpha-D-galactosamine:polypeptide N-acetylgalactosaminyltransferase 7 (GalNAc-T7)	2.23	1.821	7.782		-5.46	-6.90		3.58	4.49
SRRM1	serine/arginine repetitive matrix 1	2.07	3.014							
APOBR	apolipoprotein B receptor	2.05			2.23		-8.33	-2.49		5.42
APBB1IP	amyloid beta (A4) precursor protein-binding, family B, member 1 interacting protein	-2.11			-2.28			2.05		
MINK1	misshapen-like kinase 1	-2.27		-22.7		6.39	9.43		-9.80	-14.49
KIF13B	kinesin family member 13B	-2.48								
SNX17	sorting nexin 17	-2.62	-2.262443	-8.40						
FCHO2	FCH domain only 2	-7.09	-3.030303		-2.39			2.15		
PDXDC1	pyridoxal-dependent decarboxylase domain containing 1		5.791	4.123	-3.61	-5.03		3.24	3.28	
ATXN2L	ataxin 2-like		-2.352941		3.75		-4.65	-4.17		3.02
AKAP13	A kinase (PRKA) anchor protein 13		-2.398082	-7.52	2.98	6.08		-3.32	-9.35	
STMN1	stathmin 1			4.56	1.99	-7.19	-7.94	-2.22	4.69	5.16
PAK2	p21 protein (Cdc42/Rac)-activated kinase 2			-1.73						
DOCK2	dedicator of cytokinesis 2			-2.27	-2.05	-1.12		1.84	-1.37	
AHNAK2	AHNAK nucleoprotein 2			-7.14			4.05			-6.25
SH3TC1	SH3 domain and tetratricopeptide repeats 1			-8.70		3.55	5.01		-5.43	-7.69
EVPL	envoplakin				2.41		-4.83	-2.68		3.13
LASP1	LIM and SH3 protein 1					3.20			-4.90	
C22orf28	chromosome 22 open reading frame 28					-4.27			2.79	
MYO9B	myosin IXB						2.89			-4.44

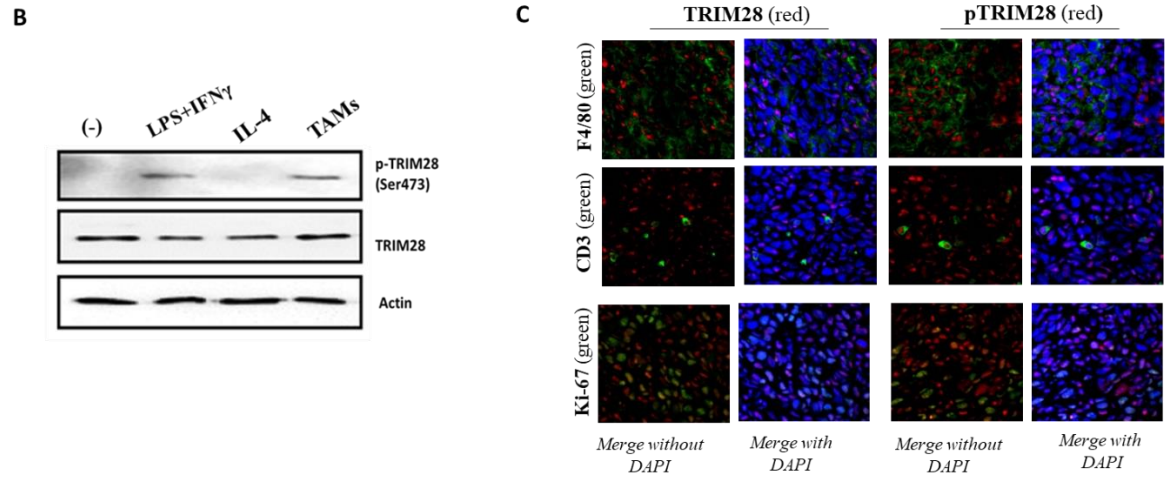

Figure 1. High levels of pTRIM28 Ser473 in M1-polarized macrophages and TAMs. (**A top**) Scheme of sample preparation for phosphoproteoma analysis: TAMs isolated from murine MN/MCA1 fibrosarcoma were compared to resting (CTR), M1 (IFNγ/LPS, 30 min) and M2 (IL-4, 8 hours) polarized macrophages**.** (**A down**) Selected proteins list defining the phosphoproteoma of TAMs as compared to naïve (CTR), M1 and M2-polarized macrophages. (**B**) Validation of the results of phospho-maps by Western Blot. PECs were left untreated (CTR) or stimulated with INFγ+LPS, for 30' (M1-polarized activation) or IL-4 for 8 hours (M2-polarized activation). TAMs were isolated from MN-MCA1 fibrosarcoma. Total proteins extracts were analyzed by Western blot for TRIM28 S473p and TRIM28. Actin was used as loading control. (**C**) Confocal microscopy analysis of TRIM28 (red) and pTRIM28 (red) in TAMs (F4/80$^+$ cells, green), T-cells (CD3$^+$ cells, green) and proliferative tumors cells (Ki-67$^+$ cells, green). The cell nuclei were counterstained with DAPI (blue). Magnification 60X.

Selected inflammatory cytokines and bacterial products trigger phosphorylation of TRIM28 at serine 473 residue through the MyD88/p38 dependent pathway

So far, phosphorylation on serine 473 (S473) has been reported in both physiological condition, such as during the late S phase of cell cycle, and in different stress setting including DNA damage[37], metabolic stress[38], viral infection[39] and T cell receptor activation[40,41]. Our results provide the first evidence that the combination of LPS and IFNγ triggers TRIM28 S473p in macrophages. To go insight the characterization of the inflammatory signals that could induce TRIM28 S473p, PECs were treated with both TLR ligands and inflammatory cytokines. Albeit we didn't observe any significant phosphorylation of TRIM28 in response to IFNγ, we confirmed TRIM28 S473p upon LPS treatment (Data not shown). Moreover, Western blot analysis showed that TNFα, IL-1β, and IL-6 activate phosphorylation of TRIM28 at Ser473 (*Fig. 2A*). Although cytokines were less potent than LPS, we observed a similar kinetic of TRIM28 S473p in response to all the M1-inducing signals (*Fig. 2A*), indicating that TRIM28 S473p is an early and transient event of the signaling cascade induced by both bacterial products and inflammatory cytokines. Beyond LPS (TLR4), we observed that either 2μg/ml PAM_3CSK_4 (TLR2) or 100ng/ml Flagellin (TLR5), were able to trigger high levels of TRIM28 S473p, whereas 10μg/ml Poly-IC (TLR3), 100μM Loxoribine (TLR7) and 1μg/ml CpG_{1826} (TLR9) didn't induce TRIM28 S473p (*Fig. 2B*). Activation of all TLRs was confirmed by IκBα degradation (*Fig. 2B*), therefore we can conclude that TRIM28 S473p is new molecular event of the plasma membrane TLR signaling cascade.

To go insight the molecular mechanisms driving TRIM28 S473 phosphorylation, we initially analyzed the impact of the adaptor protein MyD88, the first crucial molecule of the transduction pathway for all TLRs, except TLR3. PECs isolated from WT and Myd88 Knock-Out ($Myd88^{-/-}$) mice were treated with LPS for 15, 30 and 60 minutes and analyzed for TRIM28 S473p. WB showed that LPS-induced TRIM28 S473p was totally abrogated in $Myd88^{-/-}$ PECs, (*Fig. 2C*), thus demonstrating that phosphorylation of TRIM28 is under the control of the Myd88-dependent pathway.

TLR engagement activates different intracellular signaling pathways, including Phosphatidylinositol-3 kinase (PI3K)/ Akt pathway. Since in response to distinct DNA damage stimuli, PI3K-related kinases members ATM (ataxia telangiectasia mutated)/ATR (ataxia telangiectasia and Rad3 xrelated) induce TRIM28 S473p[42], we evaluated whether the PI3K/Akt signaling pathway could be involved in MyD88-dependent phosphorylation of TRIM28 at S473. To address this hypothesis, PECs were treated or not with an irreversible nonselective

inhibitor of the PI3K-related kinases members (Wortmannin, 100nM) for 1 hour. Next, medium was changed and cells were activated with LPS or PAM_3CSK_4 for 30 minutes, to induce TRIM28 S473p. WB analysis showed that both TLR agonists induced similar levels of TRIM28 S473p in cells pre-treated or not with Wortmannin (*Fig. 2D*). To confirm that Wortmannin blocks PI3K/Akt activation, we evaluated the levels of pAkt. As expected, pre-treatment of Wortmannin abrogated both LPS and PAM_3CSK_4 induced phosphorylation of Akt (*Fig.2D*). Therefore, we can conclude that TLR4 and TLR2-dependent TRIM28 S473p is independent on PI3K/Akt pathway.

Different studies have reported that TRIM28 S473p can be triggered by p38 MAPK[43]. In colorectal cancer cells, peroxide-induced p38 MAPK triggers phosphorylation of TRIM28 at S473, this event is associated with a more efficient DNA repair and tumor cell survival under oxidative stress conditions[43]. Infection of human lung epithelial cells by highly pathogenic avian influenza virus (HPAIV) strains result in PKR-mediated sensing of viral RNA and p38-MSK1-dependent TRIM28 S473 phosphorylation an event that leads to exacerbated inflammation and tissue damage[44]. The p38 MAK is also a key regulator of TLR-induced inflammatory gene expression[45,46]. Based on this evidence, we explored whether TLR dependent activation of p38 could control TRIM28 Ser473p in murine macrophages. PECs were preincubated with p38 inhibitor (SB 202190, 10 μM) for 30 minutes, and subsequently treated with LPS and PAM_3CSK_4 for 30 minutes. Western blot analysis demonstrates that p38 inhibition restrained both TLR2 and TLR4-induced TRIM28 S473p (*Figure 2E*) thus confirming p38 MAPK as a key kinase for the phosphorylation of TRIM28 at S473 under inflammatory condition

Collectively these results demonstrate that TRIM28 S473p is induced by different pro-inflammatory signals, including cytokines and microbial products, suggesting TRIM28 as a novel regulator of M1-polarized activation.

Selectively immunoregulatory M2-like signals induce TRIM28 (Ser473) phosphorylation.

To evaluate TRIM28 S473p in M2-skewed activation, PECs were treated with IL-4 for 0,5, 1, 2, 4 and 8 hours. According with phospho-proteomic analysis, we did not detect any TRIM28 S473p after 8 hours of IL-4 stimulation and we confirmed these results at earlier time points. (We used LPS treatment as positive control of TRIM28 S473p and Stat6 phosphorylation as read out of IL-4 treatment) (*Fig. 2F*). In the attempt to identify potential tumor-derived signals controlling TRIM28 S473p in TAMs, we tested immunoregulatory molecules (IL-10, PGE2) that we had found enriched in fibrosarcoma model[19,47]. WB analysis of IL-10 or PGE2 stimulated PECs showed that both immunomodulatory stimuli were able to induce TRIM S473p, with a lower potency than LPS but with a long lasting effect (*Fig. 2G*).

Finally, we evaluated whether bacterial products and cytokines were able to trigger phosphorylation of TRIM28 at S473 also in human monocytes. WB analysis confirmed TRIM28 S473p in human monocytes treated with LPS, TNFα and IL-10 for 30 minutes, indicating that our studies of TRIM28 in macrophage biology could have translational perspectives (*Fig.2H*).

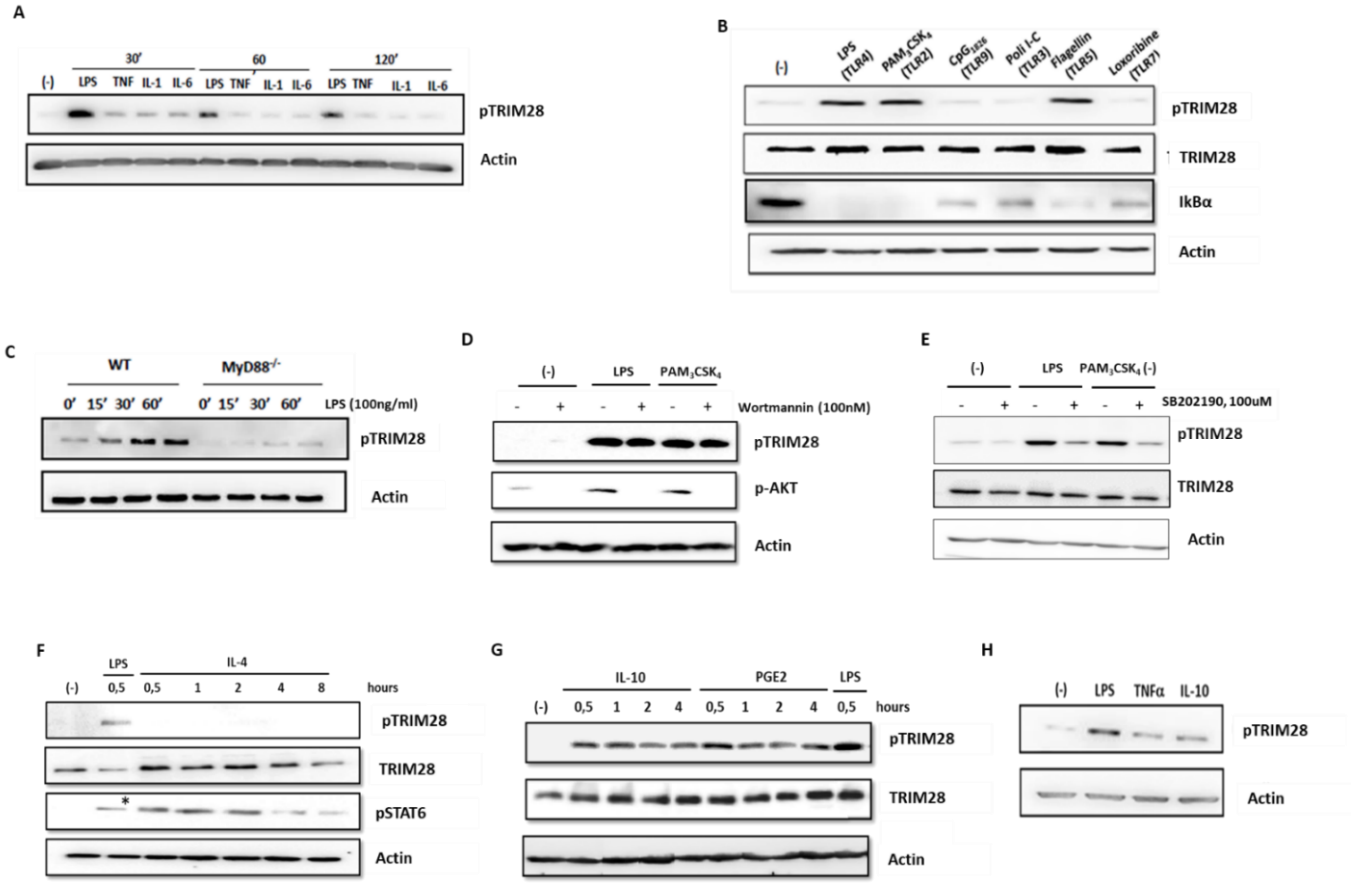

Figure 2. Both inflammatory cytokines and microbial products trigger TRIM28 S473p in PECs. (**A**) PECs were treated with TNFα (20ng/ml), IL-1b (20ng/ml), IL-6 (20ng/ml) and LPS (100ng/ml) for 30, 60, 120 minutes and were analysed for p-TRIM28 (ser473) levels by WB. Actin was used as sample loading control. (**B**) PECs were treated with 100ng/ml of LPS (TLR4), 2mg/ml of PAM_3CSK_4 (TLR2), 1mg/ml of CpG_{1826} (TLR9), 10mg/ml of PolyI-C (TLR3), 100ng/mL of Flagellin (TLR5) and 100mM of Loxoribine (TLR7) for 30 minutes and were analysed by WB for p-TRIM28(Ser473) and KAP1 levels. To verify TLR activation, membrane was immunoblotted with an anti-IκBα antibody. Actin was used as sample loading control.

LPS, PAM_3CSK_4 and Flagellin require Myd88 and p38 MAPK activation to induce TRIM28 Ser473p. (**C**) PECs from wild type (WT) and $Myd88^{-/-}$ mice were stimulated with LPS (100ng/ml) for 15, 30, 60 minutes and analysed for TRIM28 S473p by Western blot. (**D**) PECs were treated or not with Wortmannin, (100nM) for 1 hour. Next, medium was changed and cells were activated with LPS (100ng/ml) or PAM_3CSK_4 (2mg/ml) for 30 minutes. Protein extracts were analysed by Western blot. Membrane was immunoblotted with anti-pTRIM28 (Ser473) and anti-pAkt antibodies. Actin was used as sample loading control. (**E**) PECs were treated or not with p38 inhibitor (SB202190, 100μM), for 1 hour. Next, cells were activated with LPS (100ng/ml), PAM_3CSK_4 (2mg/ml) for 30 minutes. Protein extracts were analysed by Western blot. Membrane was immunoblotted with anti-pTRIM28 (Ser473) and anti-TRIM28 antibodies. Actin was used as sample loading control.

pTRIM28 are induced by selected immunoregulatory signals:(**E**) PECs were treated with IL-4 (20ng/ml) for 0,5, 1, 2, 4 and 8 hours. PECs activated with LPS (100ng/ml), were used as positive control of TRIM28 S473p. Protein extracts were analysed by WB for TRIM28 S473p. To verify IL-4 stimulation, membrane was followed immunoblotted with anti-pSTAT6 antibody. The band (*) detected in the LPS lane represents membrane bound anti-pTRIM28(Ser473) antibody. (**F**) Immunoblot analysis of TRIM28 S473p in IL-10 (20ng/ml) and PGE2 (10μM) treated PECs. Actin was used as sample loading control.

Inflammatory signals induce TRIM28 Ser473p in human monocytes:(**G**) Monocytes were isolated from peripheral blood of healthy donors (buffy-coat) and were stimulated with LPS (100ng/ml), TNFα (20ng/ml) and IL-10 (20ng/ml), for 30 minutes. Protein extracts were analysed by WB for TRIM28 S473p. Actin was used as sample loading control.

Lack of TRIM28 in myeloid cells worsens DSS-induced colitis.

To explore, *in vivo*, the functional relevance of myeloid TRIM28 in the context of cancer-related inflammation, we took advantage of *TRIM28*$^{flox/flox}$ mice to generate mice that lacks TRIM28 in myeloid cells (TRIM28$^{LysM\text{-}Cre}$).

We initially evaluated the impact of TRIM28 on TAMs activities in the fibrosarcoma model. TRIM28$^{LysM\text{-}Cre}$ and *TRIM28*$^{flox/flox}$ mice were injected with MN/MCA1 cells and monitored for fibrosarcoma growth and progression. Both tumor growth curve and lung metastasis formation were similar in the two groups of mice (*Fig. 3A*). Furthermore, FACS analysis of both primary tumor and spleen showed a similar expansion of myeloid cells (TAMs, M- and PMN-MDSC) in tumor bearing mice (Fig. *3B*) and RT-PCR analysis of TAMs indicated a mild deregulation of few M1-skewed genes (TNFα, IL-1β, IL-6, IL-23) along with an enhanced expression of CCL22 in TRIM28 KO TAMs (*Fig. 3C*). Collectively these results indicate that the total absence of TRIM28 in myeloid cells does not affect the pro-tumoral activities of TAMs in fibrosarcoma model.

Next, we investigated the effect of myeloid TRIM28 in model of inflammation-driven cancer. Lack of TRIM28 in T cells has been found associated with both increased inflammation in a T cell transfer model of colitis[48] as well as in spontaneous development of autoimmunity[41]. However, the effect of TRIM28 in myeloid cells in inflammatory response has never been investigated. We used a chemical model of acute colitis driven by the disruption of intestinal barrier integrity to evaluate the inflammatory response mounted by TRIM28$^{LysM\text{-}Cre}$ and *TRIM28*$^{flox/flox}$ mice. Mice were treated with the colitogen agent DSS in drinking water, for 5 days, followed by 2 weeks of regular water. To evaluate the clinical course of colitis, mice body weight was monitored daily and colon length was measured at the end of the experiment. The results showed that, TRIM28$^{LysM\text{-}Cre}$ mice showed a severe body weight loss and colon shortening as compared to TRIM28$^{flox/flox}$ (*Fig. 3E, F*). These results clearly demonstrated that myeloid-specific ablation of TRIM28, exacerbates DSS-induce colitis, thus supporting the analysis of CAC development in TRIM28$^{LysM\text{-}Cre}$ mice.

To induce CAC, a single intra-peritoneal injection of the pro-carcinogen AOM (10mg/kg of body weight) was followed by three rounds of DSS treatment that induce a chronic state of inflammation enabling the development of multiple colonic polyps. In response to AOM/DSS treatment, TRIM28$^{LysM\text{-}Cre}$, and *TRIM28*$^{flox/flox}$ were evaluated for both inflammatory response and development of neoplastic lesions. In keeping with acute model of colitis, lack of TRIM28 in myeloid cells resulted in increased weight loss *(Fig. 3H)* and colon shortening (*Fig. 3I).* At

necroscopy, macroscopic evaluation of colons shown a similar number of tumor lesions TRIM28$^{LysM\text{-}Cre}$, and *TRIM28$^{flox/flox}$* indicating that, lack of TRIM28 in myeloid cells doesn't alter tumor multiplicity *(Fig.3L, M)*. Whether the increased inflammation developed by TRIM28$^{LysM\text{-}Cre}$ in response to AOM/DSS might affect tumor growth and progression is a fascinating subject that warrant future studies.

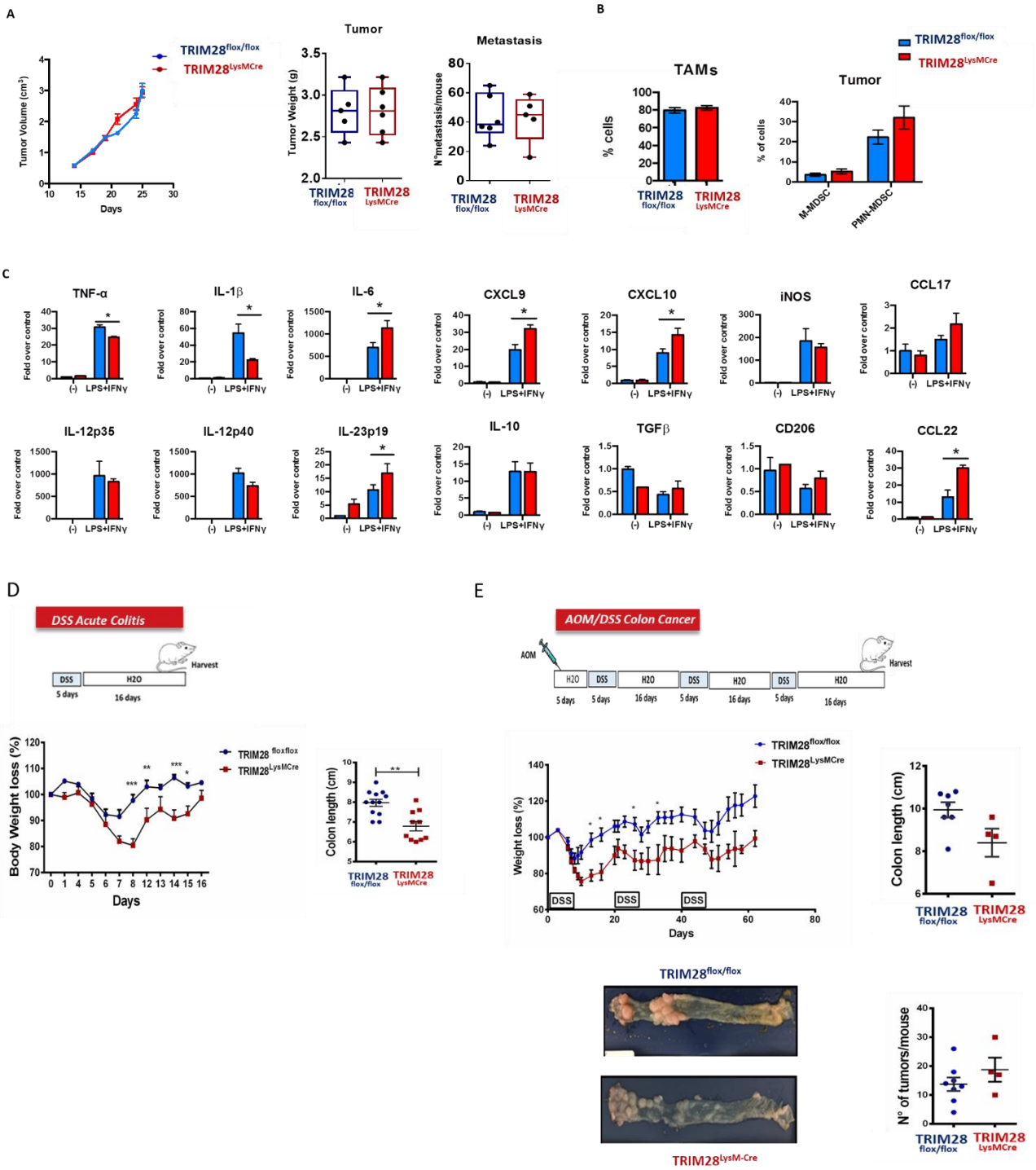

Figure 3. TRIM28 in myeloid cells does not affect the pro-tumoral activities of TAMs in fibrosarcoma model. (A) TRIM28$^{LysM\text{-}Cre}$ and TRIM28$^{flox/flox}$ mice were transplanted with 10^5 MN/MCA1 cells, starting from the 14th day, tumor growth was monitored three times a week by measuring tumor volume with a calliper. After euthanasia tumors were weighted and macroscopic lung metastases were counted (Data shown Mean ± SD and are representative of one of two independent experiments (*P<0.05 two-tailed t-test N=7). (**B**) FACS analysis of TAMs (F4/80+ cells), M-MDSC (CD11b+Ly6C+ cells) and PMN-MDSC (CD11b+Ly6C+ cells) accumulation in primary tumors and spleens of tumor bearing mice. Data from one representative experiment of 3 independent experiments (N= 5 TRIM28$^{LysM\text{-}Cre}$ mice, N=5 TRIM28$^{flox/flox}$ mice) Data shown are mean ± SEM. (**C**) RT-PCR analysis of TAMs derived from fibrosarcoma from TRIM28$^{LysM\text{-}Cre}$ and TRIM28$^{flox/flox}$ mice. TAMs were stimulated with INFγ+LPS (200U/ml INFγ+100ng/ml LPS, for 3 hours). The expression of selected M1 (TNF-α, IL1-β, IL-6, IL-12p35, IL-12p40, IL-23p19, CXCL9, CXCL10, iNOS) and M2 (IL-10, TGF-β, CD206, ArgI, CCL17, CCL22) genes were evaluated by qRT-PCR. Results are normalized on Actin mRNA levels and expressed as fold induction with respect to untreatd (ctr) TAMs. Data shown are means±SD; *P<0.05, two-tailed t-test, N=3 different biological samples.

The impact of TRIM28 ablation in myeloid cells in DSS-acute colitis and CAC model.

We took advantage of mice carrying a specific deletion of TRIM28 in myeloid cells (TRIM28-$^{LysM\text{-}Cre}$ mice to investigate its role in inflammation and cancer. (**D**) Scheme of DSS treatment in acute colitis model: to induce acute colitis, mice were treated with 1.2-1.5% of DSS in drinking water for 5 days, followed by 2 weeks of regular water. (**E**) Body weight loss was monitored every 2-3 days. At day 18th mice were euthanized, (**E**) colons were resected and measured. Data shown are mean ± SEM, two-tailed t-test, **p<0.01. Data from one representative experiment of 2 independent experiments (N= 12 TRIM28$^{LysM\text{-}Cre}$ mice and N=*12 TRIM28*$^{flox/flox}$ mice for each experiment). (**G**) Scheme of the treatment of AOM/DSS model: to induce CRC, a single intra-peritoneal injection of AOM was followed by three rounds of treatment with DSS. Each round consisted of 5 days of 1.2% DSS in drinking water, followed by 16 days of regular water. (**H**) Graphics of body weight loss during treatment and (**I**) colon length after colon resection in TRIM28$^{LysM\text{-}Cre}$ and TRIM28$^{flox/flox}$. (**L**) Representative images of CRC lesions, (**M**) colons were longitudinally opened and polyps were counted. Data shown are mean ±SEM, two-tailed t-test. Data from one representative experiment of 2 independent experiments (N= 8 TRIM28$^{LysM\text{-}Cre}$ mice and N=*4 TRIM28*$^{flox/flox}$ mice for each experiment).

TRIM28 modulates macrophage expression of LPS-induced transcriptional programs

TRIM28 interacts with KRAB-zinc finger proteins to target specific genomic regions and modulates transcription through interactions with HP1 isoforms[49]. In addition of epigenetic control, TRIM28, HP1β, and HP1γ can directly regulate initiation and/or elongation of RNA polymerase II (Pol II)-dependent transcription[50]. Since we have observed that TRIM28^{LysMCre} mice developed a more severe DSS-induced colitis, we evaluate the impact of lack of TRIM28 on LPS-induced inflammatory gene expression. We generated mRNA sequencing (mRNA-seq) data sets of WT (TRIM28^{LysMCre}) and TRIM28 KO (*TRIM28*$^{flox/flox}$) PECs under both untreated condition (Ctr) and following the treatment with 100ng/ml LPS for 4 hours to induce M1-polarized activation (LPS(4h)) or for 20 hours to induce an LPS-tolerant phenotype (LPS(18h))[51].

Data obtained with two biological replicates were highly correlated (r2>0.99) indicating high reproducibility between samples. Differential gene expression was performed using pairwise comparisons between the following experimental groups: WT_LPS (4h) vs WT_ctr, KO_LPS(4h) vs WT_ctr, KO_LPS(4h) vs KO_ctr and WT_LPS(18h) vs WT_ctr, KO_LPS(18h) vs WT_ctr, KO_LPS(18h) vs KO_ctr (*Fig 4 A, D*). To evaluate the effects of TRIM28 that are solely due to LPS treatment, we compared LPS treated TRIM28 KO to both KO_ctr and WT_ctr. As summarized by Venn diagrams, upon short exposure to LPS, 2457 (70.5%) genes are deregulated in both WT and TRIM28 KO PECs, indicated that the most of LPS-regulated genes are TRIM28 independent. However, 197 (5.7%) of genes are specifically deregulated in TRIM28 WT and 166 (4.8%) in TRIM28 KO only, overall indicating that TRIM28 regulates the expression of specific subset genes in response to LPS (*Fig.4A*). We focused on these LPS-regulated TRIM28 dependent genes. We analyzed the 197 genes that were specifically deregulated by LPS in WT PECs. Metascape analysis indicated a consistent enrichment of gene pathways involved in pyruvate metabolism, TCA cycle, nucleotide-excision repair (e.g. Nthl1, Pold1, Pole, Ercc8, Fan1, Fen1 genes) and DNA damage response (e.g. Cdk2, Fen1, Nthl1, Pold1, Pole, Eifak4, Pagr1a, Rps27l, Bbbc3 genes), suggesting that TRIM28 modulates macrophage metabolism and repair of damaged DNA upon LPS exposure.

In addition, lack of TRIM28 (TRIM28 KO PECs) modulated genes associated with cytokines secretion, including IL-6 production, corroborating the importance of TRIM28 in the regulation of LPS-induced inflammatory response (*Fig.4B*).

Collectively, in comparison to ctr WT PECs, 4 hours of LPS activation triggers the upregulation of 1624 genes in WT and 1677 genes in TRIM28 KO PECs, whereas 1316 genes were downregulated in WT and 1337 genes in TRIM28 KO PECs (*Supplementary Fig. A-D*). For

each comparison, a pathway enrichment analysis was performed using the Gene Ontology (GO) by TopGO. In both WT and TRIM28 KO PECs, 4 hours of LPS activation triggered an up-regulation of pathways associated with immune cell activation and inflammation, however in WT PECs we observed a higher enrichment of pathways related to inflammatory cytokines production (e.g. IL-12) and MAPK activity whereas in TRIM28 PEC of those supporting mononuclear cell proliferation, leukocytes mediates cytotoxicity and inhibition of biosynthetic processes (*Supplementary Fig.2 A, B*). Among the genes that are downregulated by short LPS treatment, WT PECs showed a selective enrichment of pathways related to DNA methylation and double-strand break repair, whereas in TRIM28 KO PECs with leukocytes migration. (*Supplementary Fig.2 C, D*).

In line with short LPS treatment, we observed 259 genes (8.7%) and 328 (11.1%) that are selectively regulated by prolonged LPS stimulation in WT and KO, respectively along with a large number of genes (1802, 60.8%) that are regulated by LPS in a TRIM28 independent manner (*Fig. 4D*). Metascape analysis of TRIM28 dependent genes showed that in WT, LPS-modulated genes are related to phagocytosis, antigen processing and presentation, isoprenoid metabolism and detoxification processes; whereas in KO came up genes associated with different metabolic pathways regulating proteins and amino acids catabolism, cholesterol biosynthesis and insulin-dependent metabolic processes (*Fig.4E, F*).

Overall, prolonged exposure to LPS was associated with 1168 upregulated and 1058 downregulated genes in WT PECs; whereas in TRIM28 KO counterparts, 1276 genes are induced and 1114 genes are repressed by LPS treatment as compared to WT_ctr PECs. (*Supplementary Fig.2 E-H*).

LPS tolerant WT PECs showed a selective enrichment of pathways associated with T cell activation and biosynthetic processes involving nucleobase-containing compounds and cellular nitrogen products. In contrast in LPS tolerant TRIM28 KO PECs we observed an increase in the pathways that regulate the metabolism of organic cyclic compounds, the response to hormones, the induction of gene transcription and different cellular activity associated to virus sensitivity (e.g viral genome replication and type I interferons) (*Supplementary Fig.2 E, F*). Among the genes that are downregulated in LPS tolerant condition, WT PEC showed an enrichment of pathways related to response of oxidative stress, autophagy, IL-1 production and defense whereas in TRIM28 KO of those that are associated with the repression of gene expression (*Supplementary Fig.2 G, H*).

Collectively these results indicate that TRIM28 modulate macrophage response to both short and prolonged LPS treatment by affecting the expression of selected gene transcriptional

programs associated to activation of adaptive immunity, modulation of multiple metabolic pathways and response to oxidative stress including DNA damage response.

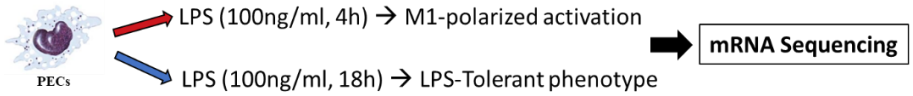

A

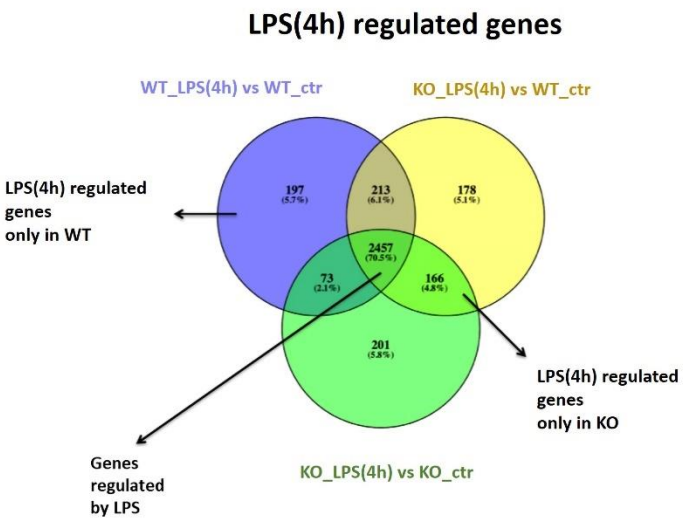

B

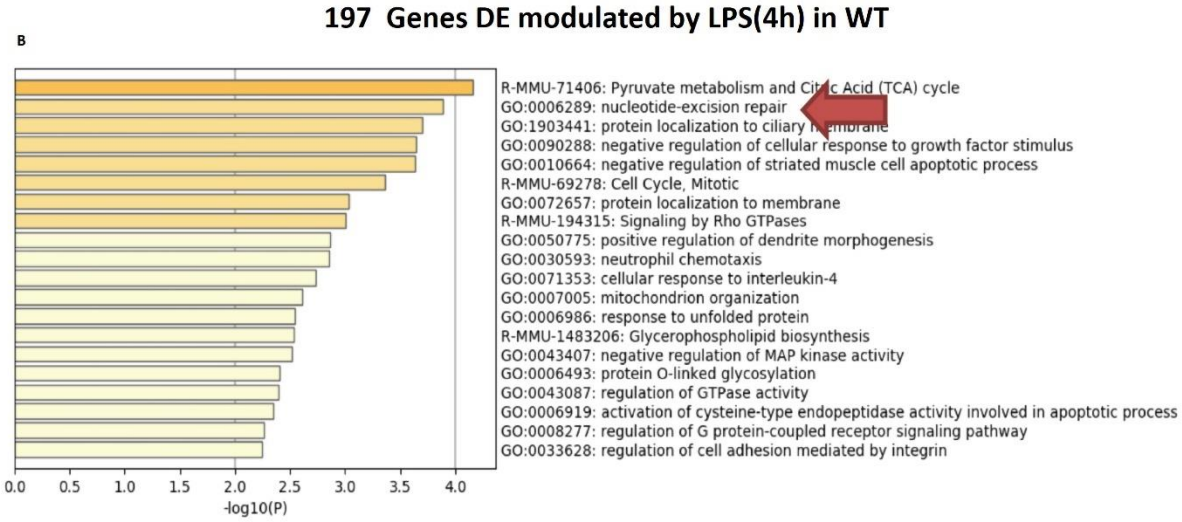

C

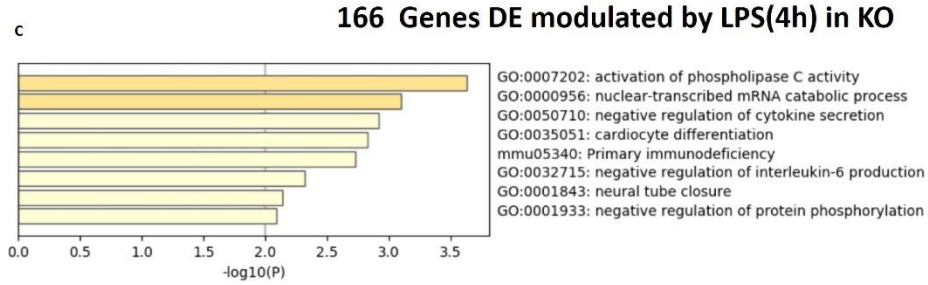

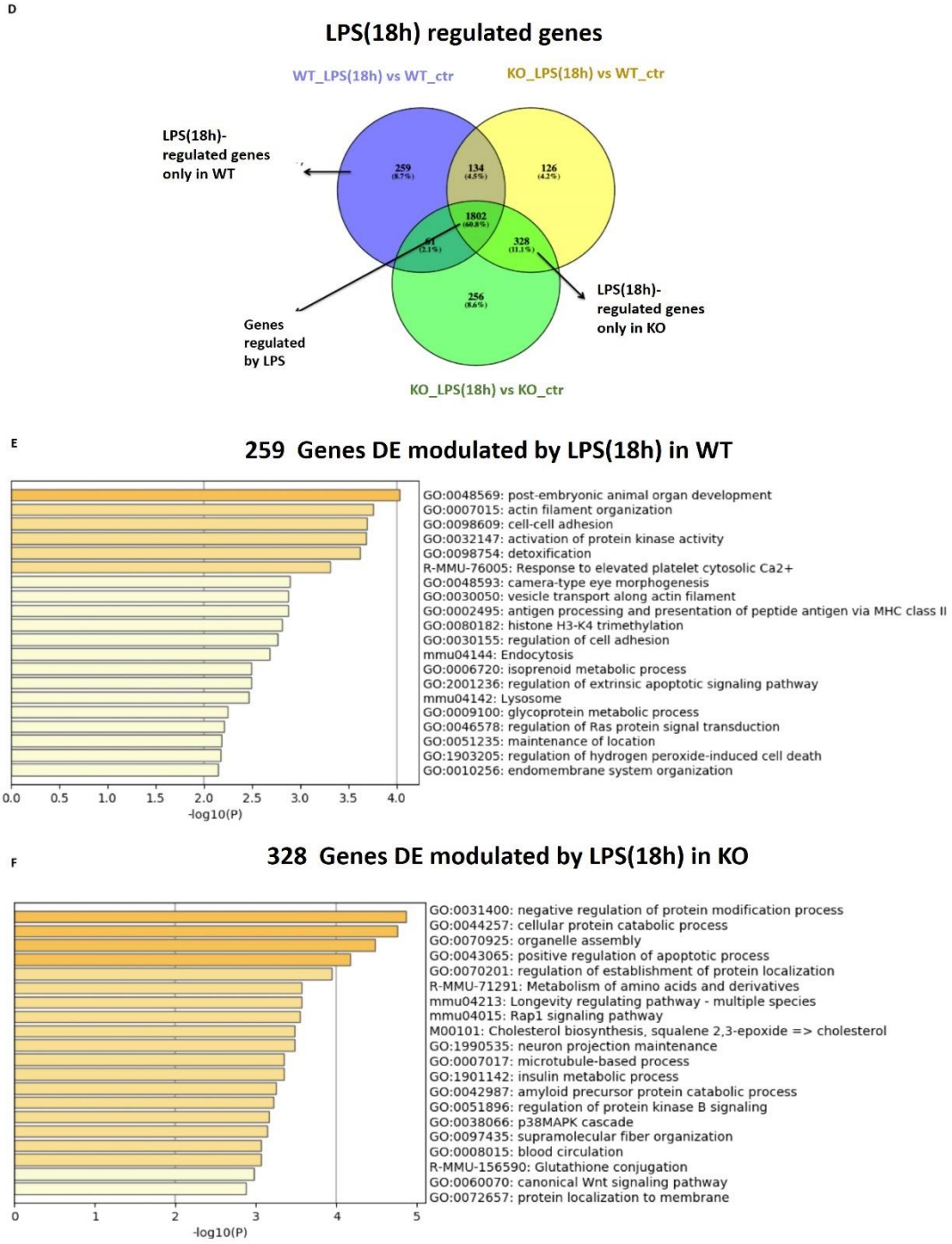

Figure 4. RNAseq analysis of "acute" and prolonged LPS treatment on PECs TRIM28_WT and TRIM28_KO. Experimental scheme. **(A, D)** Ven diagram representation of acute and prolonged LPS treatment in PECs derived from TRIM28$^{LysM\text{-}Cre}$ and TRIM28$^{flox/flox}$. PECs were stimulated with LPS (100ng/ml) for 4h or 18h, untreated PECs were left in complete medium throughout the entire experimental period. RNASeq of differential gene expressions was performed using pairwise comparisons between: WT_*LPS (4h) vs WT*_ctr, KO_LPS(4h) *vs* WT_ctr, KO_LPS(4h) *vs* KO_ctr and WT_*LPS(*18h*) vs WT*_ctr, KO_LPS(18h) *vs* WT_ctr, KO_LPS(18h) *vs* KO_ctr. DE genes were defined setting log2 fold change of ≥1 or ≤ -1 and FDR-adjusted pvalue of ≤0.01. (**B, C and E, F**) Gene set enrichment analyses performed by Metascape, with default parameters, independently on upregulated and downregulated genes (**B,C**) genes modulated by LPS_(4h) only in WT or KO mice (**E, F**) genes different modulated by LPS_(8h) only in WT or KO mice.

Lack of TRIM28 in intestinal epithelial cells (IECs) confer resistance to colitis-associated cancer (CAC).

In non-immune cells, TRIM28 has been extensively studied in different cancers, in which, depending on the type, it can exert pro- or anti-tumoral functions[52]. The tumor-suppressor activity of TRIM28 is related to the regulation of DNA repair mechanisms and epigenetic stability[53], regulated by its phosphorylation of Ser473 and/or Ser824. Given that, we have found that both TLR ligands and inflammatory cytokines can induced TRIM28 S473p, we explored the impact of inflammation on TRIM28-dependent DNA damage response and consequent susceptibility of intestinal epithelial cells (IECs) to undergo neoplastic transformation.

We initially analyzed the inflammatory response developed by TRIM28$^{flox/flox}$ and TRIM28$^{Villin\text{-}Cre}$ mice in an acute model of DSS-induced colitis. After a single round of DSS treatment, TRIM28$^{Villin\text{-}Cre}$ mice developed a more severe colitis as demonstrated by more pronounced reduction of body weight and colon length as compared to TRIM28^{floxflox} mice (*Fig. 5 B, C*). Both TRIM28$^{flox/flox}$ and TRIM28$^{Villin\text{-}Cre}$ mice control mice showed a similar colon length and body weight (data not shown) ruling out any important effects of TRIM28 under physiological condition.

Next, to explore the role of IECs- specific ablation of TRIM28 in CAC development, TRIM28$^{flox/flox}$ and TRIM28$^{Villin\text{-}Cre}$ mice were treated with azoxymethane (AOM) in combination with three rounds of DSS treatment. Albeit we confirmed an increased body weight loss in TRIM28$^{Villin\text{-}Cre}$ mice after the first DSS treatment, both mice groups showed similar flare up in response to the following rounds of DSS administration (*Fig. 5E*). In line with the body weight loss, at necroscopy, we observed a comparable colon shortening (*Fig. 5F*) However, macroscopic and histologic analysis of colons showed a drastic reduction of tumor lesions in TRIM28$^{Villin\text{-}Cre}$ mice (*Fig. 5H*). These results indicate that lack of TRIM28 in IECs enhances resistance against CAC development without affecting the overall degree of intestinal inflammation.

In conclusion, our results showed that in preclinical models of CRC, the lack of TRIM28 in intestinal epithelial cells is fundamental to confer tumor resistance only in inflammation driven-CRC model, suggesting TRIM28 as novel regulator in cancer-related inflammation.

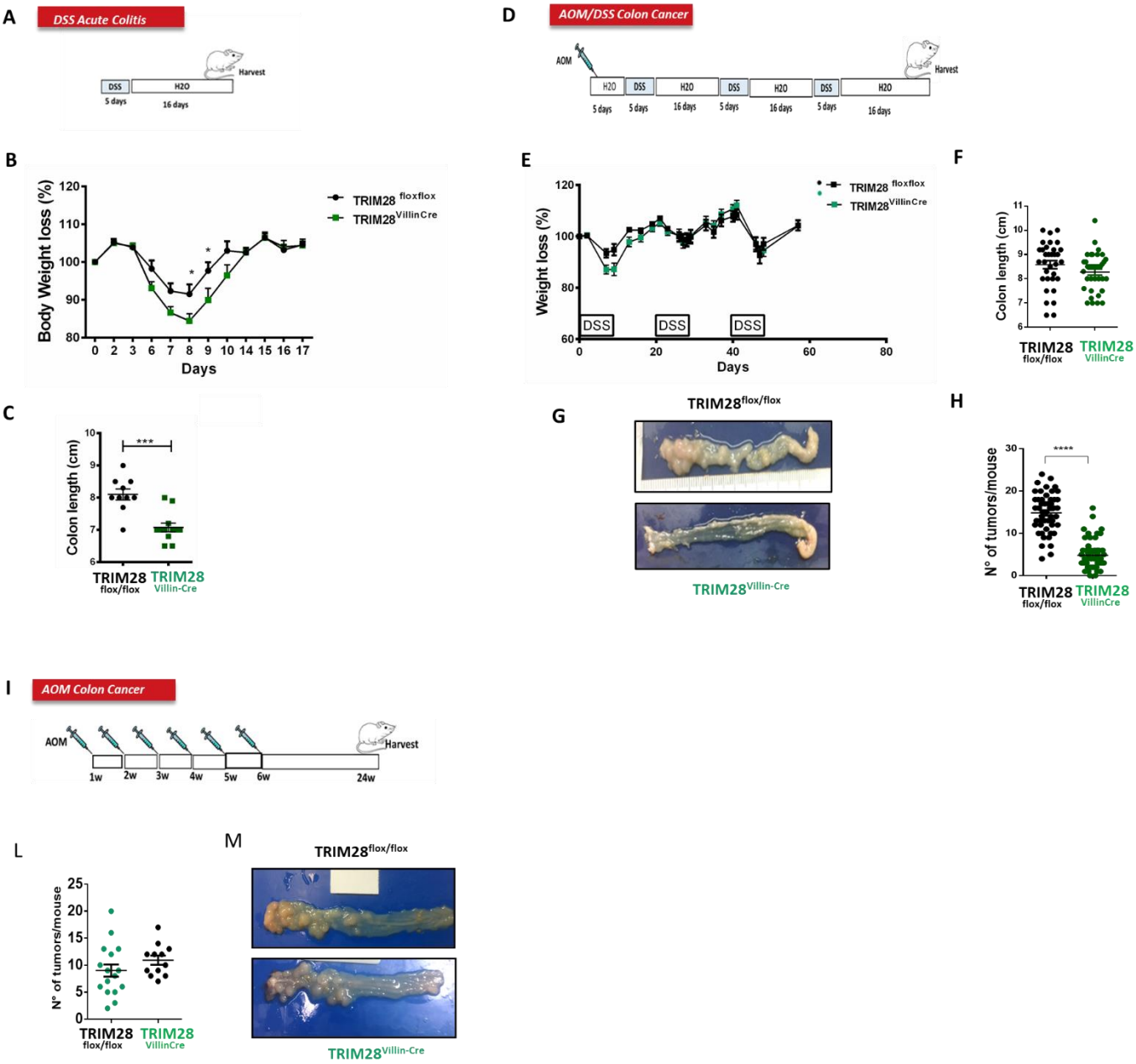

Figure 5. Study of the impact of TRIM28 ablation on IECs in DSS-induced colitis and chemically CRC models. We took advantage of mice carrying a specific deletion of TRIM28 in intestinal epithelial cells (TRIM28-^{VillinCre} mice) to investigate its role in inflammation and cancer. (**A**) Scheme of DSS treatment in acute colitis model: to induce acute colitis, mice were treated with 1.2-1.5% of DSS in drinking water for 5 days, followed by 2 weeks of regular water. (**B**) Body weight loss was monitored every 2-3 days. At day 18th mice were euthanized, (**C**) colons were resected and measured. Data shown are mean ± SEM, two-tailed t-test, **p<0.001. Data from one representative experiment of 2 independent experiments (N=10 TRIM28^{Villincre} mice and N=*10 TRIM28*$^{flox/flox}$ mice for each experiment). (**D**) Scheme of the treatment of AOM/DSS model: to induce CRC, a single intra-peritoneal injection of AOM was followed by three rounds of treatment with DSS. Each round consisted of 5 days of 1.2% DSS in drinking water, followed by 16 days of regular water. (**E**) Graphics of body weight loss during treatment and (**F**) colon length after colon resection of TRIM2^{VillinCre} and TRIM28$^{flox/flox}$.(**G**) Representative images of CRC lesions, (**H**) colons were longitudinally opened and polyps were counted. Data shown are mean ±SEM, two-tailed t-test, N=7 (N= 8 TRIM28$^{Villin\ Cre}$ mice and N=*8 TRIM28*$^{flox/flox}$ mice for each experiment). (**I**) Scheme of the treatment of AOM model: mice were treated

intraperitoneal (ip) with 10mg/kg of AOM, once a week for 6 weeks; 24 weeks after the first AOM dose, colons of mice were harvested and tumors were counted. (**L**) To analyze tumor development, colons were longitudinally opened and polyps were counted. (**M**) Representative images of CRC lesions. Data shown are mean ±SEM, two-tailed t-test. N=1 (N=15 TRIM28^{Villincre} mice and N= 18 *TRIM28*$^{flo/xflox}$ mice)

Single-Cell Transcriptome analysis of inflamed colon tissue and CRC lesions of TRIM28$^{Villin\text{-}Cre}$ and TRIM28$^{flox/flox}$ mice (AOM/DSS model).

To dissect the mechanisms whereby TRIM28 in IECs supports inflammation-driven CRC development, we treated TRIM28$^{Villin\text{-}Cre}$ and TRIM28$^{flox/flox}$ mice with AOM /DSS and we analyzed the transcriptional profile of IECs/tumor cells and lamina propria immune cells by single cell RNAseq approach. This is an absolutely state-of-the-art NGS approach that allows to improve the characterization of heterogeneous cell populations and thus the resolution of complex biological systems[54].

Since we have observed that a tumor promoting inflammatory reprograming occurred during the transition from colitis to cancer[20], we analyzed both the tumor lesions and the colon of AOM/DSS-treated mice 9 days (colitis) after the first DSS administration, when the mutant cells due to AOM treatment likely start the selection operated by immune cells.

For colitis we profiled the transcriptome of approximately 1400 epithelia cells (Epcam^{+}CD45^{-}) and 10800 immune cells (CD45^{+} Epcam^{-}) of both TRIM28$^{Villin\text{-}Cre}$ and TRIM28$^{flox/flox}$ mice, whereas for CRC lesions we analyzed 2162 epithelia cells (Epcam^{+}CD45$^{+/-}$) and 6321 immune cells (CD45^{+} Epcam^{-}) of TRIM28$^{Villin\text{-}Cre}$ and 3865 epithelia cells (Epcam^{+}CD45$^{+/-}$) and 4928 immune cells (CD45^{+} Epcam^{-}) of TRIM28$^{flox/flox}$ mice.

The analyses of the immune and epithelial cells were performed independently.

UMAP analysis and plotting identify 30 clusters of transcriptionally distinct cell types for the immune cells (CD45^{+} Epcam^{-}cells) and 9 clusters for the epithelial cells (Epcam^{+}CD45$^{+/-}$cells). We annotated immune and epithelial cell clusters by taking advantage of cell-signatures reported in published studies[55,56] or Database sets (e.g.MouseRNAseqData, HumanPrimaryCellAtlasData, BlueprintEncodeData) in combination with careful evaluation of marker genes.

We identified 9 clusters of myeloid cells, including 2 clusters of neutrophils, 3 clusters of dendritic cells (cDC1, cDC2 and pDC), 1 cluster of monocytes and 2 clusters of macrophages including a population of CD14^{high} IL1β^{high} cellsand of M2 Apoe^{high}C1q^{high} cells). We also annotated 11 clusters of lymphoid cells, including population of CD8^{+}, CD4^{+}, NK, and γδ T cells, as well as 9 clusters of B cells including population of BCR activated B cells, CCL3^{+}CCL4^{+} B cells, IgD^{high} B cells, germinal center B cells, 2 populations of antigen

presenting B cells and 3 of Plasma B cells. Next, we evaluated the frequency of each cell cluster in colon (colitis) and tumors of TRIM28$^{Villin\text{-}Cre}$ and TRIM28$^{flox/flox}$ mice. In tumor lesions of TRIM28$^{Villin\text{-}Cre}$ mice, we observed a trend towards an expansion of BCR activated B cells cluster. Interestingly, different clinical studies have pointed out the high infiltration of B lymphocytes ($CD20^+$) as favorable prognostic indicators in terms of improved disease-specific survival[57,58] and a lower risk of disease recurrence in metastatic colorectal cancer[59].

As compared to colitis, tumor lesions of both TRIM28$^{flox/flox}$ and TRIM28$^{Villin\text{-}Cre}$ mice showed a decreased frequency of the clusters related to NK (NK IL-22high), CD8 T cells (CD8 T cells and CD8 effector T + TGD cells) and γδ T cells (CD8 effector T + TGD cells). Of note, in the colon of TRIM28^{VillinCre} mice, the clusters of NK IL-22high cells and early memory CD8 T cells tend to augment under "colitis" stage. In addition, the clusters of early memory CD8 T cells, CD4 effectors and TGD-Th2 T cells seem to be expanded in the tumor of TRIM28$^{Villin\text{-}Cre}$ mice. In contrast to lymphoid cell clusters, the results suggest a reduction of tumor associated myeloid clusters. In particular, monocytes, neutrophils and both $CD14^{high}IL1^{high}$ and $Apoe^{high}C1q^{high}$ macrophage clusters tend to be lower in CRC lesions of TRIM28$^{Villin\text{-}Cre}$ than in TRIM28$^{flox/flox}$ mice, whereas under "colitis" stage the population of colonic neutrophils seem to be expanded in absence of TRIM28. Overall, these observations warrant further studies to evaluate whether the tumor resistance in TRIM28$^{Villin\text{-}Cre}$ might be associated to the expansion of cytotoxic lymphoid cells along with the reduction of pro-tumoral myeloid cells.

Among the 9 clusters of epithelial cells (Epcam+CD45+/- cells) we were able to identify 4 clusters including populations of colonic cells, namely bottom Enterocytes, MUC3+ Enterocytes, Goblet and Paneth cells and stem cells. We also annotated as neoplastic cells the cluster enriched in epithelial-mesenchymal transition (EMT) genes and we found 2 clusters characterized by the high expression of Mitochondrial genes (cluster 1 and 5) that likely include populations of apoptotic cells. Finally,3 clusters have cell signature of fibroblasts and immune cells (mast cells and intraepithelial B and T cells). As expected, the cluster of neoplastic cells with a higher EMT signature selectively expanded in tumors, in particular in those of TRIM28$^{flox/flox}$ mice. In contrast the cluster of Goblet and Paneth cells is reduced during the transition from colitis to cancer, and seems to be lightly decreased in the colon of TRIM28$^{Villin\text{-}Cre}$ as compared to TRIM28$^{flox/flox}$ mice. These last observations suggest a potential impairment of Goblet and Paneth cells in TRIM28$^{Villin\text{-}Cre}$ as a pathogenic event contributing to increased intestinal inflammation.

Collectively these results suggest that lack of TRIM28 in IECs impact on immune cells composition during the transition from colitis to cancer along with mild effects on the expansion

of neoplastic cells with an EMT^{high} gene signature and accumulation of Goblet and Paneth cells under colitis stage.

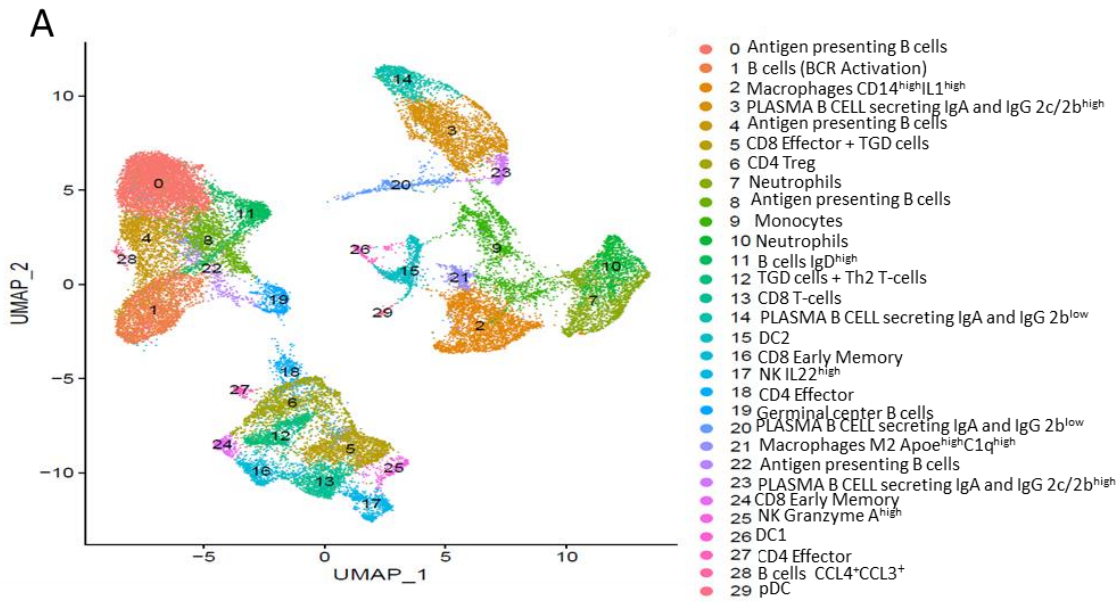

B

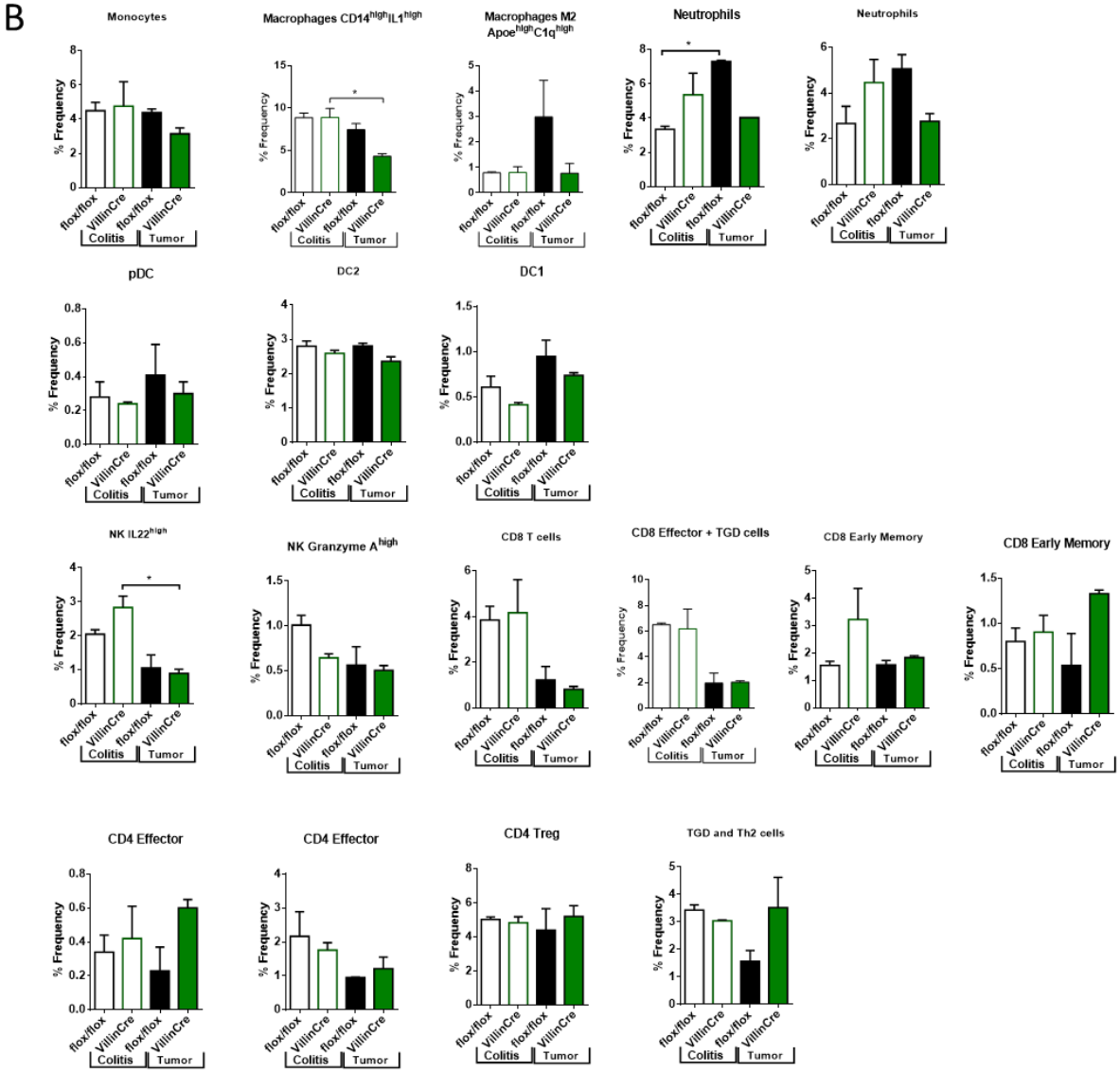
Monocytes
Macrophages CD14highIL1high
Macrophages M2 ApoehighC1qhigh
Neutrophils
Neutrophils
pDC
DC2
DC1
NK IL22high
NK Granzyme Ahigh
CD8 T cells
CD8 Effector + TGD cells
CD8 Early Memory
CD8 Early Memory
CD4 Effector
CD4 Effector
CD4 Treg
TGD and Th2 cells
% Frequency
flox/flox
VillinCre
Colitis
Tumor

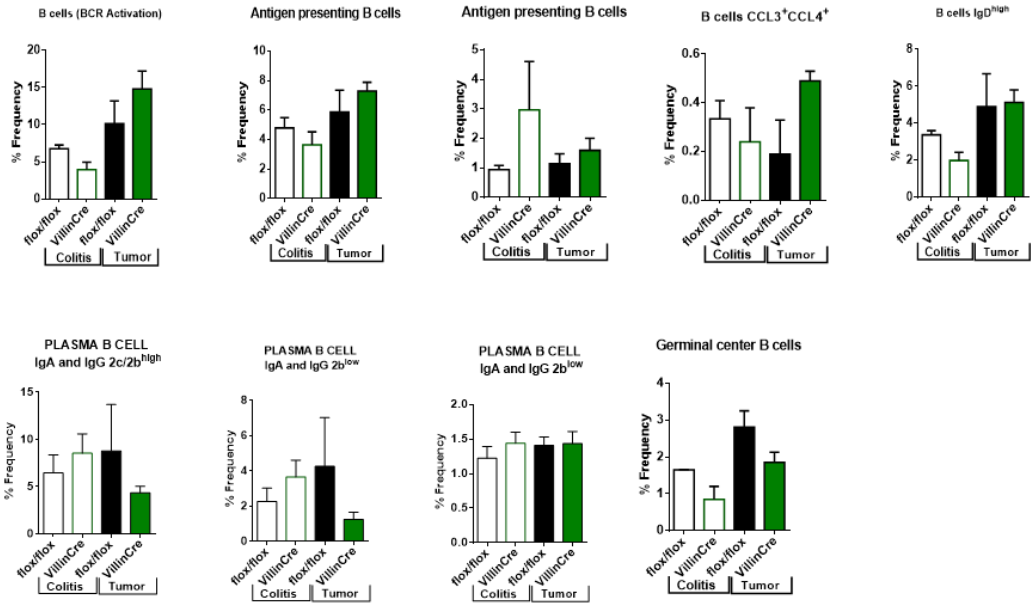
B cells (BCR Activation)
Antigen presenting B cells
Antigen presenting B cells
B cells CCL3+CCL4+
B cells IgDhigh
PLASMA B CELL
IgA and IgG 2c/2bhigh
PLASMA B CELL
IgA and IgG 2blow
PLASMA B CELL
IgA and IgG 2blow
Germinal center B cells
% Frequency
flox/flox
VillinCre
Colitis
Tumor

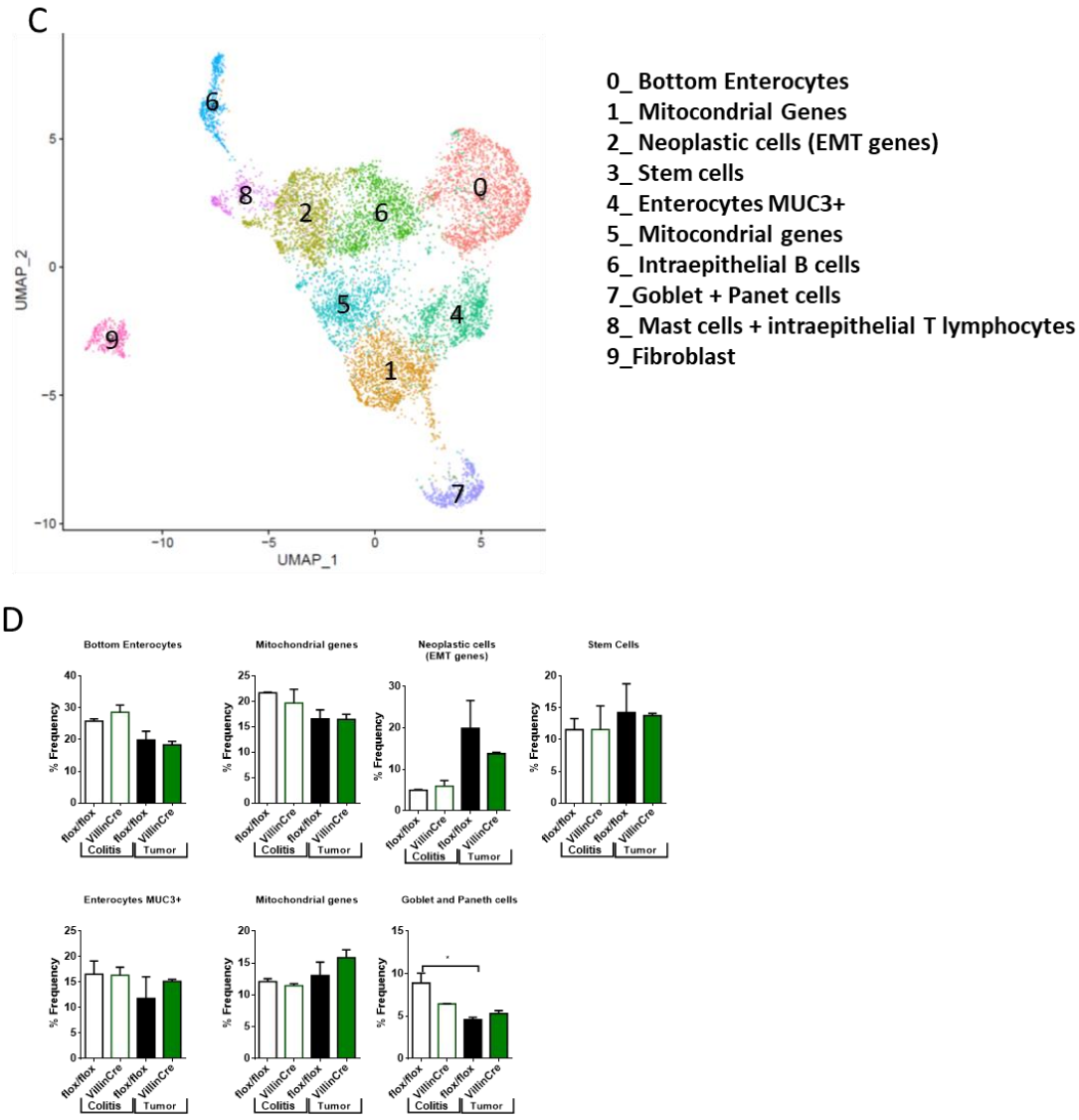

Figure 6. Single cell-RNAseq analysis of immune cells infiltrate (CD45^{+}, Epcam^{-}cells) and Epithelial cells (Epcam^{+}CD45^{-} cells) of inflamed colon tissue and CRC lesions, during acute phase of DSS colitis and after tumor development in AOM/DSS CRC model. (A) UMAP of integrated biological replicates identified 30 unique cell clusters for immune cells. Resolution 1.0. For 1st time point 10874 cells for TRIM28$^{Villin\text{-}Cre}$ mice and 10821 cells for TRIM28$^{flox/flox}$ mice were analyzed; for the 2nd analysis 6321 cells for TRIM28$^{Villin\text{-}Cre}$ mice and 4928 cells for TRIM28$^{flox/flox}$ mice. **(B)** Distribution in terms of percentage of all immune cells across clusters 0–30 between TRIM28$^{Villin\text{-}Cre}$ and TRIM2$^{flox/flox}$ mice, in colitic colon tissue and tumors. **(C)** UMAP of integrated biological replicates identified 10 unique cell clusters for Epithelial cells (clusters 6,8 and 9 were excluded). Resolution 0.4 was chosen. For 1st time point 1431 cells for TRIM28^{VillinCre} mice and 1427 cells for TRIM28$^{flox/flox}$ mice were analyzed; for the 2nd analysis 2162 cells for TRIM28$^{Villin\text{-}Cre}$ mice and 3875 cells for TRIM28$^{flox/flox}$ mice. **(D)** Distribution in terms of percentage of all epithelial cells across clusters 0–7 between TRIM28$^{Villin\text{-}Cre}$ and TRIM28$^{flox/flox}$ mice, in colitic colon tissue and tumors. Statistical comparisons were performed using one-way A-NOVA, significance level was set a *p<0.05. For each condition, experiments were performed in duplicate, for a total of 12 samples.

Discussion

Tumor Associated Macrophages (TAMs) are the major population of inflammatory cells infiltrating tumors, and the crucial orchestrators of tumor-promoting inflammation.

Accumulating evidence indicates that TAMs-centred strategies may serve as promising candidates for cancer therapy. Understanding the molecular determinants underlying TAMs polarized activation represents a crucial challenge to identify new targets for more powerful therapeutic approaches.

The biological activity of the majority of the proteins is regulated at the post-translational level[60]; in particular, the addition of phosphate groups to Serine, Tyrosine, Histidine and Threonine residues is a reversible modification that regulates several aspects of protein biology. Here we used mass spectrometry-based phosphoproteomics, a powerful methodology for the study of kinase signaling. To dissect the molecular pathways underlying the pro-tumoral activities of TAMs.

Comparing the alterations of the phospho-proteoma of TAMs isolated from murine MN/MCA1 fibrosarcoma, as compared to resting (ctr), M1 (IFNγ/LPS for 30 minutes) and M2 (IL-4 for 8 hours) polarized macrophages we originally found the phosphorylation of Tripartite motif-containing 28 (TRIM28) at Ser473 (TRIM28 S473p) in both M1-polarized PECs and TAMs.

The tripartite motif containing protein 28 (TRIM28), also known as KRAB (Kruppel-associated box)- associated protein or transcription intermediary factor 1β (TIF1β) is a pleiotropic protein that participates in the dynamic organization of chromatin and regulates numerous different processes including gene expression, DNA repair, pluripotency, proliferation, differentiation and cell survival. TRIM28 biological activity is mainly regulated by post-translational modifications including sumoylation, ubiquitination and phosphorylation.

So far, phosphorylation on serine 473 (S473) has been reported in both physiological condition, such as during the late S phase of cell cycle, and in different stress setting such as DNA damage[37], metabolic stress[38], viral infection[39,61] and T cell receptor activation[40,41]. Our results provide the first evidence of TRIM28 S473p in macrophages activated by different inflammatory triggers.

Confocal analyses of MN/MCA1 fibrosarcoma sections, confirmed TRIM28 S473p in TAMs and extended this observation to tumor cells, suggesting that TRIM28 could play a role in tumor development by modulating both neoplastic cells activities and cancer-related inflammatory microenvironment.

Immunoregulatory molecules (IL-10, PGE2) that we have previously found enriched in fibrosarcoma, represent potential tumor-derived signals controlling TRIM28 S473p in TAMs. Indeed, we found that they were able to induce long-lasting TRIM28 S473p in PECs.

Additionally, we found that several M1-inducing stimuli, including inflammatory cytokines (TNFα, IL-1β, IL-6) and plasma membrane toll-like receptor ligands (LPS, PAM_3CSK_4 and Flagellin) induce transient TRIM28 S473p in PECs

Given that TLRs play a key role in the initiation of host defense against a wide range of threats and can contribute to the development and progression of inflammatory and autoimmune diseases and cancers[62] we decided to investigate the molecular mechanisms driving TRIM28 S473p upon plasma membrane TLRs engagement. We focused on the adaptor protein MyD88, which is the first crucial molecule of the transduction pathway for all TLRs, except TLR3, and we demonstrated that TRIM28 S473p is totally abrogated in $Myd88^{-/-}$ PECs, thus demonstrating that the Myd88-dependent pathway control TRIM28 S473p.

Ligands of TLRs trigger several intracellular signaling pathways, such as the Phosphatidylinositol-3 kinase (PI3K) and the downstream serine/threonine kinases (Akts). Besides inflammation, PI3K/Akt dependent pathway plays an important role in the regulation of many cellular processes, including survival, proliferation, differentiation and metabolism[63]. Furthermore, several growth-factors induce the activation of this signaling pathway which are frequently altered in cancers[64–66]. Noteworthily, it was recently reported that the PI3K-related kinases members ATM (ataxia telangiectasia mutated)/ATR (ataxia telangiectasia and Rad3 related) induce TRIM28 S473p in response to distinct DNA damage stimuli[42].

Therefore, we have hypothesized that PI3K/Akt signalling pathway could be involved in MyD88-dependent TRIM28 S473p induction. In contrast, our results reveal that TLR4- and TLR2-dependent TRIM28 S473p is independent of PI3K/Akt pathway.

Another crucial protein in the MyD88-dependent pathway, is represented by p38, a member of the MAPKs signaling cascade, involved in the production of inflammatory mediators, including TNF-α and COX-2[67]. P38 plays an essential role in regulating cellular processes, especially inflammation and it is activated downstream of MyD88 by stimulation of TLR2 and TLR4[46].

In colorectal cancer cells, peroxide-induced p38 MAPK triggers phosphorylation of TRIM28 at S473, this event is associated with a more efficient DNA repair and tumor cell survival under oxidative stress conditions[68]. Moreover, infection of human lung epithelial cells by highly pathogenic avian influenza virus (HPAIV) strains result in PKR-mediated sensing of viral RNA and p38-MSK1-dependent TRIM28 S473 phosphorylation an event that leads to exacerbated inflammation and tissue damage[39]. In summary, overall *in vitro* studies demonstrate that

TRIM28 S473p is induced by different pro-inflammatory signals, including cytokines and microbial products, suggesting TRIM28 as a novel regulator of M1-polarized activation.
Finally, we confirmed TRIM28 phosphorylation in human monocytes treated with selected inflammatory stimuli. thus indicating that our finding could have translational perspectives.
Although TRIM28 is involved in immune responses by controlling T cells[69] and B cells[70] development, its function in macrophages differentiation is largely unknown.
To establish the role of TRIM28 in macrophages and better characterized its impact on their activation, we analyzed the transcriptome of murine macrophages, derived from TRIM28^{LysMCre} and *TRIM28*$^{flox/flox}$ mice, after acute and prolonged treatment with LPS, by RNA sequencing (RNAseq) technique. As expected, acute and prolonged exposition to LPS enhances the expression of different classes of genes; although the most of the induced are exclusively dependent by LPS approximately 10% of them are influenced by genotype. Collectively our data indicate that TRIM28 modulate macrophage response to both short and prolonged LPS treatment by affecting the expression of selected gene transcriptional programs associated to activation of adaptive immunity, modulation of multiple metabolic pathways and response to oxidative stress including DNA damage response.
In future, we're going to better characterize the pathways involved in the acute and prolonged inflammatory response, in order to dissect the impact of TRIM28 on macrophages phenotype and functional activation. TRIM28 can regulate gene transcription by, acting as a scaffold for different transcriptional factor. In the attempt scout potential TRIM28 dependent transcription factors, we are going to analyze the upstream regions of LPS-induced TRIM28-dependent genes for the the enrichment transcriptional binding motifs
In vivo, to study the circuits involved in cancer-related inflammation, we focused on DSS-acute colitis model and DSS/AOM CAC model. Our data showed that in DSS-acute colitis model TRIM28$^{LysM\text{-}Cre}$ mice worsens intestinal inflammation in response to the treatment, but in contrast, despite the increased inflammatory response, lack of TRIM28 in myeloid cells seems not alter tumor multiplicity in AOM/DSS-induced CRC, in order to clarify this data, we're going to perform histologically analysis on CRC lesions, evaluating the colitis and dysplasia grade, immune infiltrated, apoptosis, proliferation, stemness, DNA-damage and EMT process.
Given that in non-immune cells, TRIM28 has been extensively studied in different cancers, in which, depending on the type, it can exert pro- or anti-tumoral functions we explored the impact of inflammation on TRIM28-dependent DNA damage response and consequent susceptibility of intestinal epithelial cells (IECs) to undergo neoplastic transformation. Taking advantage of mice lacking of TRIM28 in IECs and we discovered that IEC- specific ablation of TRIM28

worsens DSS-induced colitis and in AOM/DSS model, mice carrying IECs specific ablation of TRIM28 developed less number of tumor lesions, demonstrating that the ablation of TRIM28 in IECs confers resistance against inflammation-driven tumor development under

Our results suggest that TRIM28 modulates CRC development in both cell-specific and disease stage-specific dependent manner.

This unexpected result obtained in TRIM28$^{Villin\text{-}Cre}$ brought us to perform the single cell transcriptome analysis of immune infiltrated and epithelial cells during the acute phase of colitis, that represents the elimination phase and when tumors were formed (escape phase), when CRC lesions were formed.

These preliminary results gave us an overview of the cellular population expression in the inflammatory condition and during tumor development, defining the difference between the two phenotype. In particular, in acute colitis, in TRIM28$^{Villin\text{-}Cre}$ mice had an increase in the percentage of NK, CD8+ and CD4+ T cells, to confirm they higher inflammatory status as compare to TRIM28$^{flox/flox}$ mice. Whereas, in tumors TRIM28$^{Villin\text{-}Cre}$ mice have a higher expansion of B cells clusters, that could be related with a good prognostic value, as demonstrated by different clinical studies, in which patients whose tumors are highly infiltrated by B lymphocytes (CD20^{+}) have a significantly improved disease-specific survival. The most interesting results emerged in the distribution of myeloid clusters, indeed, in TRIM28$^{Villin\text{-}Cre}$ mice the presence of the tumor infiltrating neutrophils (TANs) and TAMs was considerably decreased in CRC lesions, as well as a reduction of colon cells expressed EMT genes.

Collectively these results suggest that lack of TRIM28 in IECs impact on immune cells composition during the transition from colitis to cancer along with mild effects on the expansion of neoplastic cells with an EMT^{high} gene signature and accumulation of Goblet and Paneth cells under colitis stage.

Further analyses are essential to better understand the mechanism involved in TRIM28$^{Villin\text{-}Cre}$ protection.

In conclusion, overall our *in vitro* and *in vivo* results bring us to consider TRIM28 as a novel regulator of cancer-related.

Bibliography

1. Balkwill, F. & Mantovani, A. Inflammation and cancer: back to Virchow? *The Lancet* **357**, (2001).
2. Mantovani, A., Allavena, P., Sica, A. & Balkwill, F. Cancer-related inflammation. *Nature* vol. 454 436–444 (2008).
3. Erreni, M., Mantovani, A. & Allavena, P. Tumor-associated Macrophages (TAM) and Inflammation in Colorectal Cancer. *Cancer Microenvironment* **4**, (2011).
4. Wang, K. & Karin, M. Tumor-Elicited Inflammation and Colorectal Cancer. in (2015). doi:10.1016/bs.acr.2015.04.014.
5. Canli, Ö. *et al.* Myeloid Cell-Derived Reactive Oxygen Species Induce Epithelial Mutagenesis. *Cancer Cell* **32**, 869-883.e5 (2017).
6. Bollrath, J. *et al.* gp130-Mediated Stat3 Activation in Enterocytes Regulates Cell Survival and Cell-Cycle Progression during Colitis-Associated Tumorigenesis. *Cancer Cell* **15**, (2009).
7. Karin, M. & Greten, F. R. NF-κB: Linking inflammation and immunity to cancer development and progression. *Nature Reviews Immunology* vol. 5 749–759 (2005).
8. Wadgaonkar, R. *et al.* CREB-binding Protein Is a Nuclear Integrator of Nuclear Factor-κB and p53 Signaling. *Journal of Biological Chemistry* **274**, (1999).
9. Ikeda, A. *et al.* p300/CBP-Dependent and -Independent Transcriptional Interference between NF-κB RelA and p53. *Biochemical and Biophysical Research Communications* **272**, (2000).
10. Anfray, Ummarino, Andón & Allavena. Current Strategies to Target Tumor-Associated-Macrophages to Improve Anti-Tumor Immune Responses. *Cells* **9**, (2019).
11. Sica, A. & Mantovani, A. Macrophage plasticity and polarization: in vivo veritas. *Journal of Clinical Investigation* **122**, (2012).
12. Miyagi, S. *et al.* The TIF1β-HP1 System Maintains Transcriptional Integrity of Hematopoietic Stem Cells. *Stem Cell Reports* **2**, (2014).
13. Stout, R. D. & Suttles, J. Functional plasticity of macrophages: reversible adaptation to changing microenvironments. *Journal of Leukocyte Biology* **76**, 509–513 (2004).
14. Stout, R. D. & Suttles, J. *T CELL SIGNALING OF MACROPHAGE FUNCTION IN INFLAMMATORY DISEASE*. *Frontiers in Bioscience* vol. 2 (1997).
15. Isidro, R. A. & Appleyard, C. B. Colonic macrophage polarization in homeostasis, inflammation, and cancer. *American Journal of Physiology - Gastrointestinal and Liver Physiology* vol. 311 G59–G73 (2016).
16. Mantovani, A. *et al.* The chemokine system in diverse forms of macrophage activation and polarization. *Trends in Immunology* vol. 25 677–686 (2004).
17. Mantovani, A., Marchesi, F., Malesci, A., Laghi, L. & Allavena, P. Tumour-associated macrophages as treatment targets in oncology. *Nature Reviews Clinical Oncology* **14**, (2017).
18. Rooney, J. W. TIF1beta functions as a coactivator for C/EBPbeta and is required for induced differentiation in the myelomonocytic cell line U937. *Genes & Development* **15**, (2001).

19. Saccani, A. *et al.* p50 nuclear factor-κB overexpression in tumor-associated macrophages inhibits M1 inflammatory responses and antitumor resistance. *Cancer Research* **66**, 11432–11440 (2006).

20. Porta, C. *et al.* Protumor steering of cancer inflammation by p50 nf-kb enhances colorectal cancer progression. *Cancer Immunology Research* **6**, 578–593 (2018).

21. Dobin, A. *et al.* STAR: Ultrafast universal RNA-seq aligner. *Bioinformatics* **29**, 15–21 (2013).

22. Anders, S., Pyl, P. T. & Huber, W. HTSeq--a Python framework to work with high-throughput sequencing data. *Bioinformatics* **31**, (2015).

23. Babraham Bioinformatics - FastQC A Quality Control tool for High Throughput Sequence Data. https://www.bioinformatics.babraham.ac.uk/projects/fastqc/.

24. Wang, L., Wang, S. & Li, W. RSeQC: quality control of RNA-seq experiments. *Bioinformatics* **28**, (2012).

25. Ewels, P., Magnusson, M., Lundin, S. & Käller, M. MultiQC: summarize analysis results for multiple tools and samples in a single report. *Bioinformatics* **32**, (2016).

26. Love, M. I., Huber, W. & Anders, S. Moderated estimation of fold change and dispersion for RNA-seq data with DESeq2. *Genome Biology* **15**, (2014).

27. Zhou, Y. *et al.* Metascape provides a biologist-oriented resource for the analysis of systems-level datasets. *Nature Communications* **10**, (2019).

28. Okayasu, I., Ohkusa, T., Kajiura, K., Kanno, J. & Sakamoto, S. Promotion of colorectal neoplasia in experimental murine ulcerative colitis. *Gut* **39**, 87–92 (1996).

29. Bissahoyo, A. *et al.* Azoxymethane Is a Genetic Background-Dependent Colorectal Tumor Initiator and Promoter in Mice: Effects of Dose, Route, and Diet. *Toxicological Sciences* **88**, 340–345 (2005).

30. Zheng, G. X. Y. *et al.* Massively parallel digital transcriptional profiling of single cells. *Nature Communications* **8**, (2017).

31. Hafemeister, C. & Satija, R. Normalization and variance stabilization of single-cell RNA-seq data using regularized negative binomial regression. *Genome Biology* **20**, 296 (2019).

32. Zappia, L. & Oshlack, A. Clustering trees: a visualization for evaluating clusterings at multiple resolutions. *GigaScience* **7**, 1–9 (2018).

33. Savage, S. R. & Zhang, B. Using phosphoproteomics data to understand cellular signaling: A comprehensive guide to bioinformatics resources. *Clinical Proteomics* vol. 17 27 (2020).

34. Cox, J. & Mann, M. MaxQuant enables high peptide identification rates, individualized p.p.b.-range mass accuracies and proteome-wide protein quantification. *Nature Biotechnology* **26**, 1367–1372 (2008).

35. Cheng, C.-T. KAPtain in charge of multiple missions: Emerging roles of KAP1. *World Journal of Biological Chemistry* **5**, (2014).

36. Czerwińska, P., Mazurek, S. & Wiznerowicz, M. The complexity of TRIM28 contribution to cancer. *Journal of Biomedical Science* **24**, (2017).

37. White, D. *et al.* The ATM Substrate KAP1 Controls DNA Repair in Heterochromatin: Regulation by HP1 Proteins and Serine 473/824 Phosphorylation. *Molecular Cancer Research* **10**, (2012).

38. Cheng, C.-T. *et al.* Metabolic Stress-Induced Phosphorylation of KAP1 Ser473 Blocks Mitochondrial Fusion in Breast Cancer Cells. *Cancer Research* **76**, (2016).

39. Krischuns, T. *et al.* Phosphorylation of TRIM28 Enhances the Expression of IFN-β and Proinflammatory Cytokines During HPAIV Infection of Human Lung Epithelial Cells. *Frontiers in Immunology* **9**, (2018).

40. Zhou, X.-F. *et al.* TRIM28 mediates chromatin modifications at the TCR enhancer and regulates the development of T and natural killer T cells. *Proceedings of the National Academy of Sciences* **109**, (2012).

41. Chikuma, S., Suita, N., Okazaki, I. M., Shibayama, S. & Honjo, T. TRIM28 prevents autoinflammatory T cell development in vivo. *Nature Immunology* **13**, 596–603 (2012).

42. Hu, C. *et al.* Roles of Kruppel-associated box (KRAB)-associated co-repressor KAP1 Ser-473 phosphorylation in DNA damage response. *Journal of Biological Chemistry* **287**, 18937–18952 (2012).

43. Shen, L. T.-W., Chou, H.-Y. E. & Kato, M. TIF1β is phosphorylated at serine 473 in colorectal tumor cells through p38 mitogen-activated protein kinase as an oxidative defense mechanism. *Biochemical and Biophysical Research Communications* **492**, (2017).

44. Krischuns, T. *et al.* Phosphorylation of TRIM28 Enhances the Expression of IFN-β and Proinflammatory Cytokines During HPAIV Infection of Human Lung Epithelial Cells. *Frontiers in Immunology* **9**, 2229 (2018).

45. Feuillet, V. *et al.* Involvement of toll-like receptor 5 in the recognition of flagellated bacteria. *Proceedings of the National Academy of Sciences of the United States of America* **103**, 12487–12492 (2006).

46. An, H. *et al.* Involvement of ERK, p38 and NF-κB signal transduction in regulation of TLR2, TLR4 and TLR9 gene expression induced by lipopolysaccharide in mouse dendritic cells. *Immunology* **106**, 38–45 (2002).

47. Porta, C. *et al.* Tumor-Derived Prostaglandin E2 Promotes p50 NF-κB-Dependent Differentiation of Monocytic MDSCs. *Cancer Research* **80**, (2020).

48. Gehrmann, U. *et al.* Critical role for TRIM28 and HP1β/γ in the epigenetic control of T cell metabolic reprograming and effector differentiation. *Proceedings of the National Academy of Sciences* **116**, (2019).

49. Iyengar, S. & Farnham, P. J. KAP1 protein: An enigmatic master regulator of the genome. *Journal of Biological Chemistry* vol. 286 26267–26276 (2011).

50. Bunch, H. & Calderwood, S. K. TRIM28 as a novel transcriptional elongation factor. *BMC Molecular Biology* vol. 16 1–7 (2015).

51. Porta, C. *et al.* Tolerance and M2 (alternative) macrophage polarization are related processes orchestrated by p50 nuclear factor B. *Proceedings of the National Academy of Sciences* **106**, (2009).

52. Hatakeyama, S. TRIM proteins and cancer. *Nature Reviews Cancer* vol. 11 792–804 (2011).

53. Noon, A. T. *et al.* 53BP1-dependent robust localized KAP-1 phosphorylation is essential for heterochromatic DNA double-strand break repair. *Nature Cell Biology* **12**, 177–184 (2010).

54. Stubbington, M. J. T., Rozenblatt-Rosen, O., Regev, A. & Teichmann, S. A. Single-cell transcriptomics to explore the immune system in health and disease. *Science* vol. 358 58–63 (2017).

55. Haber, A. L. *et al.* A single-cell survey of the small intestinal epithelium. *Nature* **551**, (2017).

56. Wang, Y. *et al.* Single-cell transcriptome analysis reveals differential nutrient absorption functions in human intestine. *Journal of Experimental Medicine* **217**, (2020).

57. Edin, S. *et al.* The Prognostic Importance of CD20+ B lymphocytes in Colorectal Cancer and the Relation to Other Immune Cell subsets. *Scientific Reports* **9**, (2019).

58. Berntsson, J., Nodin, B., Eberhard, J., Micke, P. & Jirström, K. Prognostic impact of tumour-infiltrating B cells and plasma cells in colorectal cancer. *International Journal of Cancer* **139**, (2016).

59. Meshcheryakova, A. *et al.* B Cells and Ectopic Follicular Structures: Novel Players in Anti-Tumor Programming with Prognostic Power for Patients with Metastatic Colorectal Cancer. *PLoS ONE* **9**, (2014).

60. de Sio, F. R. S. *et al.* KAP1 regulates gene networks controlling T-cell development and responsiveness. *FASEB Journal* **26**, 4561–4575 (2012).

61. King, C. A. Kaposi's Sarcoma-Associated Herpesvirus Kaposin B Induces Unique Monophosphorylation of STAT3 at Serine 727 and MK2-Mediated Inactivation of the STAT3 Transcriptional Repressor TRIM28. *Journal of Virology* **87**, (2013).

62. Rakoff-Nahoum, S. & Medzhitov, R. Toll-like receptors and cancer. *Nature Reviews Cancer* vol. 9 57–63 (2009).

63. Green, B. D. *et al.* Akt1 is the principal Akt isoform regulating apoptosis in limiting cytokine concentrations. *Cell Death and Differentiation* **20**, 1341–1349 (2013).

64. Akira, S. & Takeda, K. Toll-like receptor signalling. *Nature Reviews Immunology* vol. 4 499–511 (2004).

65. McNamara, C. R. & Degterev, A. Small-molecule inhibitors of the PI3K signaling network. *Future Medicinal Chemistry* vol. 3 549–565 (2011).

66. Fresno Vara, J. Á. *et al.* P13K/Akt signalling pathway and cancer. *Cancer Treatment Reviews* vol. 30 193–204 (2004).

67. Yang, L. & Zhang, Y. Tumor-associated macrophages: from basic research to clinical application. *Journal of Hematology & Oncology* **10**, (2017).

68. Shen, L. T.-W., Chou, H.-Y. E. & Kato, M. TIF1β is phosphorylated at serine 473 in colorectal tumor cells through p38 mitogen-activated protein kinase as an oxidative defense mechanism. *Biochemical and Biophysical Research Communications* **492**, (2017).

69. Sio, F. R. S. *et al.* KAP1 regulates gene networks controlling T-cell development and responsiveness. *The FASEB Journal* **26**, (2012).

70. Santoni De Sio, F. R. *et al.* KAP1 regulates gene networks controlling mouse B-lymphoid cell differentiation and function. *Blood* **119**, 4675–4685 (2012).

Supplementary Figures

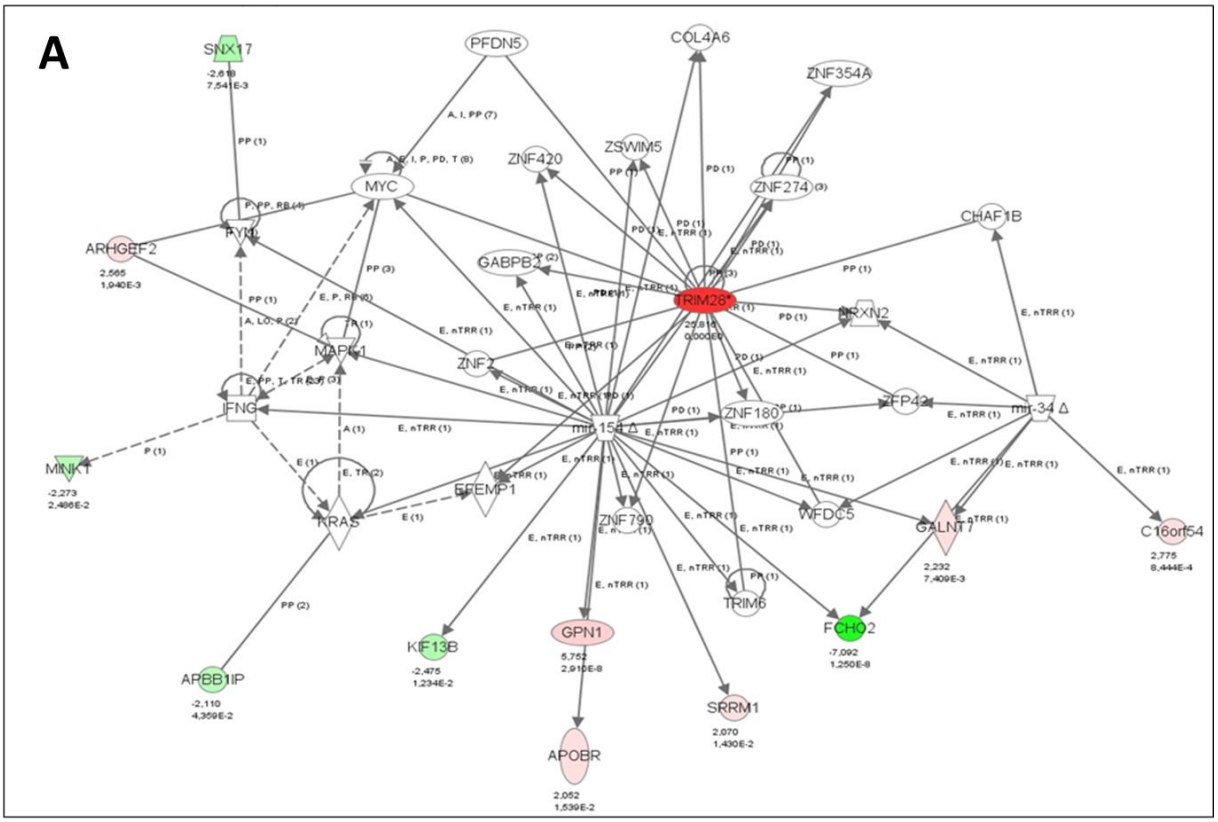

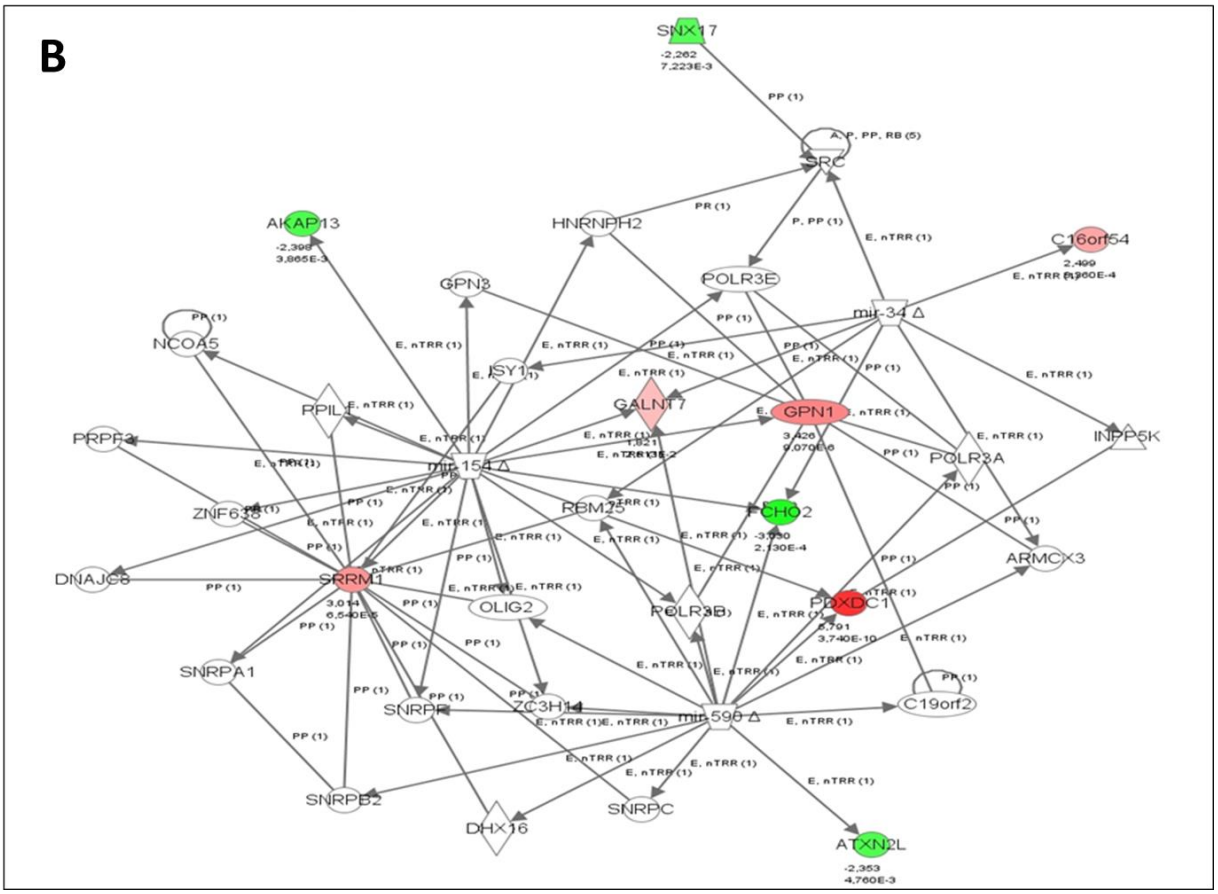

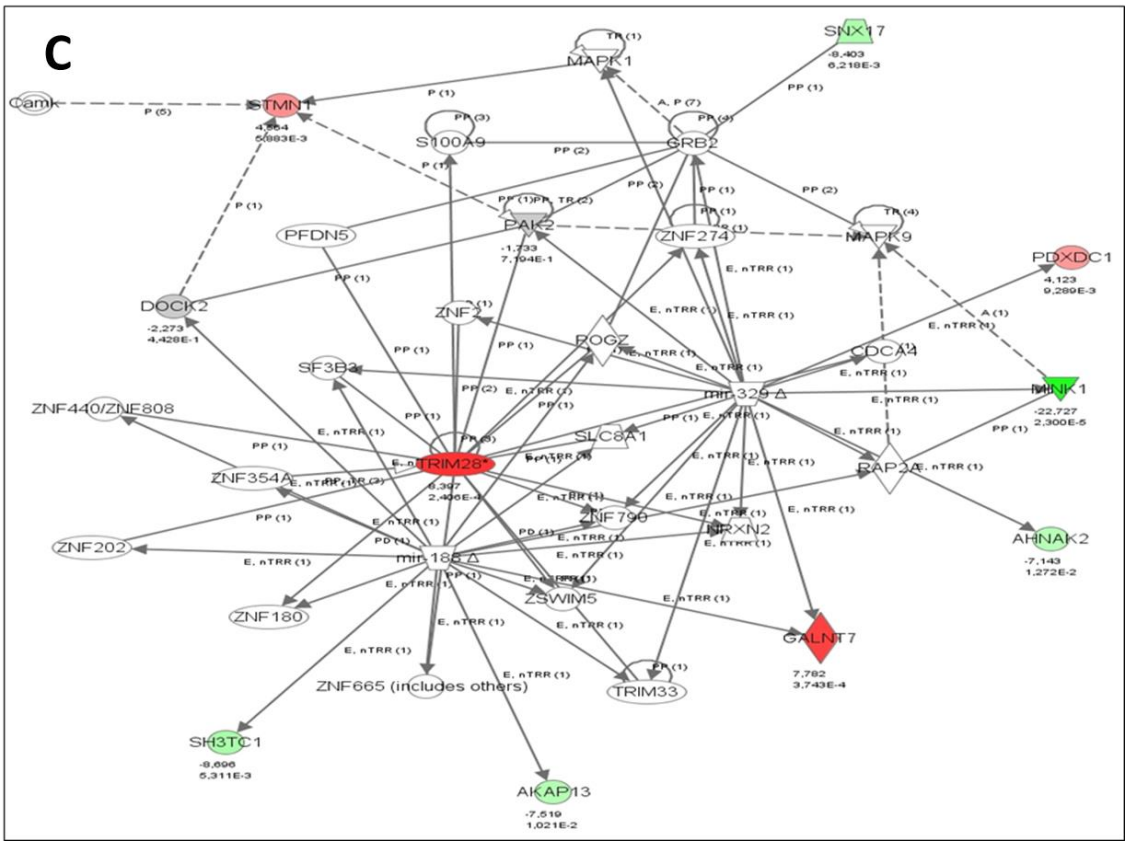

Supplementary Figure 1. Analyse of the phosphoproteoma of PECs and TAMs. Representative maps of CTR vs M1 PECs (A); CTR vs M2 PECs (B) and CTR PECs vs TAMs (C). Proteins with higher levels of phosphorylation are in red, proteins with lower levels of phosphorylation are in green. Maps of phosphorylated proteins were generated by using the Ingenuity Pathways Analysis (IPA) software.

A

LPS-upregulated genes in WT (1624)

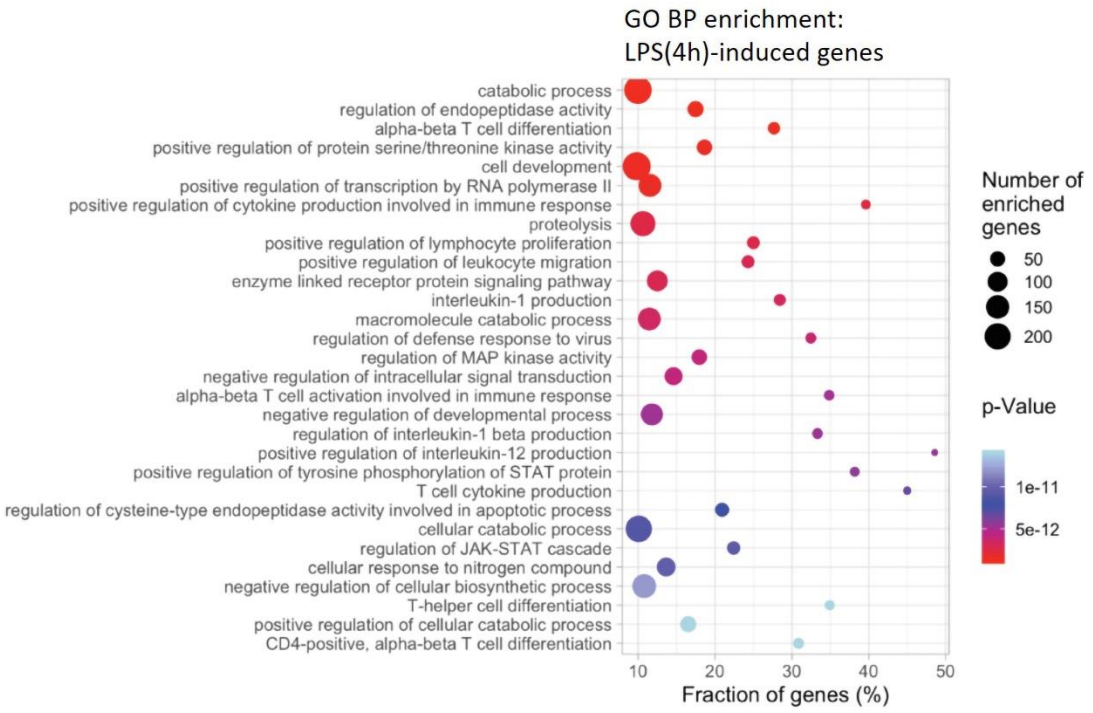

B

LPS-upregulated genes KO_LPS(4h) vs WT_ctr (1677)

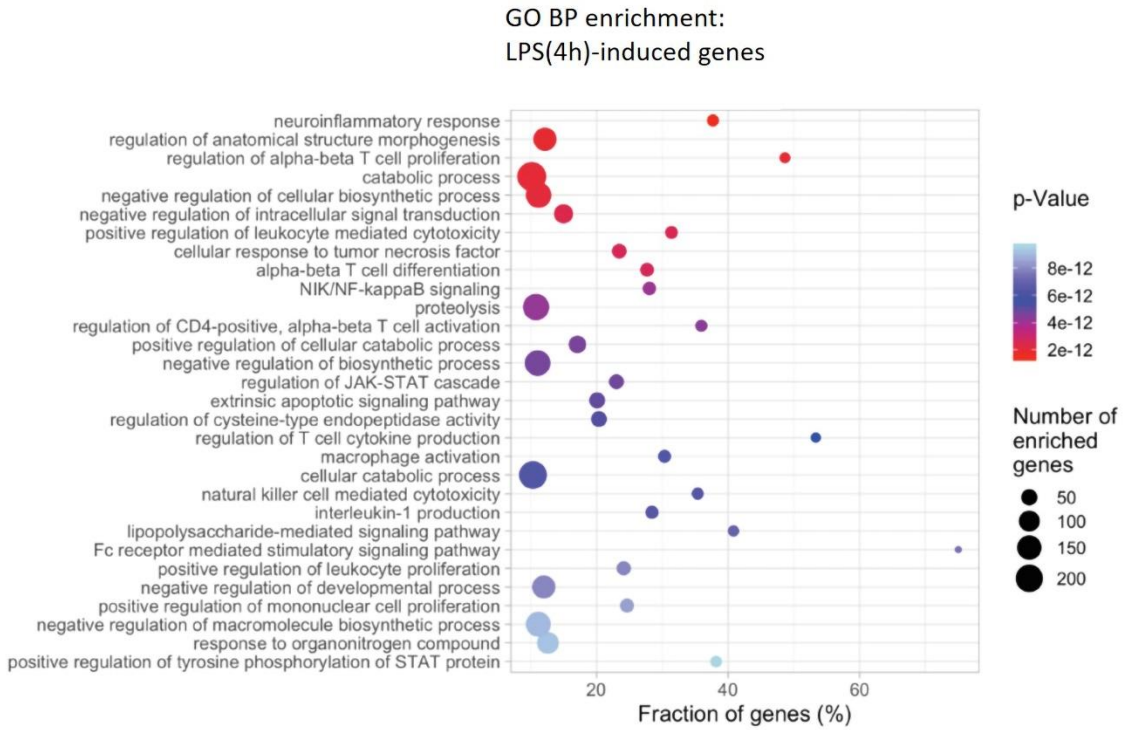

C

LPS-downregulated genes in WT(1316):

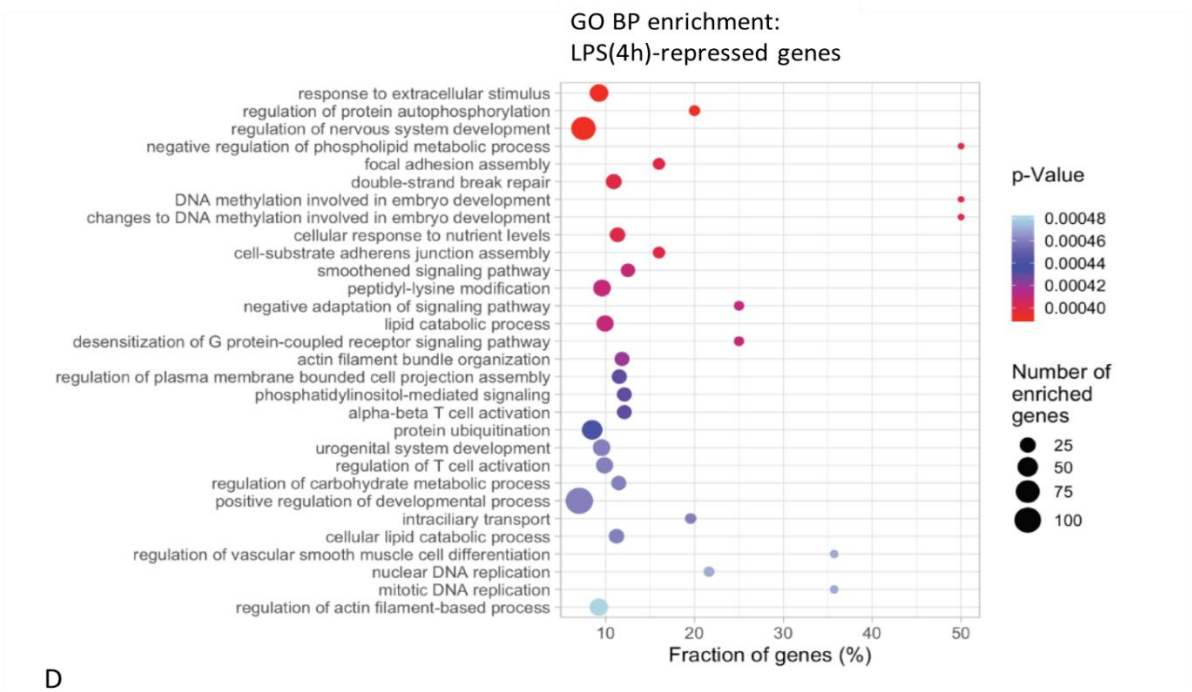

D

LPS-downregulated genes KO_LPS(4h) vs WT_ctr (1337)

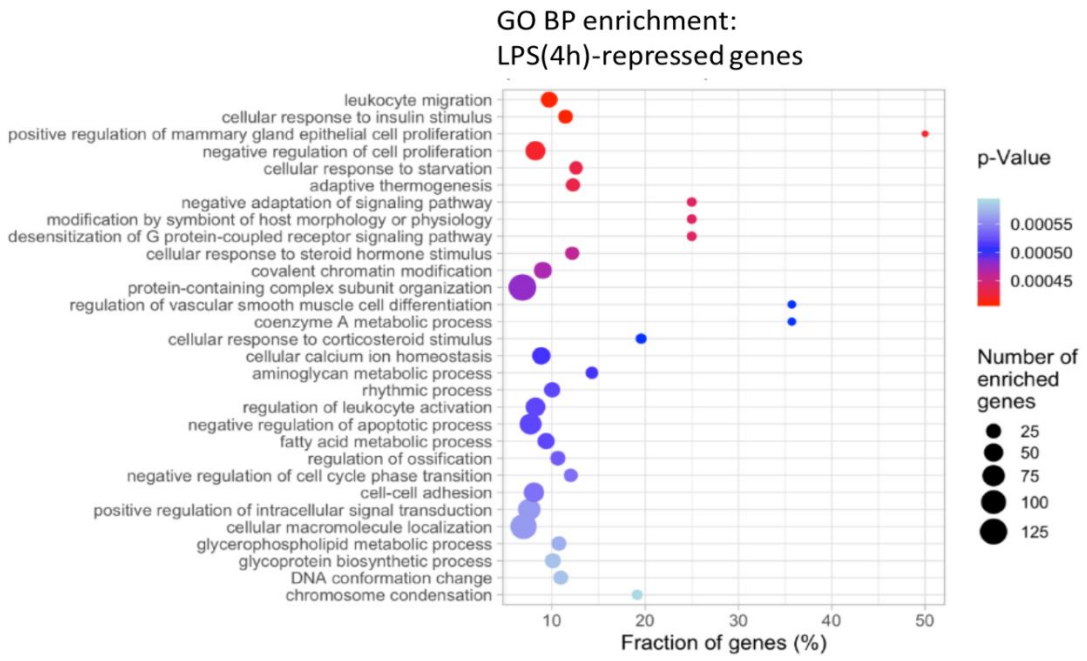

E

LPS(18h)-upregulated genes in WT (1198):

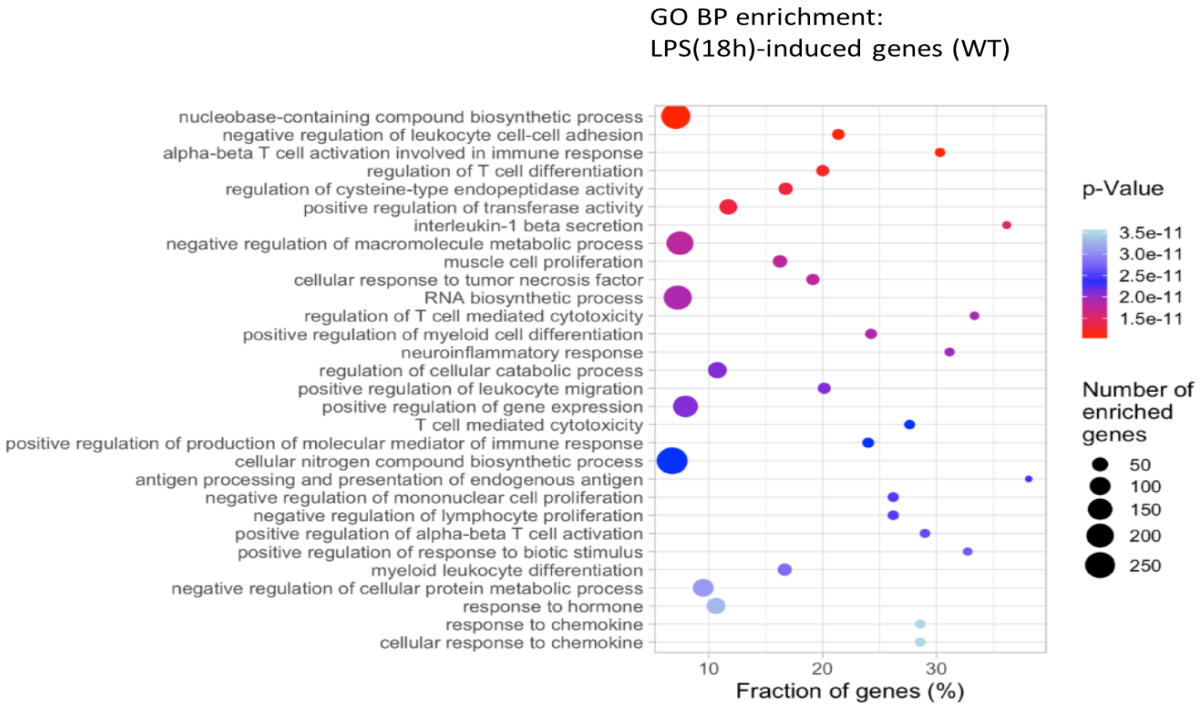

F

LPS(18h)-upregulated genes KO_LPS(18h) vs WT_ctr (1276)

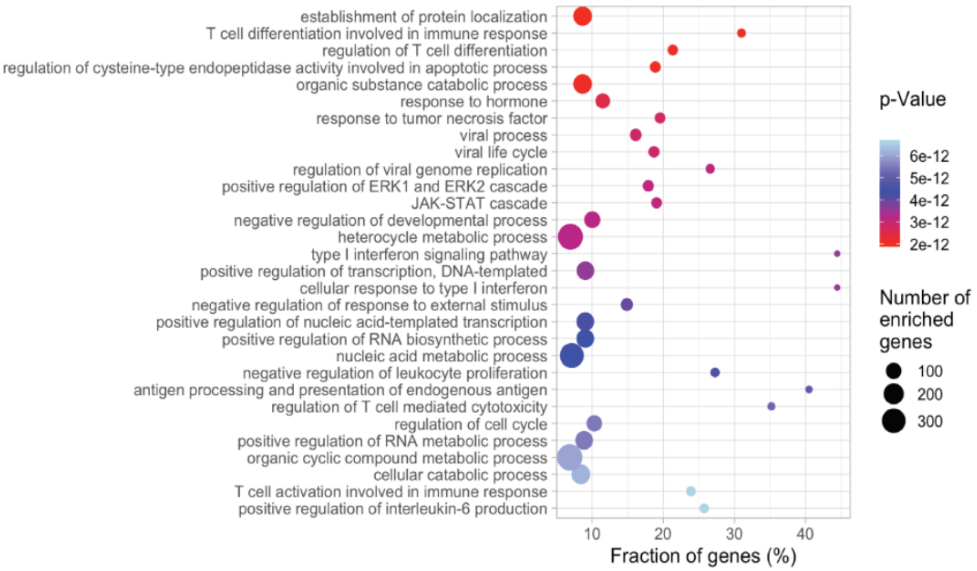

G

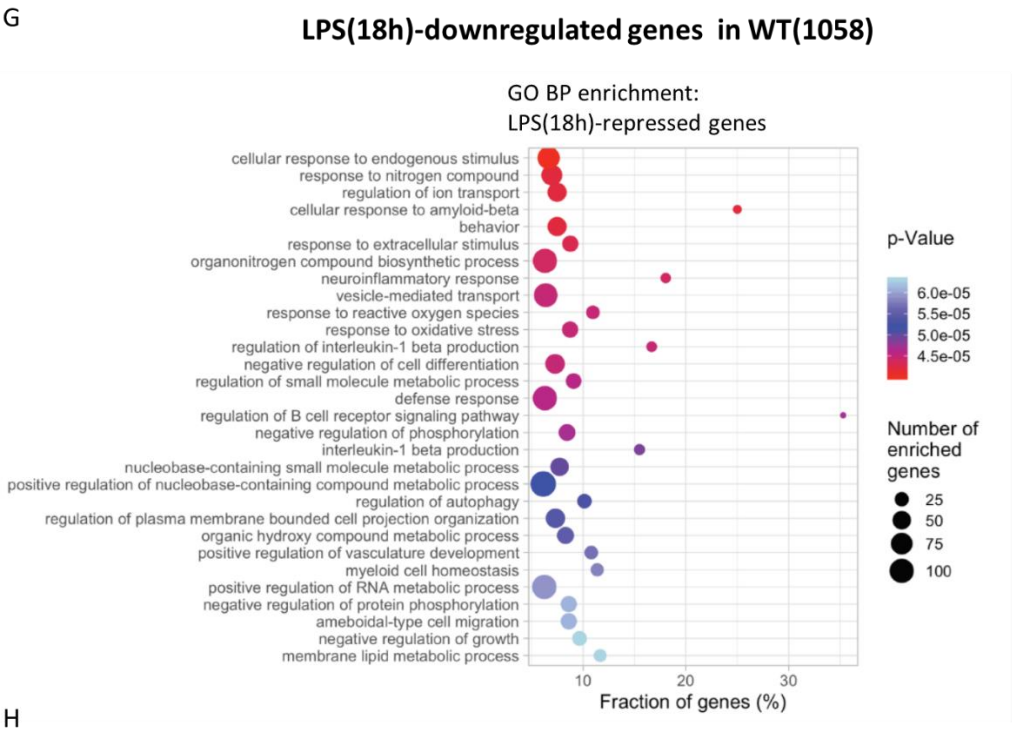

H

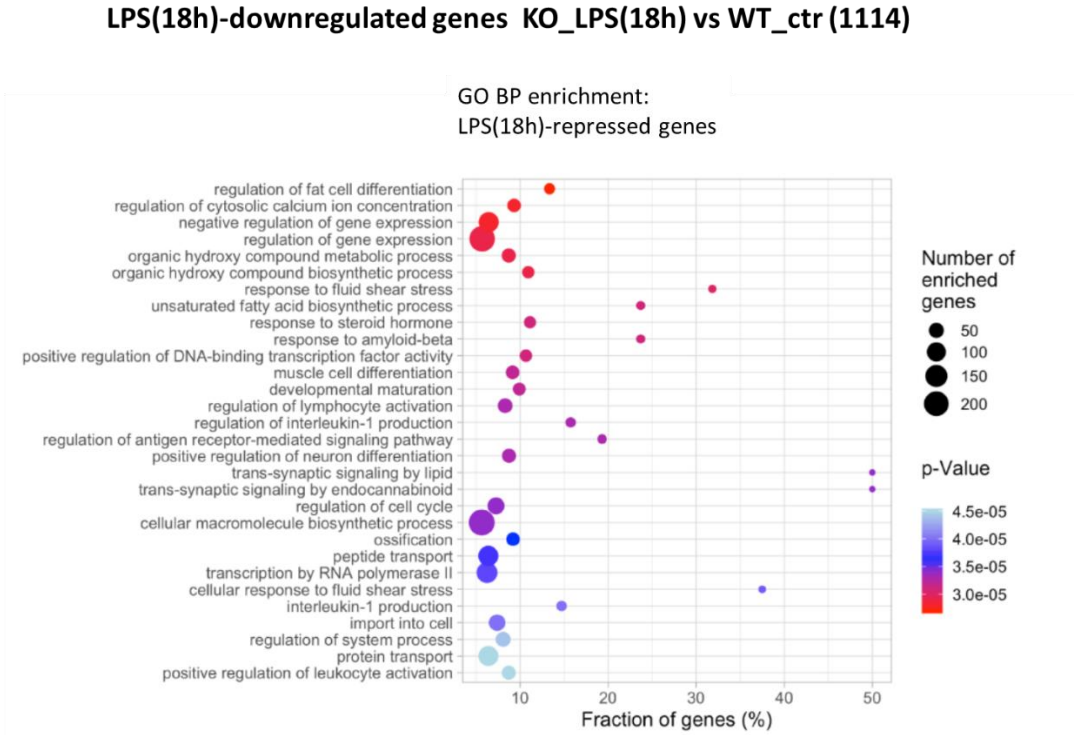

Supplementary Figure 2. TopGO analysis of acute and prolonged LPS treatment on PECs TRIM28_WT and TRIM28_KO. Comparison of genes regulated by LPS in acute (LPS(4h)) and prolonged (LPS(18h)) exposition in KO mice using a different basal (CTR) condition, WT or KO mice. DE genes were defined setting log2FC <=-1 or >=1 and FDR-adjusted pvalue <=0.01 **(B-O)** Gene set enrichment analyses performed by TopGo Bioconductor package for the following comparisons: *WT_LPS(4h) vs WT_CTR, KO_LPS(4h) vs WT_CTR* or *WT_LPS(18h) vs WT_CTR, KO_LPS(18h) vs WT_CTR* of genes up-regulated by acute (**A, B**) or prolonged exposure to LPS (**C, D**) or downregulated by LPS(4h) (**E, F**) or LPS(18h)(**G, H**). DE genes were defined setting log2 fold change of ≥1 or ≤ -1 and FDR-adjusted pvalue of ≤0.01.

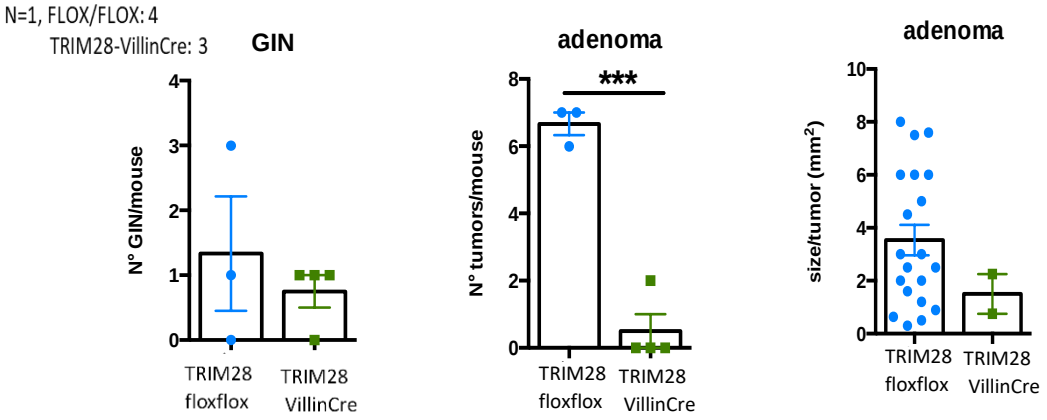

Supplementary Figure 3. Preliminary histological analysis of formalin-fixed, paraffin-embedded of colon swiss rolls sections from TRIM28$^{Villin\text{-}Cre}$ and TRIM28$^{flox/flox}$ mice after AOM/DSS treatment. Error bars, SEM. ***, $P < 0.001$ by two-tailed unpaired *t* test.

Supplementary Table 1. Real-Time PCR primers list

Gene	Forward	Reverse
	Forward	*Reverse*
Actin	cccaaggccaaccgcgagaagat	gtcccggccagccaggtccag
Arginase I	cagaagaatggaagagtcag	cagatatgcagggagtcacc
CD206	tctttgcctttcccagtctcc	tgacacccagcggaatttc
CCL2	ccgtcattttctgcctcatcc	ccctatggccctcattctca
CCL17	agtgctgcctggattacttcaaag	ctggacagtcagaaacacgatgg
CCL22	taacatcatggctaccctgcg	tgtcttccacattggcacca
CXCL9	tctcggacttcactccaacaca	actccacactgctggaggaaga
CXCL10	ccgtcattttctgcctcatcc	ccctatggccctcattctca
IL 1β	aagttgacggaccccaaaagat	tgttgatgtgctgctgcga
IL 6	ggataccactcccaacagacct	gccattgcacaactcttttctc
IL 10	ggttgccaagccttatcgga	acctgctccactgccttgct
IL 12p35	ctatctgagctccgcctgaaag	ggccaagaccacctgactctta
IL 12p40	ggaagcacggcagcagaata	aacttgagggagaagtaggaatgg
IL 23p19	agccagttctgcttgcaaagg	ggaggttgtgaagttgctccatg
i-NOS	gccaccaacaatggcaaca	cgtaccggatgagctgtgaatt
KAP1	gctcgtccctgtacatt	aatccaccatagcgccgtc
TGF-β	accaactattgcttcagcttcagctccac	gatccacttccaacccaggtc
TNFα	gaaaagcaagcagccaacca	cggatcatgctttctgtgctc

Authors'Contribution

Conception and design: C. Porta, A. Sica.

Acquisition of data and interpretation of results: S. Mola, V. Garlatti, A. Ippolito, L. Carraro, C. Porta, F. M. Consonni, J. Cibella and C. Peano.

Bio-informatics analysis (data processing and integration): A. Termanini, R. Carriero, P. Kunderfranco (Single-Cell RNA Seq); G. Soldà (RNA-Seq).

Writing: S. Mola, C. Porta.

Review: A. Sica.

Supervision: A. Sica.

CHAPTER 2

Inhibition of the histone methyltransferase EZH2 enhances monocyte recruitment in malignant pleural mesothelioma spheroid impairing anti-tumor activity of EPZ-6438.

Silvia Mola[1,2], Giulia Pinton[1], Marco Erreni[3], Marco Corazzari[2,4,7], Marco De Andrea[2,5], Ambra A. Grolla[1], Veronica Martini[2,6], Laura Moro[1], Chiara Porta[1,2]

[1]Department of Pharmaceutical Sciences, University of Piemonte Orientale "A. Avogadro", Novara, Italy

[2]Center for Translational Research on Autoimmune & Allergic Diseases (CAAD), University of Piemonte Orientale "A. Avogadro", Novara, Italy

[3] Unit of Advanced Optical Microscopy, IRCCS Humanitas Research Hospital -, via Manzoni 56, 20089 Rozzano, Milan, Italy

[4]Department of Health Sciences, University of Piemonte Orientale "A. Avogadro", Novara, Italy

[5]Department of Public Health and Pediatric Sciences, University of Turin, Medical School, Turin, Italy.

[6]Department of Translational Medicine (DIMET) University of Piemonte Orientale "A. Avogadro", Novara, Italy

[7] Interdisciplinary Research Center of Autoimmune Diseases (IRCAD), University of Piemonte Orientale, Novara, Italy

Under Review

Abstract

Malignant Pleural Mesothelioma (MPM) is a highly aggressive cancer with long latency period and dismal prognosis. Recently, EPZ-6438 (tazemetostat), an inhibitor of the histone methyltransferase EZH2, has entered in clinical trials due to the anti-proliferative effects reported on MPM cells. However, the direct and indirect effects of epigenetic reprograming on the tumor microenvironment (TME), is hitherto unexplored. Tumor Associated Macrophages (TAMs), expressing an M2-like phenotype are the major infiltrating immune cells supporting tumor growth and progression. To investigate the impact of TAMs on MPM cell responsiveness to EPZ-6438, we set up a reliable 3D MPM-monocytes spheroid model that recapitulates *in vitro*, both monocytes recruitment in tumor and their functional differentiation towards a TAM-like phenotype (Mo-TAMs). Along with an increased expression of genes for M2 and immunosuppressive molecules, monocytes-recruiting chemokine and inhibitory immune checkpoints, Mo-TAMs promote tumor cell proliferation and spreading. Prolonged treatment of MSTO spheroids with EPZ-6438 enhances both the recruitment of Mo-TAMs and the expression of tumor promoting inflammatory genes overall suppressing the anti-proliferative effects due to EZH2 inhibition in MPM cells. Albeit M1-polarized monocytes exert a significant cytotoxic effect against MPM cell monolayer, they were not able to kill MPM cell in a 3D spheroid model. Overall, our findings indicate that TAMs are a driving force for MPM growth, progression and resistance to EPZ-6438, therefore the combination of pharmacological inhibition of EZH2 with strategies of either TAM depletion or inhibition of monocyte recruitment might lead to enhanced therapeutic efficacy.

Introduction

Introduction

Malignant pleural Mesothelioma (MPM) is a rare and aggressive tumor that originates from mesothelial cells lining the pleural cavity. MPM has a strong causal link to the airborne exposure of asbestos fibers and a long latency period of outcome; therefore, the incidence of MPM is expected to rise in the following years, even though many developed countries have banned the use of asbestos in the late nineteenth century[1–3]. Based on cell morphology, MPM is classified in three major histologic subtypes associated with a different prevalence and prognosis[4]. Epithelioid MPM is the most common and favorable subtype; although patients' median survival is only 13 months after the diagnosis[5]. The sarcomatoid is the rarest and the most aggressive subtype, it does not benefit of surgery and has a median survival of 4 months, despite chemotherapy[6]. The biphasic is characterized by a mixed population of square-shaped (epithelioid) with elongated and spindle-shaped (sarcomatoid) cells, it accounts for 10-15% of MPM cases and has an intermediate prognosis between the other two subtypes (median survival of 8 months) that might be linked to proportion of sarcomatoid component[4].

The long latency of tumor development along with the non-specific nature of the clinical symptoms, (e.g. pleural effusion, dyspnea and chest pain) hinder the diagnosis, therefore MPM is often detected at advanced stage, in elderly patients, lowering further the chance of treatment[3,7]. MPM cells are highly resistant to conventional chemotherapy or radiotherapy and surgery is rarely an option due to its complexity (extra-pleural pneumonectomy, or pleurectomy or decortication) and the health status of the patients[8]. Despite the poor therapeutic benefits, since 2003 chemotherapy based on pemetrexed and cisplatin has remained the cornerstone of treatment, with no approved second line treatments[9]. Identification of new therapeutic strategies is an urgent medical need.

Enhancer of zeste homolog 2 (EZH2) is the catalytic subunit of polycomb repressive complex 2 (PRC2), that plays a key role in the trimethylation of lysine 27 on histone H3 (H3K27me3), leading to chromatin compaction and gene repression[10]. In addition of being a crucial regulator of cell lineage determination [11], EZH2 is involved in several biological activities (e.g cell cycle progression, autophagy, apoptosis, senescence and repair of damaged DNA) and acts as a crucial oncogenic driver in many different malignancies[12]. EZH2 is frequently overexpressed in MPM, where it represents both a useful biomarker for discriminating MPM form reactive mesothelial hyperplasia[13,14] and a promising prognostic and therapeutic target [15]. Indeed, different studies have shown that high expression of EZH2 is associated with diminished patient

survival[15,16] and its ablation or pharmacological inhibition significantly reduced proliferation, migration, clonogenicity, and tumorigenicity of MPM cells[16,17]. In addition to MPM, hyperactivation of EZH2 due to gain of function mutations or overexpression has been reported in different types of cancer, leading to the development of different EZH2 inhibitors[12]. Among these, tazemetostat/EPZ-6438 (Epizyme, Inc.) has been recently approved by FDA for patients with advanced epithelioid sarcoma[18] and has also entered into clinical trials for diffuse large B-cell lymphoma[19], follicular lymphoma[20] and relapsed or refractory MPM with BAP1 inactivation[21,22].

Beyond the direct anti-proliferative effect on tumor cells, EPZ-6438-driven epigenetic reprogramming can both directly and indirectly affect the tumor microenvironment (TME). Accumulating evidence highlights the importance of EZH2 in survival and activity of both effector T cells[23,24] and Treg [25,26], as well as in reducing T cell infiltration by inhibiting Th-1-chemokine expression by ovarian and melanoma cancer cells[27,28]. So far, the impact of EZH2 inhibition on human tumor associated macrophages (TAMs) accumulation and functional activation is still largely unexplored.

Macrophages play a key role in both MPM development and progression. In the attempt to clear asbestos fiber, "frustrated phagocytosis" triggers lung macrophages to release copious amount of reactive oxygen species (ROS) and inflammatory cytokines leading to an increased recruitment and activation of immune cells and consequent generation of a chronic inflammatory state, promoting malignant transformation[29]. Macrophages are highly plastic cells, despite they can be powerful inflammatory and effector cells (M1-polarized activation), local microenvironmental changes associated to tumor development and growth, re-program tumor associated macrophages (TAMs) towards an immunosuppressive M2-like phenotype, supporting immune escape[30–32]. Accordingly, in MPM patients, the number of stromal macrophages positively correlates with Tregs, and the amount of $CD163^+$ TAMs negatively correlated with overall survival[30,31]. Ablation of macrophages in mice also delayed tumor growth in different MPM models[30,33].

In addition of being central orchestrators of immunosuppressive TME[34], TAMs play a crucial role in dictating the efficacy of different therapies. Here we set up a 3D spheroid model based on the co-culture of human bi-phasic MSTO-211H cells and monocytes isolated from the peripheral blood of healthy donors to evaluate both the effects of EZH2-dependent epigenetic reprograming on TAM accumulation and the impact of TAMs on MPM cell responsiveness to EPZ-6438.

Materials and Methods

Isolation and purification of human Monocytes

Monocytes were isolated from buffy coats of healthy donors, using sequential Ficoll and Percoll density gradient centrifugations as previously described[35].

For gene expression or Western blot analysis, cells were seeded in incomplete RPMI medium and incubated at 37°C and 5% of CO_2. After 1 hour, monocytes selectively attached to the plate and non-adherent cells were vigorously washed out with saline. Monocytes were cultured in RPMI 1640 supplemented with 1% L-Glutamine and 1% penicillin-streptomycin and 10% of FBS and treated as following described.

For co-culture with MPM spheroids, after Percoll gradient, $CD14^+$ monocytes were purified by using Miltenyi Biotech CD14 MicroBeads kit, for positive magnetic separation, according to the manufacturer's instructions.

In vitro generation of Monocytes-Derived Macrophages (M-DM)

$CD14^+$ monocytes, were seeded in complete RPMI at the concentration of 2 million cells/ml in low adherence plates and cultured in the presence of human M-CSF (40 ng/mL, Miltenyi) for 6 days. Macrophage differentiation was evaluated by flow-cytometry. Cells were stained in 0.5% FBS, HBSS solution with: anti-human CD14-FITC (clone M5E2, Bio-Legend) and anti-human CD16-PE (clone 3G8, Bio-Legend) and analyzed by a S3 Cell Sorter (Biorad). When more than 90% CD14+ cells co-express the macrophage differentiation marker CD16, M-DMs were used as following described.

MPM cells lines

MSTO-211H cell line derives from biphasic MPM, harbors fibroblast-like morphology, was obtained from the Istituto Scientifico Tumori (IST) Cell-bank of Genoa; whereas the epithelioid BR-95 cell line was obtained from the biobank of the Hospital of Alessandria. All cell lines were routinely tested for mycoplasma contamination by PCR. Cells were grown in RPMI 1640, supplemented with 1% L-Glutamine and 1% penicillin-streptomycin and 10% of FBS and placed in a 37 °C humidified incubator with 5% CO_2.

Cell treatments

To evaluate the effect of EZH2 inhibition on H3K27me3, MSTO-211H, monocytes, M-DMs were treated with EPZ-6438 (10 μM, Selleckchem) for the indicated time, then core histone proteins were extracted and analyzed by Western blot. Control cells were treated with the same

amount of DMSO (Sigma). Due to the low stability of EPZ-6438, for treatments longer than 24 hours, cells were rechallenged with the same dose of drug or vehicle (DMSO) each 24 hours.
To evaluate the effect of EPZ-6438 on M1-polarized activation, monocytes and M-DMs were treated with EPZ-6438 (10 μM) for 24 hours and stimulated with LPS (100ng/ml, Enzo Life Science) during the last 4 hours. Control cells were kept in culture for the entire experimental period. In addition, cells were treated with EPZ (10μM) for 24 hours or maintained untreated for 20 hours and stimulated with LPS (100ng/ml) for the last 4 hours.
To evaluate the effect of EPZ-6438 on M2-polarized activation, monocytes and M-DMs were pre-treated with EPZ-6438 (10μM) for 24 hours and rechallenged with EPZ-6438 along with IL-4 (20ng/ml, Miltenyi) or IL-10 (20ng/ml, Miltenyi) for the following 18 hours. Control cells were kept in culture for the entire experimental period. Additionally, cells were treated with EPZ-6438 (10μM) for 42 hours, and cells were maintained untreated for 24 hours and stimulated with IL-4 or IL-10 (20ng/ml) for the last 18 hours.

Production of monocytes conditional media and treatment of MPM cells

Monocytes isolated from buffy coat were cultured in complete RPMI 1640. To induce M1 polarized activation, cells were stimulated with h-IFNγ (20ng/ml, Miltenyi) and LPS (100 ng/ml, Enzo Life Science). After 24 hours, medium was collected, centrifuged at 1400rpm, RT, 10 minutes, filtered and stored at -20°C in aliquots until use. In the same way, aliquots collected from untreated monocytes (M0) and control RPMI 1640 medium containing the polarizing stimuli and left in incubator for 24 hours were stored.
MSTO-211H and BR-95 cells were plated in 100mm-dishes in complete RPMI 1640, until 60% of confluence, then culture medium was replaced with fresh medium containing 50% of control, M0 or M1 monocytes-conditioned medium. Cells were monitored for the following 48-72 hours by optical microscope. To evaluate cell viability cells were harvested, proteins and total RNA were extracted and analyzed by Western Blot and RT-PCR respectively.

Generation of m-Cherry MSTO-211H cells

mCherry expressing MSTO-211H cells were generated by infecting MSTO-211H cells with a lentiviral vector of 3rd generation, that constitutively expressed the fluorescent reporter mCherry. HEK293T cells were transfected with pRRLsinPPTCherry_peo, pMDL, pREV and pVSVG plasmids by using Lipofectamine 2000 (Invitrogen), according to the manufacturer's instructions. After 48 hours, the medium, containing the viral particles, was collected, filtered and ultracentrifuged at 70.000 g, +4°C, 2 hours. The lentiviral pellet was resuspended in complete medium and directly added on semiconfluent MSTO-211H cells. Infected mCherry

MSTO-211H were selected by cell sorting (S3 Cell Sorter, Biorad), expanded and maintained in culture in complete RPMI 1640, in a 37 °C humidified incubator with 5% CO_2.

MPM multicellular spheroids (MCS)

MCS were generated according to a published protocol (Manente, Pinton, et al, Epigenomics, 2016) with light modifications. Specifically, we coated the 96-well plates with a thin layer of 1% sterile agarose (Sigma) in water solution. Before use, the coated plates were sterilized by UV light for 20 min. In each well we seeded 10.000 MSTO-211H cells resuspended in 100µl of RPMI 1640 medium, supplemented with 1% L-Glutamine and 1% penicillin-streptomycin and 10% of FBS. After an overnight culture in humidified incubator, at 37 °C, 5% CO_2, MSTO-211H cells aggregate to form an MCS/well. MCS were kept in culture for 96 hours maximum, according to the experimental procedures following described.

Co-culture of MSTO-211 spheroids and Monocytes

MCS were pre-treated for 48 hours with EPZ-6438 (10µM) or DMSO then, 50.000 monocytes were added to each MCS and co-cultured for additional 48 hours in presence or absence of EPZ-6438. MCS were mechanically disaggregated and both $CD14^+$ (monocyte-derived TAMs) and $CD14^-$ (tumor cells) cells were isolated by using Miltenyi Biotech CD14 MicroBeads kit, for positive magnetic separation, according to the manufacturer's instructions. Both cell populations were analyzed for gene expression by RT-PCR.

Monocytes were left untreated (M0) or were M1-polarized by IFNγ (20ng/ml) and LPS (100nl/ml) treatment for 4 hours. M0 or M1 monocytes were added to MSTO-211H spheroids 72 hours after their formation, at the concentration of 50.000 cells/spheroid and subsequently co-cultured for 24 hours. MCSs were kept untreated (DMSO challenged) or treated with EPZ-6438 (10µM) for the entire experimental period.

Re-adherence of MSTO-211H spheroids

MCS were pre-treated for 48 hours with EPZ-6438 (10µM) or DMSO then, 30.000 monocytes were added to each MCS and co-cultured for additional 24 hours in presence or absence of EPZ-6438. Next, MSTO-211H spheroids were plated in standard conditions and cultured for the last 24 hours. To evaluate the proliferating cells around the spheroid, the images were captured using an optic microscope (Leica MB5000B), and the area of spreading cells was quantified by ImageJ-WIN64 software.

Total protein extraction

Cells were washed twice with cold saline solution and lysed by directly adding 1% NP-40 lysis buffer (1% NP-40, 150 mM NaCl, 50 mM Tris-HCl pH 8.5 10 mM EDTA, 10 mM NaF, 10 mM $Na_4P_2O_7$, 0.4 mM Na_3VO_4) with freshly added protease inhibitors (10 µg/ml leupeptin, 4 µg/ml pepstatin and 0.1 Unit/ml aprotinin). Cell lysates were collected and centrifuged at 13000 rpm, +4°C, 20 minutes. The pellets were discarded and the supernatants, containing proteins, were collected and assayed for protein concentration with the Bradford method.

Acidic Extraction of Histone Core proteins

Cells were collected and washed twice with cold saline. Next, the pellet was resuspended in 1X packed bed volume of ice cold 5% perchloric acid lysis solution (5% PCA, 10mM N-ethylmaleiamide, 10 mM NaF, 10 mM $Na_4P_2O_7$, 0.4 mM Na_3VO_4, Cocktail α-proteasi 1X), kept on ice for 10 minutes and centrifuged at 13000rpm, +4°C, for 10 minutes. The extraction was repeated three times. The remaining pellet was resuspended in 2X packed bed volume of ice cold solution of HCl 0.4N, 10mM N-ethylmaleiamide and protease inhibitors, centrifuged at 13000rpm, +4°C, for 10 minutes. The extraction was repeated three times. Supernatants were collected and histone core proteins were precipitated with ice-cold solution of 25% trichloroacetic acid (TCA) on ice for 30 minutes and collected by centrifugation at 1300rpm, +4°C, 20 minutes. The protein pellet was sequentially washed with 1ml of ice-cold 100% acetone + 0.006% HCl solution and 1ml of ice-cold 100% acetone solution.

The dry pellet was resuspended in Tris-HCl (50mM) and quantified with the Bradford assay method.

Immunoblot

Proteins were separated by SDS-PAGE under reducing conditions, transferred onto nitrocellulose membrane and incubated with H3K27me3(ab6002, Abcam), H3, (ab1791, Abcam), PARP1, (sc8007, Santa Cruz), α-Tubulin (Sigma-Aldrich), p21 (C-19, Santa Cruz) antibodies. After incubation with peroxidase-conjugate Goat-α-Rabbit (7074S, Cell Signaling), Goat-α-Mouse (7076S, Cell Signaling) antibodies, chemioluminescent ECL reagent (Biorad) were added and the signals were detected at trans-illuminator Chemidoc (Biorad).

Gene expression analysis

Total RNA was extracted according to the manufacturer's instructions of RNeasy Mini Kit (Qiagen).

RNA was quantified by using Nanodrop spectrophotometer. RNA quality was assessed as 260/280 and 260/230 OD ratio >1.5, 1 μg of RNA was reverse transcribed by the Script Advanced cDNA Synthesis Kit (Biorad). 20ng of template was amplified using SYBER Green Master Mix (Biorad) and detected by the CFX96 Real-Time System (BioRad). All samples were run in triplicate. Expression data were normalized to β-Actin housekeeping mRNA and were analyzed by the $2^{-(\Delta Ct)}$ method. Results are expressed as fold upregulation respect to the control cell population. The sequences of gene-specific were designed by using https://www.ncbi.nlm.nih.gov/tools/primer-blast/. The primers are synthetized by Sigma-Aldrich, the sequences are reported in Supplementary Table S1.

Fluorescence-activated cell sorting (FACS) analysis

$1x10^6$ cells were stained with antigen-specific antibodies. Cells were stained in 0.5% FBS, HBSS solution with: anti-human CD14-FITC (clone M5E2, Bio-Legend) or anti-human CD14-BUV737 (clone MΦP9, BD-OptiBuild) and anti-human CD16-PE or-PE-Cy7 (clone 3G8, Bio-Legend or BD-Pharmigen). Cells were acquired usiging S3 Cell Sorter (Biorad) or BD FACSymphony A5 (BD Bioscence) and analyzed using FlowJo (9.3.2) software.

Time-lapse

For time-lapse analysis, mCherry-MCS were cultured for 72 hours and followed co-cultured with CFSE-labeled monocytes (10.000 cells/spheroid) for 2.5 hours. After addition of monocytes, the plate was placed in an incubator maintained at 37°C in a humidified 5% CO_2 atmosphere and migration of monocytes towards the MCS was monitored by Leica THUNDER Imager 3D Live Cell microscope.

Confocal Microscopy analysis

Confocal acquisitions were performed on mCherry-MCS co-cultured with or without CSFE-labeled monocytes. MCS were fixed with 4% paraformaldehyde (PFA), at room temperature (RT) for 1 hour and mounted with Fluoromount™ Aqueous Mounting Medium (Sigma-Aldrich).

MCS were acquired as z-stack of the entire sections using a Leica TCS SP8 Laser scanning confocal microscope, equipped with a HC PL APO CS2 10x/0.40 dry objective. Emission filter bandwidths and sequential scanning acquisition were set up in order to avoid any possible spectral overlap between fluorophores. ImageJ-win64 software package and Imaris (Bitplane) software were used for image analysis and 3D reconstruction.

Analysis of the monocyte infiltration within the MCS was performed using the macro reported below. Briefly, after channel separations, using the "Image Calculator" process, monocytes located within the MCS were selected. Subsequently, the volume of infiltrating monocytes and the MCS were calculated using the "Voxel Counter" plugin.

Proliferation assay

MSTO-211H cells were stained with CellTrace™ CFSE Cell Proliferation Kit (Thermo Fisher Scientific), according to the manufacturer's instructions. Next CFSE-labelled MSTO-211H were seeded in low adherence 96 well to generate MCSs and treated with EPZ (10μM) or DMSO for 96 hours. During the last 48 hours some MCSs were co-cultured with monocytes (50.000 cells/spheroids). Next, MCS were fixed with 4% PFA, RT, for 1 hour and mounted with Fluoromount™ Aqueous Mounting Medium (Sigma-Aldrich). Confocal acquisitions were performed using Leica SP8 LIGHTNING Confocal Microscope. The cell proliferation was quantified in term of Mean of Fluorescence (MFI), using ImageJ-win64 software.

Statistical analysis

Statistical significance between two groups was assessed by unpaired, Student t test and among multiple groups by one-way or two-way ANOVA (GraphPad Prism software). All statistical assessments were two-sided, and a value of $P<0.05$ was considered statistically significant.

Results

MSTO-211H cells form multicellular spheroids (MCS) that are sensitive to EZH2 inhibition and capable to recruit human monocytes

Multicellular spheroid (MCS) is increasingly appreciated as a useful *in vitro* model to evaluate drug response[36–39].

Based on this evidence, we decided to investigate the effects of TAMs on human bi-phasic MPM cells (MSTO-211H cell line) responsiveness to EPZ-6438 through a 3D MCS model.

At first, we tested the effect of EPZ-6438 on MCS growth. We generated mCherry-expressing MSTO-211H and we cultured these MPM cells in low adherence condition, according to a well-established protocol[40].

After 24 hours, MSTO-211H cells assemble a 3D MCS that can be kept in culture for 4 days. Therefore, mCherry-MCS were treated with EPZ-6438 or vehicle (DMSO) for 96 hours and analyzed by confocal microscopy. As compared to control (DMSO treated), we observed that EPZ-6438 triggered a significant reduction of MCS volume (*Fig. 1A*). In addition, Western blot analysis showed a consistent upregulation of the cell cycle inhibitor p21 in EPZ-6438-treated MCS (*Fig.1B*). These results confirm anti-tumor activity of EZH2 inhibition in our MCS model.

Next, to go insight in the construction of an *in vitro* tumor model that better recapitulates TME, we evaluated whether human peripheral blood monocytes might be recruited into MCS.

After 72 hours of culture, CSFE-labeled monocytes were added to mCherry-MCS and monitored by time lapse imaging. We observed that monocytes quickly migrated towards MCS, leading to their close localization around it as early as 2 hours of co-culture (*Fig.1C*). Next, confocal microscopy analysis demonstrates that monocytes were able to infiltrate the MCS after 24 hours of co-culture and were maintained up to 48 hours of co-culture (*Fig.1D*).

Moreover, FACS analysis of the MCS shows that almost the half of $CD14^+$ monocytes upregulated the macrophage differentiation marker CD16 after 48 hours of co-culture (*Fig. 1E*).

Collectively, these results indicate that human monocytes can be recruited into MCS, where they start to differentiate in macrophages.

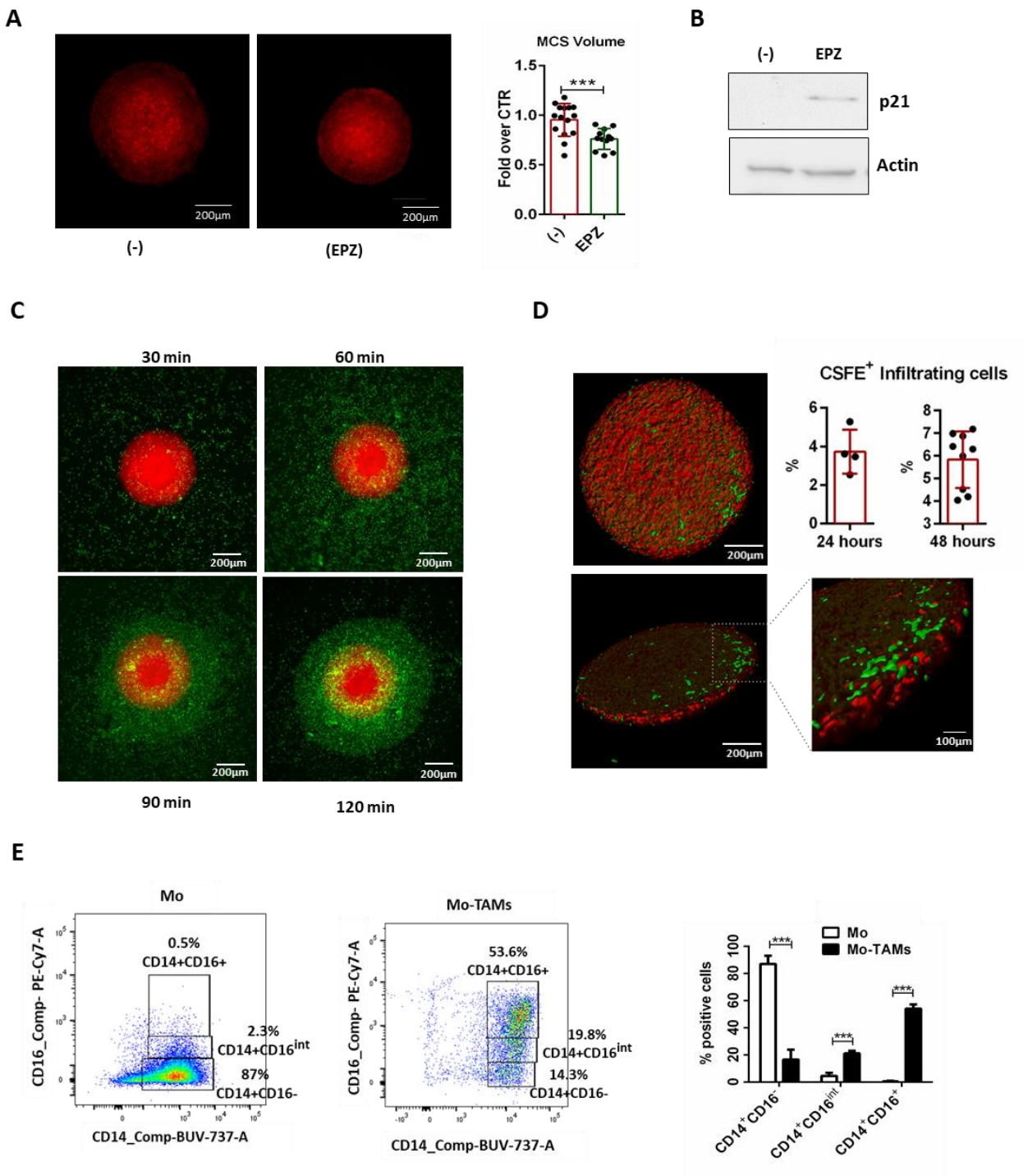

Figure 1. Human monocytes infiltrate MPM MCS (**A**) Volume of mCherry-MSTO-211H MCS treated with EPZ-6438 (EPZ, 10µM) or vehicle (-) for 96 hours was evaluated by confocal microscopy and calculated by ImageJ-win64 software. The results are shown as fold over vehicle treated MCS (-). data are shown as mean mean±SD ***P<0.001 by two-tailed *t*-test, N (-)=11 and N (EPZ)=10. Representative images are shown. Scale bars: 200µm. (**B**) Western blot analysis of p21 expression of MSTO-211H MCS, treated with vehicle (-) or EPZ-6438 (10µM) for 96 hours (EPZ). Total cell lysates were resolved by 10% SDS-PAGE. β-Actin was used as loading control. (**C**) Migration of CSFE-labeled monocytes towards mCherry-MCS was monitored every 10 minutes, by time-lapse microscopy using Leica THUNDER Imager 3D Live Cell microscope equipped with an environmental chamber maintained at 37°C, 5% CO_2 humidified atmosphere. Representative frames are shown. Scale bars: 200µm. (**D**) mCherry-MCS were cultured for 72 and 48 hours, then co-cultured with CSFE-labeled monocytes for additional 24 or 48 hours,

respectively. MCS were analyzed by confocal microscopy and infiltrating monocytes ($CSFE^+$ cells) were quantified using ImageJ-win64. Representative confocal images after 48 hours of co-culture are shown. Scale bars: 200µm or 100µm, N (24 hours) =4 and N (48 hours) =9. (**E**) Representative dot plot of FACS analysis of monocytes (CD14+ cells) co-cultured with MCS co-cultured for 48 hours to check their macrophage differentiation (CD14+CD16+ cells). Data are shown as mean±SEM *P < 0.05, ** P < 0.01 and *** P < 0.001 by two-way ANOVA N= 3.

MCS-infiltrating monocytes acquire a functional TAM-like phenotype supporting tumor growth

It has been reported that different tumor cell lines produce soluble molecules that can skew the differentiation of human monocytes-derived macrophages (M-DM) towards a TAM-like phenotype[41]. We evaluated whether the monocytes co-cultured with MCS underwent functional differentiation towards a TAM-like phenotype. After 48 hours of co-culture, MCS were disaggregated and $CD14^+$ cells (monocytes-derived TAMs) were magnetically sorted and analyzed for the expression of selected M1 and M2 genes by RT-PCR. Untreated monocytes, as well as M1-polarized monocytes by LPS treatment and M2-skewed monocytes by IL-4 or IL-10 treatment, were used as controls. The results show a significant induction of typical M2 genes (IL10, CD163, CD206, CD209 and CD301) in both monocytes-derived TAMs (Mo-TAMs) and IL-4/IL-10-treated (M2-like) monocytes as compared to the untreated ones. In contrast, all the genes encoding inflammatory mediators (e.g. TNFA, IL1B, IL6, IL12B, COX2 and CD80) were highly induced in LPS-(M1) activated monocytes but were not significantly modulated in Mo-TAMs (*Fig. 2A*). Overall, these results indicate that, similar to TAMs of MPM patients[34], *in vitro* Mo-TAMs acquire an M2-skewed phenotype. Moreover, TAMs usually support their accumulation in solid tumors through the production of chemokines (e.g. CCL2 and CXCL12) and growth factors (e.g. CSF1 and VEGF), accordingly, in our model, we observed a significant upregulation these chemo-attractants by Mo-TAMs, as compared to control monocytes (*Fig. 2B).*

Next, we analyzed the expression of the major enzymes (IDO1, NOS2, ARG1) and immune checkpoints (CD-47/SIRPα[42], PD-L1/PD1[43] and HLA class I/LILRB1[44]), that respectively drive the immunosuppressive activity of tumor-infiltrating myeloid cells and hamper the ability of macrophages to eliminate cancer cells by phagocytosis (*Fig. 2C-D)*. In comparison to control monocytes, Mo-TAMs showed a consistent increased expression of IDO1 and ARG1 along with a light upregulation of NOS2 and PD-L1 (*Fig. 2C*). These results along with the higher expression of IL10 and the low expression of the inflammatory cytokines indicate that Mo-TAMs have acquired an immunosuppressive signature resembling human TAMs of MPM patients.

In addition, Mo-TAMs expressed SIRPA and showed a selective upregulation of PD1 and leukocyte immunoglobulin-like receptor LILRB1 (*Fig. 2D*), two additional inhibitory receptors impairing macrophage-dependent clearance of cancer cells. In parallel, MSTO-211H cells isolated from MCS-monocytes co-culture expressed the "don't eat me" signal CD47 as well as PD-L1 and HLA molecules (HLA-A and HLA-B), that are recognized ligands for PD-1 and LILRB1, respectively (*Fig. 2E*). Overall, these results suggest that tumor cells likely escape phagocytosis by Mo-TAMs.

To address the functional relevance of Mo-TAMs, after 48 hours of co-culture MCS growth were analyzed by confocal microscopy, then the $mCherry^{+}$ tumor volume was calculated by ImageJ-win64 software. The results show a clear increase of tumor volume in co-culture condition, thus indicating that Mo-TAMs support the growth of MCS (*Fig. 2F*).

Overall, these results demonstrate that MCS-infiltrating monocytes underwent a functional differentiation towards a TAM-like phenotype endowed of tumor-promoting activities. Therefore, we have generated a reliable MPM 3D model to investigate *in vitro* the effects of TAMs on biphasic MPM responsiveness to EPZ-6438.

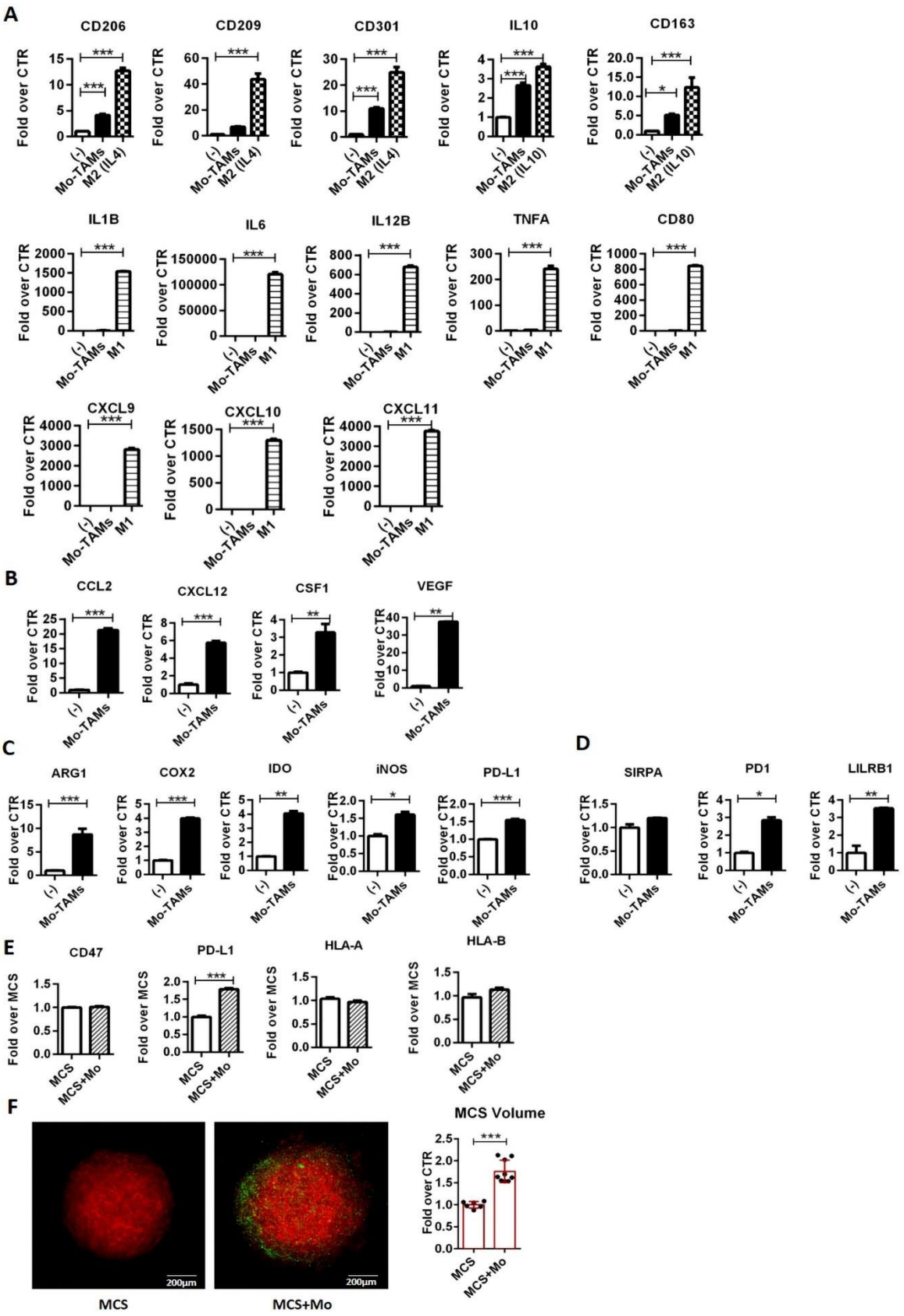

Figure 2. MCS-infiltrating monocytes acquire a functional TAM-like phenotype. (**A-D**) Monocytes-derived TAMs (Mo-TAMs) were isolated from MCS by magnetic cell sorting and analyzed by RT-PCR for the expression of genes encoding for selected (**A**) M1 (IL1, IL6, IL12B, TNFA, COX2 and CD80) and M2 (CD206, CD209, CD301, IL10 and CD163) molecules, (**B**) TAM-recruiting

chemokines (CCL-2 and CXCL12) and growth factors (CSF1 and VEGF) (**C**) immunosuppressive molecules (IDO, NOS2, ARG1, PD-L1) and (**D**) immune checkpoint receptors (SIRPA, PD1 and LILRB1). M1-polarized monocytes by a 4-hour treatment with IFNγ (20ng/ml) and LPS (100ng/ml) and M2-skewed monocytes by an 18-hour treatment with IL-4 (20ng/ml) or IL-10 (20ng/ml) were used as positive controls for M1 and M2 gene expression, respectively. β-Actin was used as housekeeping gene. Normalized RT-PCR results are shown as fold increase over untreated monocytes (-). Data are shown as mean±SD and are representative of one out of three independent experiments with similar results. **P* < 0.05, ***P*< 0.01 and ****P*< 0.001 by two-tailed one-way ANOVA or unpaired *t* test, N= 3. (**E**) MSTO-211H cells isolated from MCS co-cultured with monocytes were analyzed by RT-PCR for the expression of ligands for inhibitory phagocytosis receptors (CD47, PD-L1, HLA-A and HLA-B). β-Actin was used as housekeeping gene. Normalized RT-PCR results are shown as fold increase over MCS alone (MCS). Data are shown as mean±SD and are representative of one out of three independent experiments with similar results **P* < 0.05, ** *P* < 0.01 and *** *P* < 0.001 by two-tailed unpaired *t* test, N=3. (**F**) Volume of mCherry-MCS culture without (MCS) or with CSFE-labelled monocytes (MCS+Mo) was evaluated by confocal microscopy and calculated by ImageJ-win64 software. The results are shown as fold over MCS. Data shown are mean±SD ****P*<0.001 by two-tailed *t*-test N(MCS)=7 and N(MCS+Mo)=9). Representative images are shown. Scale bars:200µm.

EPZ-6438 enhances monocyte recruitment in the MCS

Cancer cell epigenetic reprogramming is associated with the expression of new transcriptional programs that impact on anti-tumor immunity through different mechanisms, including the upregulation of chemo-attractants that shape the composition tumor immune infiltrate[45]. In both ovarian and melanoma cells, EZH2 inhibition has been reported associated to the upregulation of Th1-recruiting chemokines[27,28].

We evaluated whether EZH2 inhibition in MSTO spheroids could modulate the expression of chemokines (CCL2, CCL5 and CXCL12) and growth factors (CSF1 and VEGF) associated with monocyte recruitment and survival. Western blot analysis showed that H3K27 trimethylation of MSTO-211H cells was fully suppressed after a 24 hour treatment with EPZ-6438 (10 μM) (*Fig. 3A*). Therefore, tumor MCS were cultured in presence of EPZ-6438 (10 μM) or vehicle (-) for 48, 72 and 96 hours, then RNA was extracted and analyzed by RT-PCR. Control MCS (-) express similar levels of chemo-attractants at each time points. In contrast, after 48 hours (CCL2 and CSF1) or 72 hours (CCL5, CXCL12 and VEGF) of EPZ-6438 treatment, MCS started to express increasingly amount of mRNA of the selected monocyte-recruiting molecules (*Fig. 3B*). These results suggest that prolonged treatment with EPZ-6438 might increase TAM accumulation.

To test this hypothesis, we analyzed the recruitment of CSFE-labeled monocytes into mCherry-MCS, by confocal microscopy. According to their time of life (96 hours), mCherry-MCS were treated with EPZ-6438 for 72 or 48 hours and co-cultured with CSFE-labeled monocytes for the following 24 and 48 hours, respectively. In both experimental conditions, confocal microscopy analysis showed a consistent increased infiltration of monocytes in EPZ-6438 treated MCS (*Fig. 3C*).

Besides the effects of EZH2 inhibition on MSTO cells, EPZ-6438 could also alter the responsiveness of monocytes to the chemo-attractants. To address this aspect, we treated monocytes with EPZ-6438 for 48 hours and we analyzed the expression of chemokine/growth factor receptors by RT-PCR. The results showed a similar mRNA level of CCR2, CCR5, CXCR4 and CSFR1 in both DMSO and EPZ-6438 treated monocytes, ruling out a direct effect of EPZ-6438 on monocytes' ability to sense chemo-attractants (*Fig. 3D*).

Overall, these results demonstrate that prolonged treatment of MCS with EPZ-6438 enhances the expression of monocyte-recruiting molecules in association with an increased accumulation of tumor infiltrating monocytes.

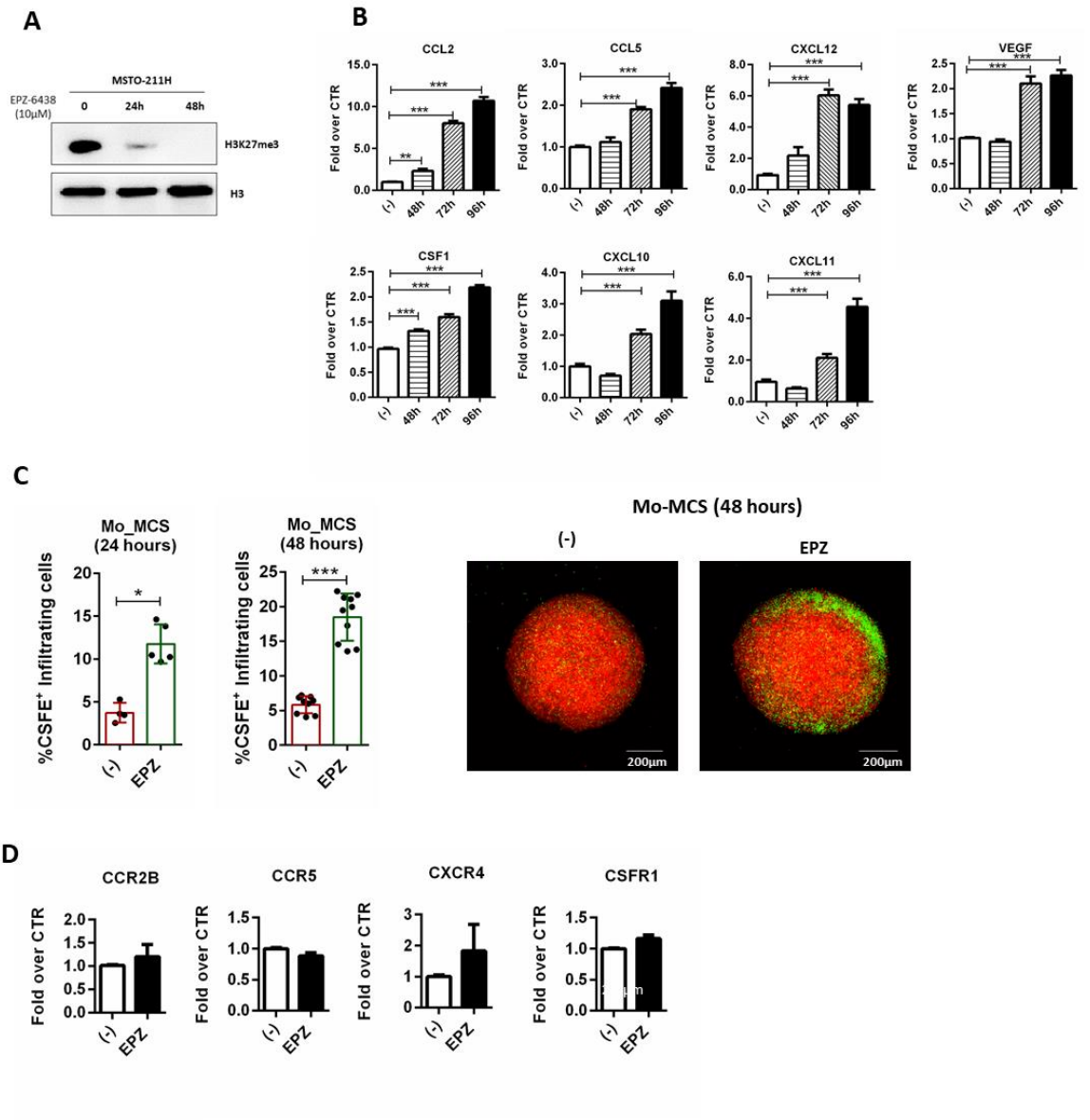

Figure 3. EZH2 inhibition enhances monocyte recruitment in MCS.

(**A**) MSTO-211H cells were left untreated (-) or treated with EPZ-6438 (10μM) for 24 and 48 hours, then core histone proteins were extracted and analyzed by Western blot for H3K27me3 levels. Histone H3 was used as loading control. (**B**) RT-PCR analysis of total RNA extracted from MCS treated or not (-) with EPZ-6438 (10μM) for 48, 72 and 96 hours. Selected monocyte chemo-attractants (CCL2, CCL5, CXCL12, CSF1, VEGF) were evaluated. β-Actin was used as housekeeping gene. Normalized qPCR results are shown as fold increase over control (-). *P < 0.05, ** P < 0.01 and *** P < 0.001 by two-tailed one-way ANOVA, N= 3 technical replicates. Data shown are mean±SD from one out of three independent experiments with similar results. (**C**) MCSs were treated with EPZ-6438 (10μM) for 72 or 48 hours and subsequently co-cultured with CSFE-labeled monocytes for 24 or 48 hours, respectively. Infiltrating monocytes was quantified using ImageJ-win64. Representative images are shown. Scale bars: 200 μm. * P< 0.05 and *** P< 0.001 by two-tailed unpaired t-test; 24 hours N(EPZ)=5; 48 hours N(-)=7 , N(EPZ)=12). (**D**) Monocytes were treated with EPZ-6438 (10μM) for 48 hours and analyzed for the expression of chemokine/growth factor-receptors (CCR2B, CCR5, CXCR4 and CSFR1) by qPCR. β-Actin was used as housekeeping gene. Normalized qPCR results are shown as fold increase over untreated monocytes Data shown are mean±SD from one out of three independent experiments with similar results.* P < 0.05, ** P< 0.01 and *** P< 0.001 by two-tailed unpaired t test N=3 technical replicates.

EZH2 inhibition enhances Mo-TAM pro-tumor phenotype

Epigenetic modulators can also directly modulate tumor infiltrating immune cells[46]. EZH2 modulate gene expression programs associated with differentiation and functional activation of T and NK cells, therefore its inhibition has been found associated with an enhanced anti-tumor immunity[47], but also with an increased expansion of myeloid derived suppressor cells and consequent suppression of anti-tumor immunity (MDSCs)[48].

Macrophages are extremely plastic cells therefore we evaluated whether the epigenetic reprogramming associated with EZH2 inhibition might alter the pro-tumor phenotype of TAMs. So far, the effect of EPZ-6438 on human monocyte/macrophage polarized activation has still poorly explored, hence we started by evaluating whether EZH2 inhibition might alter their responsiveness to either M1 (LPS) or M2 (IL-4 or IL-10) polarizing stimuli.

Both primary human monocytes and M-DM, obtained by culturing peripheral blood monocytes with MCSF (40ng/ml) for 6 days, were treated with EPZ-6438 (10 μM) for 24 hours and analyzed by western blot. In response to the EZH2 inhibitor, H3K27me3 dropped in both cell types (*Fig. 4A and Supplementary Fig. 1A*).

Then, to analyze the effects of EZH2-dependent H3K27me3 on cell response to IL-4, monocytes and M-DM were treated or not with EPZ-6438 for 24 hours and subsequently challenged with IL-4 (20ng/ml) plus or not EPZ-6438 for additional 18 hours. Control cells were maintained in standard medium plus DMSO throughout the entire experimental period. An additional group of cells was cultured in the presence of EPZ-6438 for the entire experimental period, to evaluate the effects that are solely due to EZH2 inhibition.

We analyzed the expression of typical IL-4-induced genes by RT-PCR. Consistent, the results obtained from monocytes isolated from different donors showed that, both control and EPZ-6438-treated cells expressed comparable levels of the tested genes. In contrast we observed a little upregulation of CD206, CCL17, CD209 and CD301 along with a light downregulation of CCL22 in monocytes treated with EPZ-6438 plus IL-4, as compared to those activated with IL-4 only (*Fig. 4B*) Similarly, in M-DM we confirmed that EPZ-6438 alone did not alter the expression of the selected IL-4 inducible genes, whereas EZH2 inhibition faintly modulated IL-4-induced gene expression (*Supplementary Fig.1B*).

Next, we analyzed the effects of EZH2 inhibition on monocyte response to IL-10, an immunosuppressive cytokine that is abundantly present in MPM microenvironment[49].

In both monocytes and MDM, we observed that EZH2 inhibition lightly increased IL-10-induced IL10 gene expression, whereas CD163 seems to be EZH2 independent (*Fig. 4C and*

Supplementary Fig. 1C). Furthermore, in both cells type we confirmed that EPZ-6438 was able to induce VEGF expression either alone or in combination with IL-10 (*Fig. 4C and Supplementary Fig. 1C*). These results indicate that EZH2 contributes modulating myeloid cell response to selected IL-10-induced genes.

Next, we explored whether the EZH2-dependent H3K27me3 might selectively affect the expression of inflammatory (M1) genes. Therefore, human monocytes and M-DM were cultured in presence of EPZ-438 (10μM) for 24 hours and activated with LPS (100ng/ml) for the last 4 hours.

RT-PCR analysis confirmed that EPZ-6438 only did not affect gene expression, whereas pharmacological inhibition of EZH2 in both monocytes and M-DM sharply heightened the expression of selected inflammatory genes in response to LPS stimulation. Noteworthy, along with the anti-tumor cytokine IL12B, the other EZH2-dependent genes include monocyte recruiting chemokine (CCL2), pro-tumor cytokines (IL1B, IL6) and immunosuppressive molecules (PD-L1, IDO1, COX2) (*Fig. 4D and Supplementary Fig. 1D*).

Finally, to figure out the effect of EZH2 inhibition on Mo-TAMs, monocytes were co-cultured with MCS in presence or absence of EPZ-6438 for 48 hours. In comparison to controls (DMSO-treated cells), Mo-TAMs isolated from MCS exposed to the EZH2 inhibitor showed a significant upregulation of selective genes, in particular the pro-tumor inflammatory cytokines IL1B and IL6 along with the chemokines CCL2 and CCL17 (*Fig. 4E*) and growth factors CSF1 and VEGF. With the exception of TNFA, the other upregulated genes also encode for pro-tumor (IL10, CD301, CD206 and COX2) mediators, immunosuppressive enzymes (IDO and ARG1) and immune checkpoints (LILRB1, SIRPA, PD1), (*Fig. 4E*), overall suggesting that EPZ-6438 treatment will reasonable support the protumor activity of Mo-TAMs.

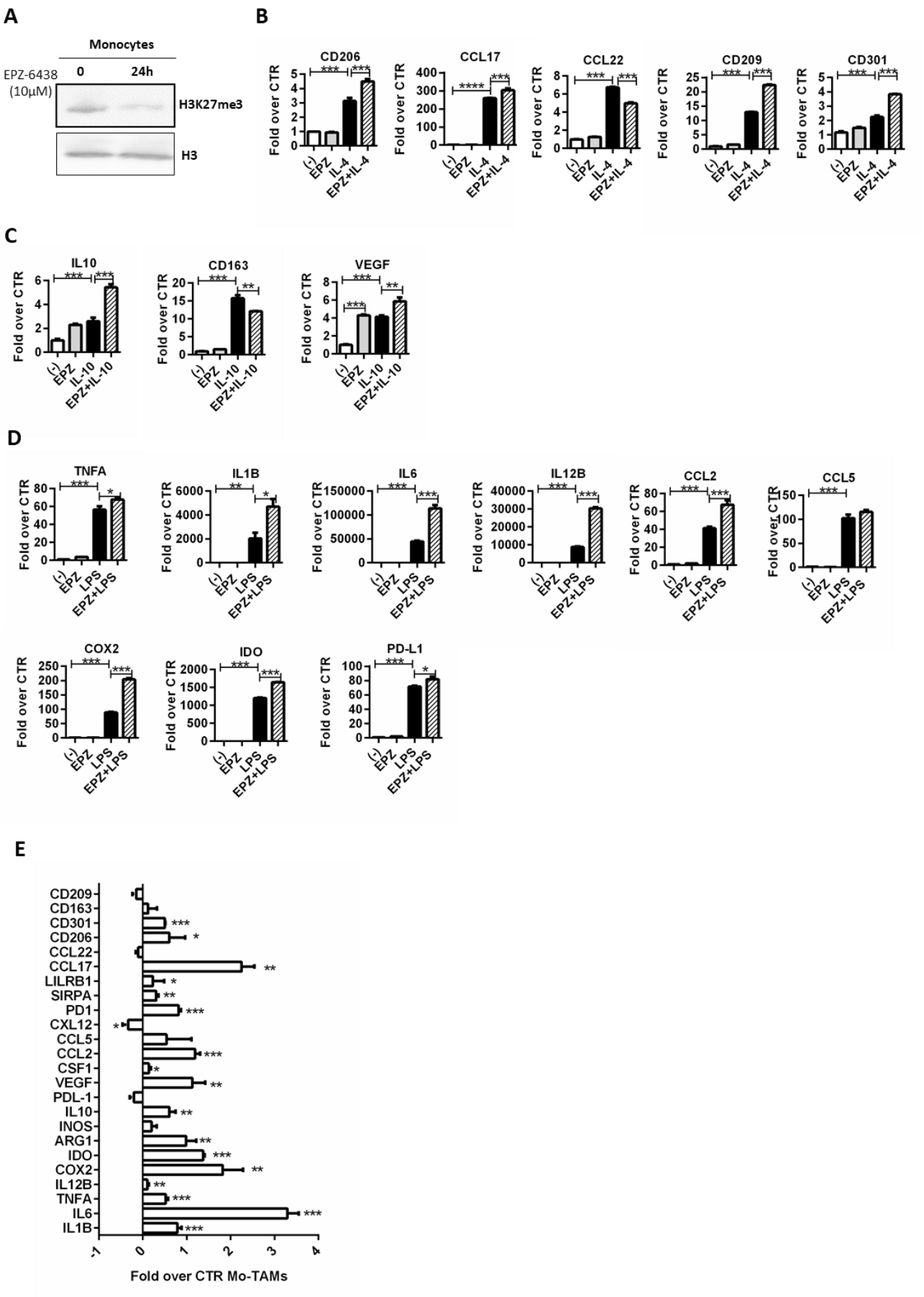
A
Monocytes
EPZ-6438 (10μM)
0
24h
H3K27me3
H3
B
CD206
CCL17
CCL22
CD209
CD301
C
IL10
CD163
VEGF
D
TNFA
IL1B
IL6
IL12B
CCL2
CCL5
COX2
IDO
PD-L1
Fold over CTR
(-)
EPZ
IL-4
EPZ+IL-4
IL-10
EPZ+IL-10
LPS
EPZ+LPS
E
CD209
CD163
CD301
CD206
CCL22
CCL17
LILRB1
SIRPA
PD1
CXL12
CCL5
CCL2
CSF1
VEGF
PDL-1
IL10
INOS
ARG1
IDO
COX2
IL12B
TNFA
IL6
IL1B
Fold over CTR Mo-TAMs

Figure 4. EZH2 inhibition affects human monocyte polarized activation. (**A**) Human monocytes were treated with 10μM EPZ-6438 or DMSO (-) for 24hours, then core histone proteins were extracted and analyzed by Western blot for H3K27me3 levels. Histone H3 was used as loading control. (**B, C**) Cells were pre-treated with EPZ-6438 (10μM) for 24 hours and rechallenged with EPZ-6438 along with (**B**) IL-4 (20ng/ml) or (**C**) IL-10 (20ng/ml) for additional 18 hours. Control cells were maintained in standard medium throughout the entire experimental period. An additional group of cells were treated with EPZ-6438 (10μM) for 42 hours and M2-polarized monocytes were maintained untreated for 24 hours and then stimulated with (**B**) IL-4 (20ng/ml) or (**C**) IL-10 (20ng/ml) for the last 18 hours. The expression of selected (**B**) IL-4 (CD206, CCL17, CCL22, CD209 and CD301) and (**C**) IL-10 (IL10, CD163 and VEGF) inducible genes was analyzed by RT-PCR. β-Actin was used as housekeeping gene. Normalized RT-PCR results are shown as fold increase over untreated monocytes (-). Data are shown as mean±SD and are representative of one out of four independent experiments with similar results. **P*< 0.05, ***P*< 0.01 and ****P*< 0.001 by two-tailed one-way ANOVA, N=3. (**D**) Monocytes were pre-treated with EPZ-6438 (10 μM) for 20 hours, and then stimulated with LPS (100ng/ml) for the following 4 hours. Control cells were kept in culture for the entire experimental period. Additionally, a group of cells was treated with EPZ-6438 (10 μM) for 24 hours and a group of cells was M1-polarized by LPS (100ng/ml) stimulation during the last 4 hours. Monocytes were analyzed to evaluate the expression typical M1-inflammatory genes (TNFA, IL1B, IL6, IL12B, CCL2 and CCL5) by RT-PCR. β-Actin was used as housekeeping gene. Normalized RT-PCR results are shown as fold increase over untreated monocytes (-). Data are shown as mean±SD and are representative of one out of four independent experiments with similar results. **P*< 0.05, ***P*< 0.01 and ****P*< 0.001 by two-tailed one-way ANOVA; N= 3. (**E**) Monocytes were co-culture with MCS in presence or absence of EPZ-6438 (10 μM). After 48 hours, Mo-TAMs were purified by magnetic separation and analyzed for the expression of selected genes including inflammatory cytokines (IL1, IL6, IL12B, TNFA, COX2), chemokines (CCL2, CCL5, CCL22, CCL17) and M2 markers (IL10, CD163, CD206, CD209 and CD301). β-Actin was used as housekeeping gene. Normalized RT-PCR results are shown as fold increase over Mo-TAMs from DMSO treated MCS (-). Data are shown as mean±SEM of three different experiments **P*< 0.05, ***P*< 0.01 and ****P*< 0.001 by two-tailed *t* test, N=3.

Mo-TAMs impair the efficacy of EPZ-6438

Given that MCS treatment with EPZ-6438 enhances the recruitment of monocytes and their functional differentiation in pro-tumoral cells, we evaluated the impact of TAMs on MPM cell responsiveness to EPZ-6438.

We analyzed the volume of mCherry-MCS treated with the EZH2 inhibitor in comparison to those pre-treated with EPZ-6438 for 48 hours and subsequently co-cultured with CSFE-labeled monocytes for additional 48 hours. Confocal microscopy analysis showed an approximately 2-fold increase of mCherry-MCS volume in co-culture condition (*Fig. 5A*). These results indicate that Mo-TAMs impair the anti-proliferative activity of EPZ-6438. To evaluate to what extent Mo-TAMs affect MSTO cell responsiveness to EPZ-6438, we labeled MSTO-211H cells with CSFE and we then tracked their proliferation in the MCS. Confocal microscopy analysis confirmed that tumor cell proliferation was reduced by EPZ-6438 treatment (*Fig. 5B*). In contrast, Mo-TAMs triggered a similar tumor cell proliferation rate in both DMSO and EPZ-6438 treated MCSs, indicating that their tumor promoting effects abolish the anti-proliferative activity of EZH2 inhibition. To corroborate these observations, we evaluated the expression of the cell cycle inhibitor p21 in tumor cells by RT-PCR and we confirmed that Mo-TAMs were able to fully revert the p21 induction triggered by EZH2 inhibition (*Fig. 5C*). These results definitely validate the ability of Mo-TAMs to impair the anti-tumor activity of EPZ-6438.

Strikingly, we noted that although MCS were extremely resistant to both mechanic and enzymatic disaggregation, the presence of Mo-TAMs lowered spheroid firmness, allowing their disassembling in a viable single cell suspension. This observation prompt us to investigate whether Mo-TAMs might affect the migratory behavior of MSTO cells under both untreated and EPZ-6438 treated conditions. MCS were pretreated or not with EPZ-6438 for 48 hours, co-cultured with monocytes for additional 24 hours and subsequently seeded in standard condition. After 24 hours, we evaluated the amount of MSTO cells grown around the MCS and we found that Mo-TAMs greatly promoted tumor cell spreading under both DMSO and EPZ-6438 treated conditions (*Fig. 5D*). Since both proliferative and migratory ability likely contribute in determining the extent of tumor cells around the MCS, to gather the effects of Mo-TAMs on tumor cell spreading behavior we isolated MSTO cells from the MCS before seeding and analyzed the expression of selected genes associated with extracellular matrix (ECM) remodeling and epithelial-mesenchymal transition (EMT). Noteworthy we found a dramatic upregulation of MMP9 in MSTO cells from MCS-monocytes co-culture (*Fig. 5E*) along with similar transcript levels of E-CADHERIN, N-CADHERIN, VIMENTIN, SNAIL and MMP2

(*Supplementary Fig. 2*). These results suggest that Mo-TAMs do not affect EMT but enhance the invasive ability of tumor cells by favoring the expression the ECM degrading enzyme MMP9. Overall, these findings indicate that Mo-TAMs play a key tumor promoting role in MCS model, hampering EPZ-6438 efficacy and favoring MSTO spreading capacity.

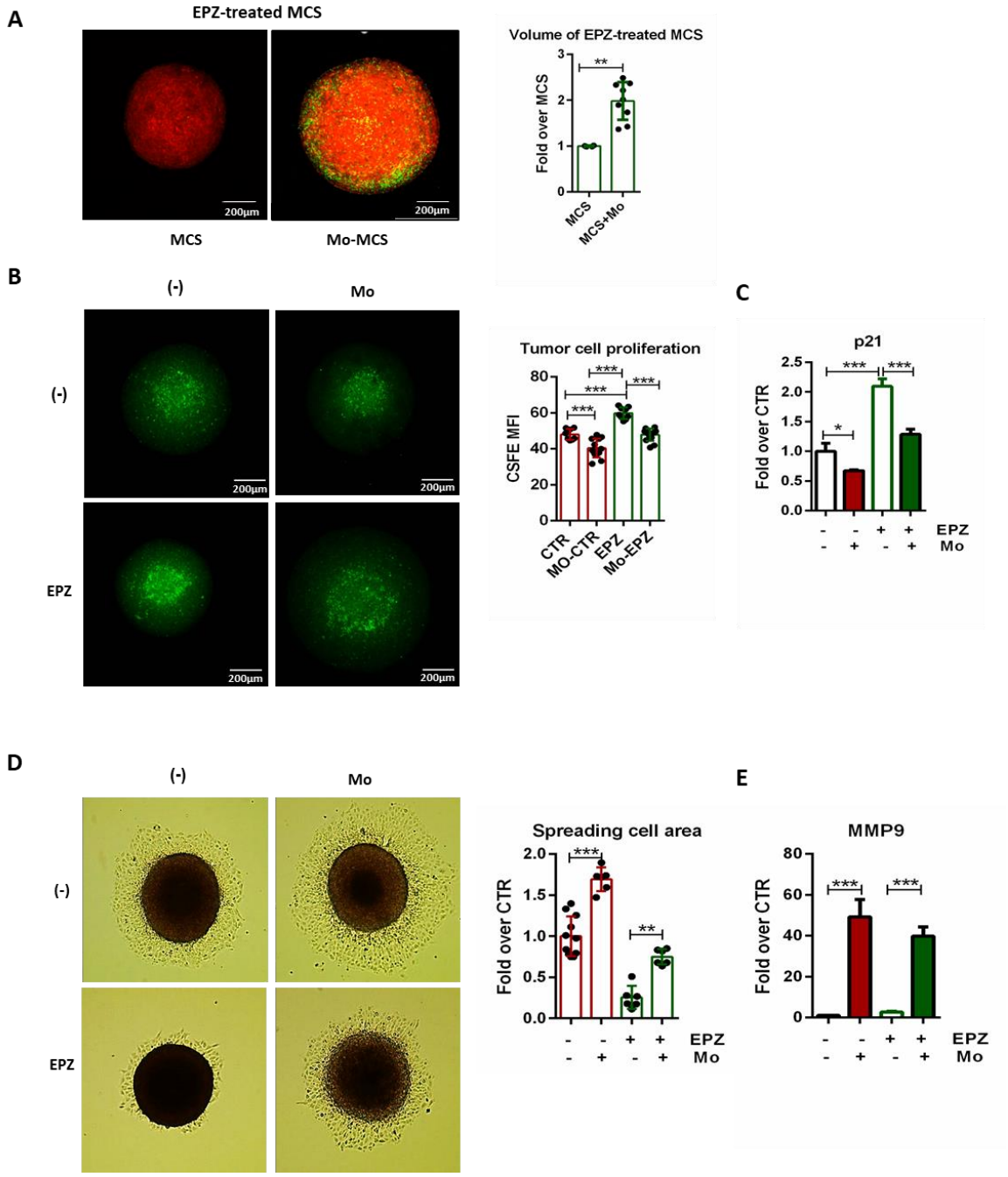

Figure 5. Mo-TAMs impair EPZ-6438 anti-tumoral effects (**A**) mCherry-MCS were treated with EPZ-6438 (10µM) for 96 hours and co-culture or not with CSFE-labeled monocytes for the last 48 hours. Volume of mCherry-MCS was evaluated by confocal microscopy and calculated by ImageJ-win64 software. Representative images are shown. Scale bars: 200 µm. Data shown are mean±SD ***P< 0.001 by two-tailed unpaired t test N (MCS)=4, N (MCS+Mo)=9 . (**B**) MCS were generated with CSFE-labeled MSTO-211H cells and cultured for 96 hours with 10µM EPZ-6438 or DMSO (-). As indicated, monocytes were added and co-cultured during the last 48 hours. MCS were analyzed by confocal microscopy then CSFE mean of fluorescence intensity (MFI) was quantified using ImageJ-win64 software. Representative images are shown. Scale bars: 200µm Data are shown as mean±SD and are representative of one out of three independent experiments with similar results. **P< 0.01 and ***P< 0.001 by two-tailed one-way ANOVA. (**C**) RT-PCR analysis of p21 expression by MSTO-211H cells derived from MCS co-cultured with monocytes. β-Actin was used as housekeeping gene. Normalized RT-PCR results are shown as fold increase over MSTO-211H cells from DMSO treated MCS (-). Data are shown as mean±SD and are representative of one out of three independent experiments with similar results. *P< 0.05 and **P< 0.01 by two-tailed one-way ANOVA, N= 3. (**D**) MCS were treated with 10µM EPZ-6438 or DMSO for 48 hours, then co-cultured or not with monocytes for additional 24 hours and seeded in standard condition. After 24 hours, spreading cells was analyzed by optical microscope and quantified by ImageJ-win64 software. Representative optical microscopic images are shown. Magnification: 10X. Representative data from one out of 6 independent experiments are shown. **P < 0.01 and *** P < 0.001 by two-tailed one-way ANOVA. (**E**) RT-PCR analysis of MMP9 expression by MSTO-211H cells derived from MCS co-cultured with monocytes. β-Actin was used as housekeeping gene. Normalized RT-PCR results are shown as fold increase over MSTO-211H cells from DMSO treated MCS (-). Data are shown as mean±SD and are representative of one out of three independent experiments with similar results. ***P< 0.01 by two-tailed one-way ANOVA, N= 3.

MSTO-211H MCS neutralize the cytotoxic activity of M1-polarized monocytes

Immunotherapeutic strategies aim to re-program TAMs in M1 effectors have been found effective in several preclinical models of cancers and are under evaluation in clinical studies for different types of human cancers[50,51]. Despite MPM cells are highly resistant to several chemotherapeutics, recent evidence indicates that LPS-activated RAW264.7 macrophages exert direct cytotoxic activity against MPM cells co-cultured in standard 2D condition[43].

Based on these premises, we started to evaluate the sensitivity of different types of human MPM cell monolayers to human M1-polarized monocytes.

Both biphasic MSTO-211H and epithelioid BR-95 MPM cells were treated with the conditioned medium (M1) collected from monocytes activated with INF-γ (20ng/ml) and LPS (100ng/ml) for 24 hours. Similarly, tumor cells were treated with medium conditioned by naïve monocytes (M0) or with "control medium" obtained by incubating monocyte cell culture medium supplemented with LPS (100 ng/mL) and INF-γ (20ng/ml) at 37°C for 24 hours. MSTO-211H and BR-95 cells treated with both control and M0-conditioned medium reached similar confluence after 48 hours and 72 hours of culture, respectively. In contrast, the treatment with M1-conditioned medium led to a drastic reduction of attached cells along with the presence of round floating cells (*Fig. 6A*). These results indicate that M1 monocytes release soluble molecules capable of impairing survival of both biphasic (MSTO-211H) and epithelioid (BR-95) cells. This hypothesis was confirmed by Western blot analysis of Poly ADP-ribose polymerase 1 (PARP-1)[52], a target of apoptotic caspases. Indeed, in both cell types we observed that exposure to M1-conditioned medium triggered a massive cleavage of PARP-1 (*Fig. 6B*). In agreement, RT-PCR analysis showed a consistent increased expression of genes encoding for the pro-apoptotic proteins BAX, BAK, NOXA, BIM and PUMA in both MSTO-211H and BR-95 cell monolayers (*Fig. 6C*).

Overall, these results demonstrate that human M1 monocytes produce soluble factors capable to kill both biphasic and epithelioid MPM cell monolayers. Next, we moved to the more reliable MCS model in the attempt to evaluate whether the cytotoxic activity of M1 monocytes could synergize with the anti-proliferative effect of EPZ-6438. Monocytes were M1 polarized by treatment with IFNγ (20ng/ml) and LPS (100ng/ml) for 4 hours or maintained in culture untreated (M0). Next, untreated or EPZ-6438-treated MCS were co-cultured with M0 or M1 monocytes for 24 hours and subsequently seeded in standard conditions for additional 24 hours. The results showed that both M1 and M0 monocytes similarly enhance tumor cell spreading and hamper the anti-tumor effect of EPZ-6438 (*Fig. 6D*). These results suggest that MPM cells

in the MCS were resistant to the cytotoxic activity of M1-polarized monocytes or were able to re-educate M1-monocytes in pro-tumoral Mo-TAMs. Therefore, to enhance the therapeutic effect of EPZ-6438, other strategies aimed to inhibit TAM accumulation rather than to re-program Mo-TAMs in M1 effectors might be considered in combination with EZH2 inhibition.

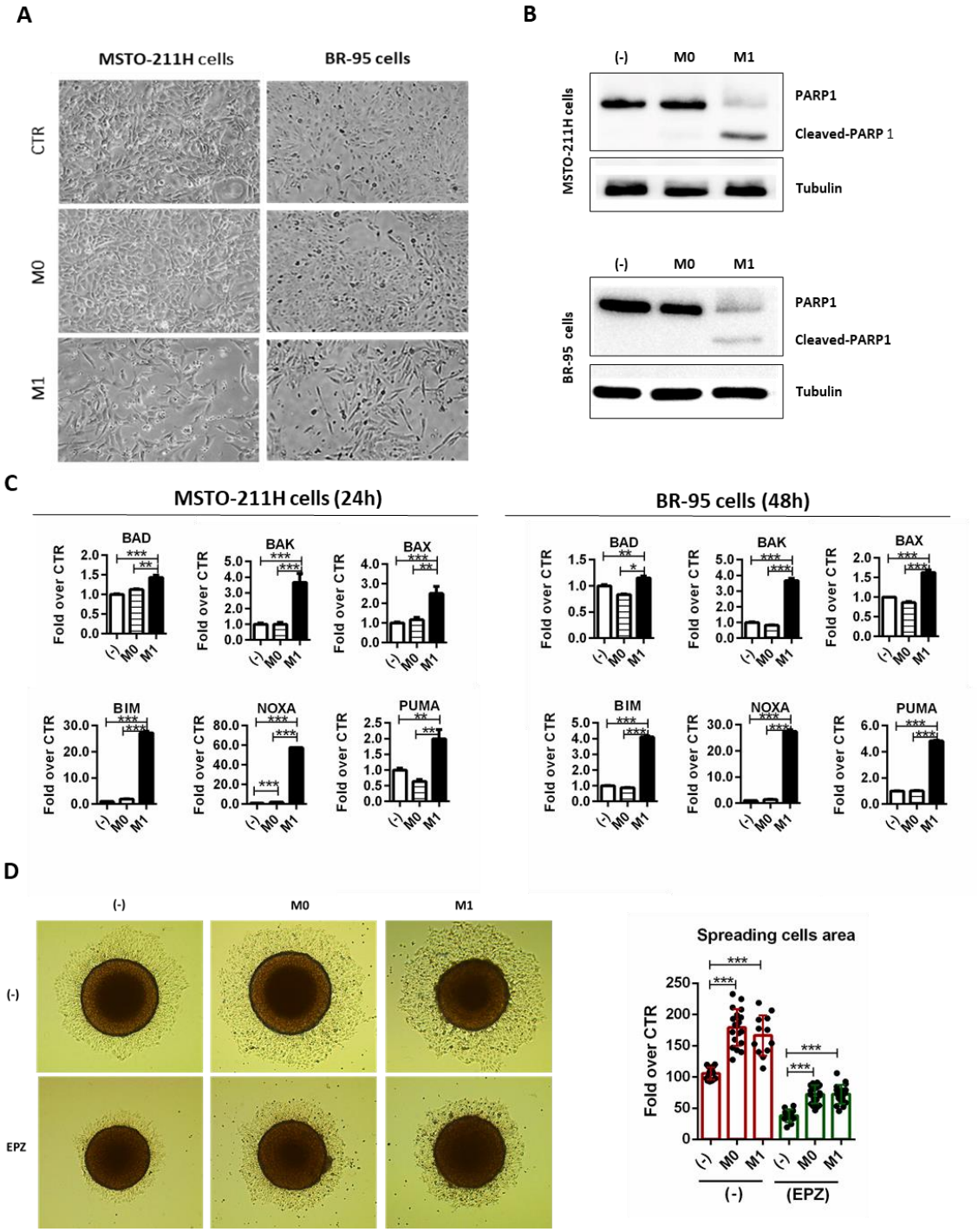

Figure 6. M1-polarized monocytes impair survival of MPM cell grown as monolayer but not as MCS.

(**A-B**) MSTO-211H and BR-95 cells were respectively cultured for 48 hours or 72 hours with 50% of control medium (ctr), M0 and M1-conditioned medium. (**A**) Representative optical microscope images are shown. Magnification: 10X. (**B**) Total

proteins were extracted and resolved by 7% SDS-PAGE. PARP1 cleavage were analyzed by Western Blot. Tubulin was used as loading control. (**C**) Total RNA was extracted from MSTO-211H cells and BR-95 cells treated with M0 or M1 monocytes-conditioned medium for 24 and 48 hours, respectively. Pro-apoptotic gene expression (BAD, BAK, BAX, BIM, NOXA, PUMA) was evaluated by RT-PCR. β-Actin was used as housekeeping gene. Normalized RT-PCR results are shown as fold increase over untreated cells (-). Data are shown as mean±SD and are representative of one out of three independent experiments with similar results. **P*< 0.05, ***P*< 0.01 and ****P*< 0.001 by two tailed unpaired *t* test. (**D**) MCS were treated with 10μM EPZ-6438 or DMSO for 48 hours, then co-cultured or not with M0 or M1 monocytes for additional 24 hours and seeded in standard condition. After 24 hours, spreading cells was analyzed by optical microscope and quantified by ImageJ-win64 software. Representative optical microscopic images are shown. Magnification: 10X. Representative data from one out of 6 independent experiments are shown. ***P* < 0.01 and *** *P* < 0.001 by two-tailed one-way ANOVA.

Discussion

EPZ-6438 is an inhibitor of the histone methyl transferase EZH2 that has recently entered in trial for MPM patients due to its anti-proliferative effects on tumor cells, however the effect of this epigenetic modulator on the TME and other way around the impact that TME has on MPM cell responsiveness to EZH2 inhibitor have never been explored.

Macrophages represent the major population of inflammatory cells present in MPM, the driving force of tumor progression by exerting immunosuppressive activities[34]. TAMs deeply affect the efficacy of anti-cancer therapies. Here we provided evidence that inhibition of EZH2 enhances the capacity of MPM cells to recruit monocytes and to drive their differentiation towards a TAM-like phenotype, that in turns impair the anti-tumor effects of EPZ-6438.

Despite studies involving research animals remain a crucial step forward the development of new drugs, the growing awareness of the Principles of Humane Experimental Technique, the 3Rs, have triggered the development of new technologies and models to improve the capacity to address biological questions *in vitro*.

In comparison to monolayer cell cultures, 3D tumor spheroids accurately mimic many features of solid tumors (e.g. gradients of nutrients, oxygen and pH establish over time, ECM deposition, cell-cell and cell-ECM interactions, cellular layered assembling) leading to a gene expression signature and drug resistance mechanisms that closely resemble those of patient-derived tumors[36,39,53].

As further improvement, we set up a 3D MPM-monocytes spheroid model, that recapitulates *in vitro*, both monocytes recruitment in tumor and their functional differentiation towards a TAM-like phenotype endowed of tumor promoting activities. Indeed, Mo-TAMs acquire a selective increased expression of genes encoding M2-like receptors (CD301, CD209, CD206, CD163), immunosuppressive molecules (IL-10, IDO1, ARG1, iNOS, PD-L1), inhibitory immune checkpoints (SIRPα, PD1, LILRB1), as well as chemokines (CCL2, CXCL12) and growth factors (M-CSF, VEGF), that are crucial drivers of monocyte recruitment in solid tumors. Accordingly, CCL2 is a significantly elevated biomarker in both pleural effusion[43] and serum[43] of MPM patients. Among the phagocytosis checkpoint, the EZH2-dependent expression of PD1 by RAW264.7 macrophages has been recently reported associated with their impaired ability to uptake mouse MPM cells[43]. Here we confirmed a higher expression PD1 in Mo-TAMs along with a consistent upregulation of LILRB1, an inhibitory receptor that recognizes MHC class I complexes and impairs the ability of TAMs to clear different types of cancer cells both *in vitro* and *in vivo*[44]. In agreement with the tumor-promoting phenotype, Mo-TAMs enhance MPM

spheroid growth by inducing tumor cells proliferation as demonstrated by the decrease of both CSFE intensity (*Fig. 5B*) and cell cycle inhibitor p21 (*Fig. 5*C). Moreover, we observed that Mo-TAMs significantly reduced spheroid firmness, in association with a selective induction of MMP9 expression and tumor cell spreading abilities. These results suggest that Mo-TAMs modulate the remodeling of extracellular matrix, creating a TME that is more permissive for tumor cells invasion. In support of this hypothesis, clinical studies have reported that high expression of MMP9 correlate with a more aggressive MPM phenotype associated with a decreased patients' survival[54,55]. Hence, the molecular characterization of the potential pro-invasive activity of Mo-TAMs warrants future studies.

Definitely, in combination with EPZ-6438 treatment, our studies demonstrate that Mo-TAMs abolish the anti-tumor activity of EZH2 inhibition in MPM cells. In comparison to EPZ-6438-treated spheroids, the presence of Mo-TAMs led to the total recover of tumor cells proliferation and spreading ability. Whereas, EZH2 inhibition in glioblastoma cells was associated to the release of soluble factors capable to shifts human M-DM and murine microglial cells towards an M1 anti-tumor phenotype[56]. Mo-TAMs isolated from EPZ-6438-treated MPM spheroids showed an enhanced expression of several M2-like genes (IL-10, CD163, CD301, CD206, CD209, CCL17) along with a consistent upregulation of pro-tumor cytokines (IL-1β, IL-6), chemokines (CCL2, CCL5) and faint induction of M1 anti-tumor genes (IL-12p40, TNFα). Therefore, in MPM spheroid model, EPZ-6438 strengthens the pro-tumoral phenotype of Mo-TAMs. This effect might be due to a modified expression of polarizing signals by MPM cells as well as an altered responsiveness of Mo-TAMs to the TME signals. Noteworthy, in both monocytes and M-DM we observed that the epigenetic reprograming driven by EPZ-6438 weakly affect the responsiveness to both IL-4 and IL-10, but strongly enhance the expression of selected LPS-induced inflammatory genes (*Fig.4I*), including IL-1β, IL-6 and CCL2. In addition, EZH2 inhibition in MSTO cells increases the expression of many monocyte chemo-attractants (CCL2, CCL5, CXCL12, M-CSF, VEGF) leading to a higher accumulation Mo-TAMs.

Overall, our findings point out a dual activity of EPZ-6438 in MPM. Since the beneficial anti-proliferative effects of EZH2 inhibition in MPM cells are counteracted by the accumulation of pro-tumoral Mo-TAMs, strategies of macrophage depletion might enhance MPM responsiveness to EPZ-6438. Even better, approaches of TAMs reprograming in M1 anti-tumor effector might work in synergism with EZH2 inhibitors leading to increased therapeutic efficacy. In line with previous studies with murine RAW264.7 macrophages[43], we observed

that M1-polarized monocytes release soluble factors capable to kill different MPM cell monolayers. However, in the 3D spheroid model, tumor cells are highly resistant to the cytotoxic activity of M1 monocytes. The observation that naïve (M0) and M1 polarized monocytes exert comparable pro-tumor effects, suggests that MPM spheroids fully re-program M1 monocytes in pro-tumoral Mo-TAMs (*Fig. 6D*). Although strategies capable to efficiently enhance TAM effector capacity would be advisable, inhibition of monocytes recruitment in MPM or TAMs depletion represent alternative valuable approaches that could be exploited to improve MPM response to EPZ-6438.

Bibliography

1. Wan, R. *et al.* Comprehensive Analysis of the Discordance of EGFR Mutation Status between Tumor Tissues and Matched Circulating Tumor DNA in Advanced Non–Small Cell Lung Cancer. *Journal of Thoracic Oncology* **12**, 1376–1387 (2017).

2. Røe, O. D. & Stella, G. M. Malignant pleural mesothelioma: history, controversy and future of a manmade epidemic. *European Respiratory Review* **24**, (2015).

3. Robinson, B. W. S. & Lake, R. A. Advances in Malignant Mesothelioma. *New England Journal of Medicine* **353**, 1591–1603 (2005).

4. Brcic, L. & Kern, I. Clinical significance of histologic subtyping of malignant pleural mesothelioma. *Translational Lung Cancer Research* vol. 9 924–933 (2020).

5. Beckett, P. *et al.* Demographics, management and survival of patients with malignant pleural mesothelioma in the National Lung Cancer Audit in England and Wales. *Lung Cancer* **88**, 344–348 (2015).

6. Aujayeb, A. & Taylor, L. Is the Deciduoid Variant of Pleural Mesothelioma Significant? *Journal of Thoracic Oncology* vol. 15 e94 (2020).

7. Rodríguez Panadero, F. Diagnosis and Treatment of Malignant Pleural Mesothelioma. *Archivos de Bronconeumología (English Edition)* **51**, (2015).

8. Bonelli, M. A., Fumarola, C., la Monica, S. & Alfieri, R. New therapeutic strategies for malignant pleural mesothelioma. *Biochemical Pharmacology* vol. 123 8–18 (2017).

9. Vogelzang, N. J. *et al.* Phase III study of pemetrexed in combination with cisplatin versus cisplatin alone in patients with malignant pleural mesothelioma. *Journal of Clinical Oncology* **21**, 2636–2644 (2003).

10. Cao, R. *et al.* Role of histone H3 lysine 27 methylation in polycomb-group silencing. *Science* **298**, 1039–1043 (2002).

11. Yin, X., Yang, S., Zhang, M. & Yue, Y. The role and prospect of JMJD3 in stem cells and cancer. *Biomedicine & Pharmacotherapy* **118**, (2019).

12. Duan, R., Du, W. & Guo, W. EZH2: A novel target for cancer treatment. *Journal of Hematology and Oncology* vol. 13 104 (2020).

13. Yoshimura, M. *et al.* Highly expressed EZH2 in combination with BAP1 and MTAP loss, as detected by immunohistochemistry, is useful for differentiating malignant pleural mesothelioma from reactive mesothelial hyperplasia. *Lung Cancer* **130**, 187–193 (2019).

14. Yoshimura, M. *et al.* Utility of highly expressed EZH2 in pleural effusion cytology for the diagnosis of mesothelioma. *Pathology International* vol. 70 831–833 (2020).

15. McLoughlin, K. C., Kaufman, A. S. & Schrump, D. S. Targeting the epigenome in malignant pleural mesothelioma. *Translational Lung Cancer Research* vol. 6 350–365 (2017).

16. Kemp, C. D. *et al.* Polycomb repressor complex-2 is a novel target for mesothelioma therapy. *Clinical Cancer Research* **18**, 77–90 (2012).

17. Lafave, L. M. *et al.* Loss of BAP1 function leads to EZH2-dependent transformation. *Nature Medicine* **21**, 1344–1349 (2015).

18. Hoy, S. M. Tazemetostat: First Approval. *Drugs* vol. 80 513–521 (2020).

19. Medicines Agency, E. *Public summary of opinion on orphan designation Polatuzumab vedotin for the treatment of diffuse large B-cell lymphoma What is diffuse large B-cell lymphoma?* www.ema.europa.eu/contact (2018).

20. Medicines Agency, E. *Public summary of opinion on orphan designation Tazemetostat for the treatment of follicular lymphoma*. www.ema.europa.eu/contact (2018).

21. Scherpereel, A., Wallyn, F., Albelda, S. M. & Munck, C. Novel therapies for malignant pleural mesothelioma. *The Lancet Oncology* vol. 19 e161–e172 (2018).

22. Zauderer, M. G. *et al.* Phase 2, multicenter study of the EZH2 inhibitor tazemetostat as monotherapy in adults with relapsed or refractory (R/R) malignant mesothelioma (MM) with BAP1 inactivation. *Journal of Clinical Oncology* **36**, 8515–8515 (2018).

23. Karantanos, T., Chistofides, A., Barhdan, K., Li, L. & Boussiotis, V. A. Regulation of T cell differentiation and function by EZH2. *Frontiers in Immunology* vol. 7 (2016).

24. Zhao, E. *et al.* Cancer mediates effector T cell dysfunction by targeting microRNAs and EZH2 via glycolysis restriction. *Nature Immunology* **17**, 95–103 (2016).

25. Goswami, S. *et al.* Modulation of EZH2 expression in T cells improves efficacy of anti-CTLA-4 therapy. *Journal of Clinical Investigation* **128**, 3813–3818 (2018).

26. Wang, D. *et al.* Pharmacological inhibition of EZH2 destabilizes FOXP3 expression and slows tumor growth d Genetic disruption of Ezh2 function in Tregs leads to robust anti-tumor immunity d Blockade of EZH2 in Tregs reprograms TI-Tregs to gain pro-inflammatory activity. *CellReports* **23**, 3262–3274 (2018).

27. Zingg, D. *et al.* The Histone Methyltransferase Ezh2 Controls Mechanisms of Adaptive Resistance to Tumor Immunotherapy. *Cell Reports* **20**, 854–867 (2017).

28. Peng, D. *et al.* Epigenetic silencing of TH1-type chemokines shapes tumour immunity and immunotherapy. *Nature* **527**, 249–253 (2015).

29. Izzi, V. *et al.* Immunity and malignant mesothelioma: From mesothelial cell damage to tumor development and immune response-based therapies. *Cancer Letters* vol. 322 18–34 (2012).

30. Jackaman, C., Yeoh, T. L., Acuil, M. L., Gardner, J. K. & Nelson, D. J. Murine mesothelioma induces locally-proliferating IL-10+TNF-α+CD206−CX3CR1+ M3 macrophages that can be selectively depleted by chemotherapy or immunotherapy. *OncoImmunology* **5**, (2016).

31. Lievense, L. A. *et al.* Pleural effusion of patients with malignant mesothelioma induces macrophage-mediated T Cell suppression. *Journal of Thoracic Oncology* **11**, 1755–1764 (2016).

32. Burt, B. M. *et al.* Circulating and tumor-infiltrating myeloid cells predict survival in human pleural mesothelioma. *Cancer* **117**, 5234–5244 (2011).

33. Miselis, N. R., Wu, Z. J., van Rooijen, N. & Kane, A. B. Targeting tumor-associated macrophages in an orthotopic murine model of diffuse malignant mesothelioma. *Molecular Cancer Therapeutics* **7**, 788–799 (2008).

34. Chéné, A. L. *et al.* Pleural effusions from patients with mesothelioma induce recruitment of monocytes and their differentiation into M2 macrophages. *Journal of Thoracic Oncology* **11**, 1765–1773 (2016).

35. Porta, C. *et al.* Tolerance and M2 (alternative) macrophage polarization are related processes orchestrated by p50 nuclear factor B. *Proceedings of the National Academy of Sciences* **106**, (2009).

36. Costa, E. C. *et al.* 3D tumor spheroids: an overview on the tools and techniques used for their analysis. *Biotechnology Advances* vol. 34 1427–1441 (2016).

37. Fontana, F. *et al.* Three-Dimensional Cell Cultures as an In Vitro Tool for Prostate Cancer Modeling and Drug Discovery. *International Journal of Molecular Sciences* **21**, (2020).

38. Zanellato, I., Colangelo, D. & Osella, D. JQ1, a BET Inhibitor, Synergizes with Cisplatin and Induces Apoptosis in Highly Chemoresistant Malignant Pleural Mesothelioma Cells. *Current Cancer Drug Targets* **18**, (2018).

39. Brüningk, S. C., Rivens, I., Box, C., Oelfke, U. & ter Haar, G. 3D tumour spheroids for the prediction of the effects of radiation and hyperthermia treatments. *Scientific Reports* **10**, (2020).

40. Manente, A. G. *et al.* KDM6B histone demethylase is an epigenetic regulator of estrogen receptor β expression in human pleural mesothelioma. *Epigenomics* **8**, (2016).

41. Sawa-Wejksza, K., Dudek, A., Lemieszek, M., Kaławaj, K. & Kandefer-Szerszeń, M. Colon cancer–derived conditioned medium induces differentiation of THP-1 monocytes into a mixed population of M1/M2 cells. *Tumor Biology* **40**, 101042831879788 (2018).

42. Schürch, C. M. *et al.* The “don’t eat me” signal CD47 is a novel diagnostic biomarker and potential therapeutic target for diffuse malignant mesothelioma. *OncoImmunology* **7**, (2018).

43. Hamaidia, M. *et al.* Inhibition of EZH2 methyltransferase decreases immunoediting of mesothelioma cells by autologous macrophages through a PD-1-dependent mechanism. *JCI Insight* **4**, (2019).

44. Barkal, A. A. *et al.* Engagement of MHC class i by the inhibitory receptor LILRB1 suppresses macrophages and is a target of cancer immunotherapy article. *Nature Immunology* **19**, 76–84 (2018).

45. Hogg, S. J., Beavis, P. A., Dawson, M. A. & Johnstone, R. W. Targeting the epigenetic regulation of antitumour immunity. *Nature Reviews Drug Discovery* vol. 19 776–800 (2020).

46. Cao, J. & Yan, Q. Cancer Epigenetics, Tumor Immunity, and Immunotherapy. *Trends in Cancer* vol. 6 580–592 (2020).

47. Kim, H. J., Cantor, H. & Cosmopoulos, K. Overcoming Immune Checkpoint Blockade Resistance via EZH2 Inhibition. *Trends in Immunology* vol. 41 948–963 (2020).

48. Huang, S. *et al.* EZH2 inhibitor GSK126 suppresses antitumor immunity by driving production of myeloid-derived suppressor cells. *Cancer Research* **79**, 2009–2020 (2019).

49. Sato, T. *et al.* Interleukin 10 in the tumor microenvironment: A target for anticancer immunotherapy. *Immunologic Research* **51**, 170–182 (2011).

50. Anfray, Ummarino, Andón & Allavena. Current Strategies to Target Tumor-Associated-Macrophages to Improve Anti-Tumor Immune Responses. *Cells* **9**, (2019).

51. Cassetta, L. & Pollard, J. W. Targeting macrophages: Therapeutic approaches in cancer. *Nature Reviews Drug Discovery* vol. 17 887–904 (2018).

52. Soldani, C. & Scovassi, A. I. Poly(ADP-ribose) polymerase-1 cleavage during apoptosis: An update. *Apoptosis* vol. 7 321–328 (2002).

53. Nunes, A. S., Barros, A. S., Costa, E. C., Moreira, A. F. & Correia, I. J. 3D tumor spheroids as in vitro models to mimic in vivo human solid tumors resistance to therapeutic drugs. *Biotechnology and Bioengineering* **116**, (2019).

54. Servais, E. L. *et al.* Mesothelin Overexpression Promotes Mesothelioma Cell Invasion and MMP-9 Secretion in an Orthotopic Mouse Model and in Epithelioid Pleural Mesothelioma Patients. *Clinical Cancer Research* **18**, (2012).

55. Štrbac, D., Goričar, K., Dolžan, V. & Kovač, V. Evaluation of Matrix Metalloproteinase 9 Serum Concentration as a Biomarker in Malignant Mesothelioma. *Disease Markers* **2019**, (2019).

56. Yin, Y. *et al.* EZH2 suppression in glioblastoma shifts microglia toward M1 phenotype in tumor microenvironment. *Journal of Neuroinflammation* **14**, 220 (2017).

Supplementary

Supplementary Table 1. Real-Time PCR primers list

Gene	Forward	Reverse
ACTB	cccaaggccaaccgcgagaagat	gtcccggccagccaggtccag
ARG1	ctgactggagacctcaagtgc	tcgtggctgtccctttgagaa
BAD	cggaggatgagtgacgagt	ccaggactggaagactcgc
BAK	aaaatggcttcggggcaag	aacgtagctgcggaaaacct
BIM	agtgggtatttctcttttga	gtgtccaattacgccgcaact
CCL2	aagatctcagtgcagaggctcg	cacagatctccttggccacaa
CCL5	gtctttgtcacccgaaag	gacaagagcaagcagaaac
CCR2B	gctggtcctgccgctg	cacacgaagcagggttttca
CCR5	ggagccctgccaaaaaatc	tgagtagagcggaggcagga
CD163	agacaaggagctgaggctagt	acagagaccgcttccatgct
CD206	cgatccgacccttccttgac	tgtctccgcttcatgccatt
CD47	tggactgagtctctgtattg	gctagagctaagatacctcaaac
CD80	tttcacttttgaccctaagc	cctgaacagaagtgagaaag
COX2	cccttgggtgtcaaaggtaa	gccctcgcttatgatctgtc
CSF1	ttaagaaggcatttctcctg	ccttgtcatgctcttcataatc
CXCL12	acactccaaactgtgcccttc	ccacgtctttgccctttcatc
CSFR1	tgagcaagacctggacaagga	ggatgcaattcttggaagcg
CXCR4	aacttcagtttgttggctg	gtgtatatactgatcccctcc
E-CADHERIN	cccttcacagcagaactaac	Cacctctaaggccatctttg
HLA-A	aaaaggagggagttacactcagag	gctgtgagggacacatcagag
HLA-B	ctaccctgcggagatca	acagccaggccagcaaca
IDO	gatgtccgtaaggtcttg	cagtttgccaagacacag
IL10	ttaagggttacctgggttgccaagc	tcttggttctcagcttggggcatca
IL12B	cggtcatctgccgcaaa	tgcccattcgctccaaga
IL1B	cctactcacttaaagcccgcc	ttagaaccaaatgtggccgtg
IL6	agaacagatttgagagtagtgaggaac	ggcatttgtggttgggtcagg
LILRB1	gcttatgcttatgacctcgaac	agaacaaatctgttgtagcc
MMP2	cacagtccgccaaatgaa	cactcctgagatctgcaaac

MMP9	ccattcacgtcgtccttatg	cgctgggcttagatcattc
N-CADHERIN	gatgaaacgccgggataaa	cttcttctcctccaccttct
NOS2	aaagaccaggctgtcgttga	acgggaccggtatttcattct
NOXA	gagatgcctgggaagaagg	ttctccggaagttcagttt
P21	cagcatgacagatttctacc	cagggtatgtatgtacatgagga
PD1	cacgagggacaataggag	atagtccacagagaacacag
PDCD1	caggagggacaataggag	atagtccacagagaacacag
PD-L1	ccgaagtcatctggacaagca	tctcttggaattggtggtggt
PUMA	gacgacctcaacgcacagta	cacctaattgggctccatct
SIRPA	gaacggaacatctatattgtgg	catgcaaccttgtagaagaag
SNAIL	gatgaggacagtgggaaa	ccaaggaagagactgaagtag
TNFA	acgaacatccaaccttccca	cccaattctctttttgagccag
VEGF	tacctccaccatgccaagtg	atgattctgccctcctccttc
VIMENTIN	ccagctaaccaacgacaaa	tcctcttctctctgaagcatctc

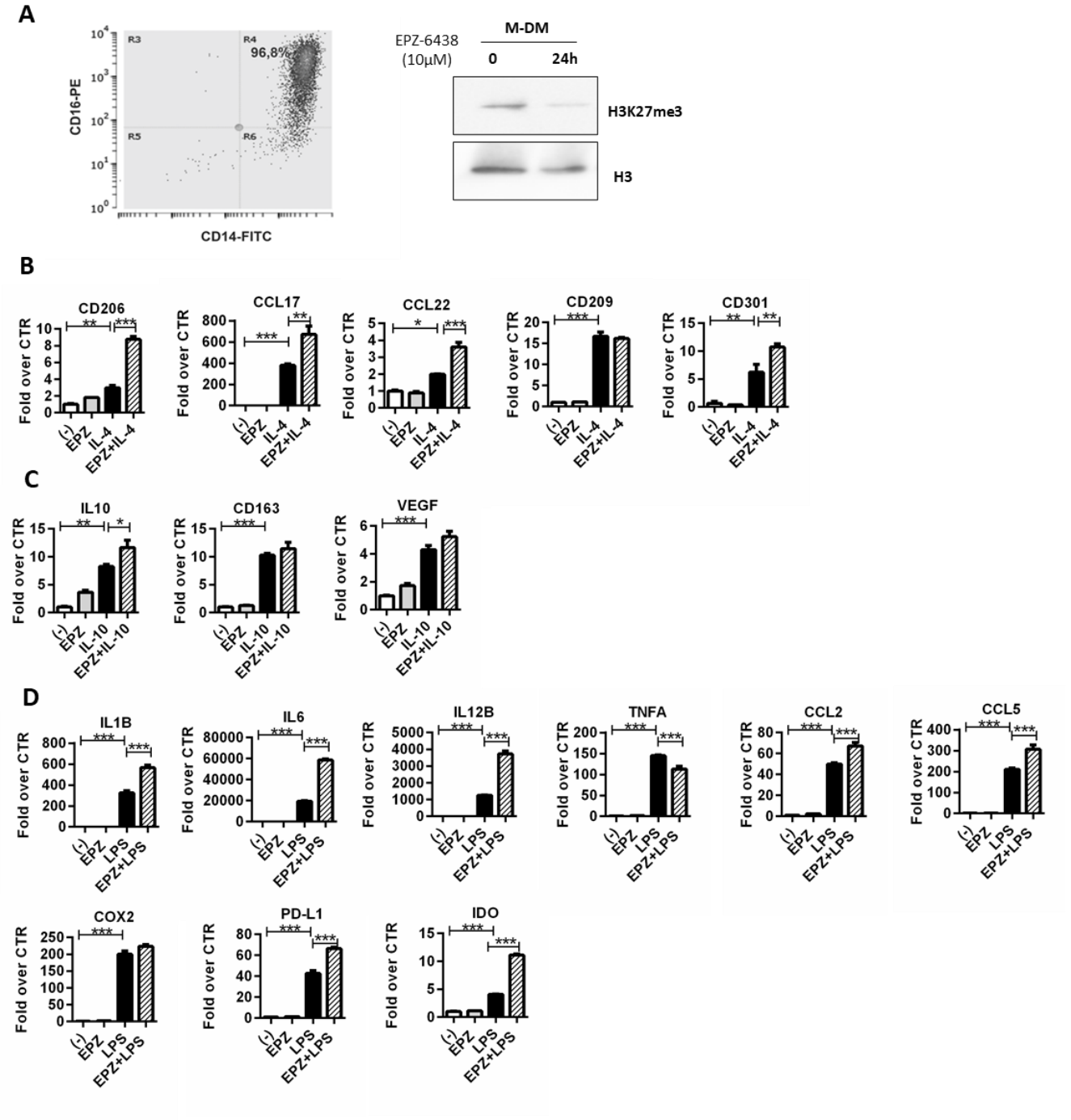

Supplementary Figure1. The effect of EZH2 inhibEZH2 inhibition affects human M-DM polarized activation. (**A**) Human monocytes cultured with 40ng/ml of MCSF for 6 days were checked for macrophage differentiation by FACS analysis of CD16 expression. Representative dot plot is shown (A, left). Human M-DM were treated with 10μM EPZ-6438 or DMSO only (-) for 24 hours, then core histone proteins were extracted and analyzed by Western blot for H3K27me3 levels. Histone H3 was used as loading control. (**B, C**) Cells were pre-treated with EPZ-6438 (10μM) for 24 hours and rechallenged with EPZ-6438 along with (**B**) IL-4 (20ng/ml) or (**C**) IL-10 (20ng/ml) for additional 18 hours. Control cells were maintained in standard medium supplemented with DMSO throughout the entire experimental period. An additional group of cells were treated with EPZ-6438 (10μM) for 42 hours and M2-polarized monocytes were cultured for 24 hours and then stimulated with (**B**) IL-4 (20ng/ml) or (**C**) IL-10 (20ng/ml) for the last 18 hours. The expression of selected (**B**) IL-4 (CD206, CCL17, CCL22, CD209 and CD301) and (**C**) IL-10 (IL10, CD163 and VEGF) inducible genes was analyzed by qRT-PCR. β-Actin was used as housekeeping

gene. Normalized RT-PCR results are shown as fold increase over control monocytes (-). Data are shown as mean±SD and are representative of one out of four independent experiments with similar results. *P< 0.05, **P < 0.01 and ***P< 0.001 by two-tailed one-way ANOVA, N=3. (**D**) Monocytes were pre-treated with EPZ-6438 (10 μM) for 20 hours, and then stimulated with LPS (100ng/ml) for the following 4 hours. Control cells were kept in culture in standard medium supplemented with DMSO for the entire experimental period. Additionally, a group of cells was treated with EPZ-6438 (10 μM) for 24 hours and a group of cells was M1-polarized by LPS (100ng/ml) stimulation during the last 4 hours. Monocytes were analyzed to evaluate the expression typical M1-inflammatory genes (TNFA, IL1B, IL6, IL12B, CCL2 and CCL5) by RT-PCR. β-Actin was used as housekeeping gene. Normalized RT-PCR results are shown as fold increase over untreated monocytes (-). Data are shown as mean±SD and are representative of one out of four independent experiments with similar results. * P< 0.05, **P< 0.01 and ***P< 0.001 by two-tailed one-way ANOVA; N= 3

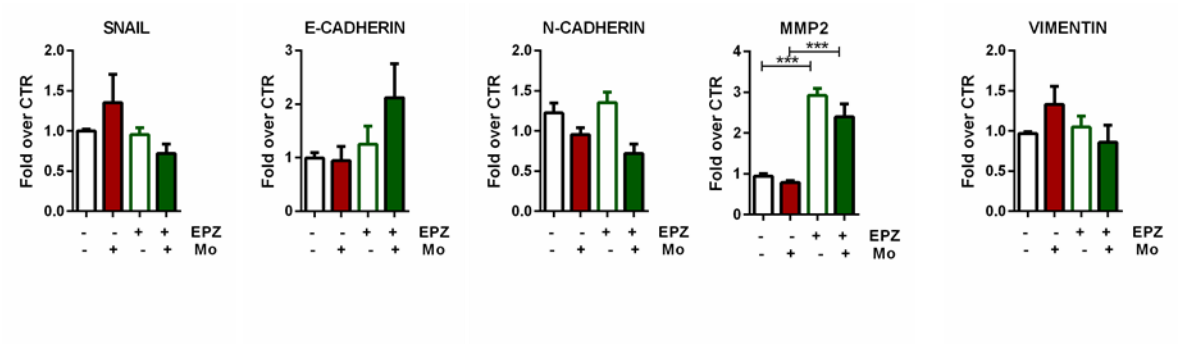

Supplementary Figure 2. Mo-TAMs do not alter EMT gene expression by MSTO-211H cells. RT-PCR analysis of EMT gene expression by MSTO-211H cells derived from MCS co-cultured with monocytes. β-Actin was used as housekeeping gene. Normalized RT-PCR results are shown as fold increase over MSTO-211H cells from DMSO treated MCS (-). Data are shown as mean±SD and are representative of one out of three independent experiments with similar results. ***P< 0.01 by two-tailed one-way ANOVA, N= 3.

Authors'Contribution

Conception and design: C. Porta, L. Moro

Acquisition of data and interpretation of results: S. Mola, G. Pinton, M. Erreni, M. Corazzari, M. De Andrea, A. Grolla, V. Martini.

Writing: S. Mola, C. Porta.

Review: G. Pinton, L. Moro.

Supervision: C. Porta

Discussion

Tumor Associated Macrophages (TAMs) are the major population of inflammatory cells infiltrating tumors, and the crucial orchestrators of tumor-promoting inflammation.

Accumulating evidence indicates that TAM-centred strategies may serve as promising candidates for cancer therapy. Understanding the molecular determinants underlying TAM polarized activation represents a crucial challenge to identify new targets for more powerful therapeutic approaches.

As it is well known, the biological activity of the majority of the proteins is regulated at the post-translational level[1]; in particular, the addition of phosphate groups to Serine, Tyrosine, Histidine and Threonine residues is a reversible modification that regulates several aspects of protein biology. To dissect the molecular pathways underlying the pro-tumoral activities of TAMs we decided to analyze the phosphoproteoma of TAMs isolated from murine MN/MCA1 fibrosarcoma, as compared to resting (ctr), M1 (IFNγ/LPS for 30 minutes) and M2 (IL-4 for 8 hours) activated macrophages.

Tripartite motif-containing 28 (TRIM28) emerged as the protein that showed the most significant different levels of Ser473 phosphorylation (S473p) in TAMs and M1 macrophages. TRIM28 is a member of the Kruppel-Associated-Box Proteins that acts as a co-repressor in gene expression[2]. TRIM28 regulates multiple cellular processes, including pluripotency, cell growth and differentiation, neoplastic transformation, apoptosis, DNA repair, and maintenance of genomic integrity. Notably, TRIM28 is involved in immune responses by controlling T cells [3]and B-cells development[4]. Although some experimental studies suggest that TRIM28 could be involved in macrophage differentiation and activation[5], its role in TAMs has never been investigated.

In our studies we focused on the inflammatory circuits involved in TRIM28 phosphorylation, in order to understand whether TRIM28 could be involved in the pro-tumoral functions exerted by TAMs. Confocal analyses of MN/MCA1 fibrosarcoma sections, reveal that both TAMs and tumor cells express TRIM28 in its Ser473 phosphorylated form, suggesting that TRIM28 could play a role in tumor development by modulating both neoplastic cells activities and cancer-related inflammatory microenvironment.

In vitro, our results provide the first observation that TRIM28 pSer473 is triggered by several M1-inducing stimuli, including inflammatory cytokines (TNFα, IL-1β, IL-6) and plasma membrane toll-like receptor ligands (LPS, PAM_3CSK_4 and Flagellin).

Given that TLRs play a key role in the initiation of host defense against a wide range of threats and can contribute to the development and progression of inflammatory and autoimmune diseases and cancers[6], we decided to investigate the molecular mechanisms driving TRIM28

S473p upon plasma membrane TLRs engagement. We focused on the adaptor protein MyD88, which is the first crucial molecule of the transduction pathway for all TLRs, except TLR3, and we demonstrated that TRIM28 S473p is totally abrogated in Myd88$^{-/-}$ PECs, thus demonstrating that the Myd88-dependent pathway control TRIM28 S473p.

Ligands of TLRs trigger several intracellular signaling pathways, such as the Phosphatidylinositol-3 kinase (PI3K) and the downstream serine/threonine kinases (Akts). Besides inflammation, PI3K/Akt dependent pathway plays an important role in the regulation of many cellular processes, including survival, proliferation, differentiation and metabolism[7,8]. Furthermore, several growth-factors induce the activation of this signaling pathway which are frequently altered in cancers[9–11]. Noteworthily, it was recently reported that the PI3K-related kinases members ATM (ataxia telangiectasia mutated)/ATR (ataxia telangiectasia and Rad3 related) induce TRIM28 S473p in response to distinct DNA damage stimuli[12]. Therefore, we have hypothesized that PI3K/Akt signalling pathway could be involved in MyD88-dependent TRIM28 S473p induction. In contrast, our results reveal that TLR4- and TLR2-dependent TRIM28 S473p is independent of PI3K/Akt pathway.

Another crucial protein in the MyD88-dependent pathway, is represented by p38, a member of the MAPKs signaling cascade, involved in the production of inflammatory mediators, including TNF-α and COX-2[13]. P38 plays an essential role in regulating cellular processes, especially inflammation and it is activated downstream of MyD88 by stimulation of TLR2 and TLR4 [14].

In colorectal cancer cells, peroxide-induced p38 MAPK triggers phosphorylation of TRIM28 at S473, this event is associated with a more efficient DNA repair and tumor cell survival under oxidative stress conditions[15]. Moreover, infection of human lung epithelial cells by highly pathogenic avian influenza virus (HPAIV) strains result in PKR-mediated sensing of viral RNA and p38-MSK1-dependent TRIM28 S473 phosphorylation an event that leads to exacerbated inflammation and tissue damage[16].

Our data demonstrated that TRIM28 phosphorylation is strictly related with the activation of p38 after TLR2 and TLR4 induction.

In summary, overall *in vitro* studies demonstrate that TRIM28 S473p is induced by different pro-inflammatory signals, including cytokines and microbial products, suggesting TRIM28 as a novel regulator of M1-polarized activation.

Furthermore, our Western blot analyses revealed that also immunosuppressive factor, such as IL-10 and PGE2, which tumor microenvironment is highly enriched, drive TRIM28 S473p.

Finally, we demonstrated that our finding could be relevant for humans, indeed, human monocytes in response to inflammatory stimuli, previous studied in murine macrophages,

induced TRIM28 phosphorylation, indicating that our studies, in macrophage biology, could have translational perspectives.

Although TRIM28 is involved in immune responses by controlling T cells[17] and B-cells[4] development, its function in macrophages differentiation is largely unknown.

To establish the role of TRIM28 in macrophages and better characterized its impact on their activation, we analyzed the transcriptome of murine macrophages, derived from TRIM28$^{LysM\text{-}Cre}$ and *TRIM28*$^{flox/flox}$ mice, after acute and prolonged treatment with LPS, by RNA sequencing (RNAseq) technique. Our preliminary data suggest, as expected, that acute and prolonged exposition to LPS enhances the expression of different classes of genes; most of gene inductions are exclusively dependent by LPS treatment and only 10% of them are influenced by genotype. Collectively our date indicate that TRIM28 modulate macrophage response to both short and prolonged LPS treatment by affecting the expression of selected gene transcriptional programs associated to activation of adaptive immunity, modulation of multiple metabolic pathways and response to oxidative stress including DNA damage response.

In future, we're going to better characterize the pathways involved in the acute and prolonged inflammatory response, in order to dissect the impact of TRIM28 in macrophages phenotype and functional activation. In addition, given that, TRIM28 is crucial of gene transcription regulation, acting as a scaffold for different transcriptional factor, we're going to perform analysis of transcriptional binding motifs enriched upstream of genes that are differentially regulated by TRIM28 during acute and prolonged exposition to LPS in order to understand how TRIM28 could modulate the inflammatory response in macrophages.

In vivo, to study the circuits involved in cancer-related inflammation, we focus on DSS-acute colitis model and DSS/AOM CAC model. Our data showed that in DSS-acute colitis model TRIM28$^{LysM\text{-}Cre}$ mice worsens intestinal inflammation in response to the treatment, but in contrast, despite the increased inflammatory response, lack of TRIM28 in myeloid cells seems not alter tumor multiplicity in AOM/DSS-induced CRC, in order to clarify this data, we're going to perform histologically analysis on CRC lesions, evaluating the colitis and dysplasia grade, immune infiltrated, apoptosis, proliferation, stemness, DNA-damage and EMT process. Given that in non-immune cells, TRIM28 has been extensively studied in different cancers, in which, depending on the type, it can exert pro- or anti-tumoral functions[18] we explored the impact of inflammation on TRIM28-dependent DNA damage response and consequent susceptibility of intestinal epithelial cells (IECs) to undergo neoplastic transformation. Taking advantage of mice lacking of TRIM28 in IECs and we discovered that DSS-acute colitis model IEC-specific ablation of TRIM28 worsens intestinal inflammation in colitis and surprising in

AOM/DSS model, mice carrying IECs specific ablation of TRIM28 developed less number of tumor lesions in colitis-associated CRC, demonstrating that the ablation of TRIM28 in IECs confers resistance only under inflammatory conditions.

Our results suggest that TRIM28 modulates CRC development in both cell-specific and disease stage-specific dependent manner.

This unexpected result obtained in TRIM28^{VillinCre} brought us to perform the single cell transcriptome analysis of immune infiltrated and epithelial cells during the acute phase of colitis, that represents the elimination phase and when tumors were formed (escape phase), when CRC lesions were formed.

These preliminary results gave us an overview of the cellular population expression in the inflammatory condition and during tumor development, defining the difference between the two phenotype. In particular, in acute colitis, in TRIM28^{VillinCre} mice had an increase in the percentage of NK, CD8+ and CD4+ T cells, to confirm they higher inflammatory status as compare to TRIM28^{floxflox} mice. Whereas, in tumors TRIM28^{VillinCre} mice have a higher expansion of B cells clusters, that could be related with a good prognostic value, as demonstrated by different clinical studies, in which patients whose tumors are highly infiltrated by B lymphocytes (CD20^{+}) have a significantly improved disease-specific survival[19,20]. The most interesting results emerged in the distribution of myeloid clusters, indeed, in TRIM28^{VillinCre} mice the presence of the tumor infiltrating neutrophils (TANs) and TAMs was considerably decreased in CRC lesions, as well as a reduction of colon cells expressed EMT genes.

Collectively these results suggest that lack of TRIM28 in IECs impact on immune cells composition during the transition from colitis to cancer along with mild effects on the expansion of neoplastic cells with an EMT^{high} gene signature and accumulation of Goblet and Paneth cells under colitis stage.

Further analyses are essential to better understand the mechanism involved in TRIM28^{VillinCre} protection, indeed, starting from these data we're performing gene ontology analysis (GO) and ingenuity pathway analysis (IPA). Moreover, by immune fluorescence analysis of γ-H2AX, a biomarker of double strand break damage[21], we wanted to investigate if the absence of TRIM28 could be led an increase of DNA damage focis, hypothesizing that the impair capacity to repair DNA double strand breaks would result in increased cell death, avoiding the surviving of transformed neoplastic cells.

Furthermore, *in vitro*, we're studying the role of TRIM28 in DNA damage-repair under inflammatory conditions, taking advantage to MC-38, murine CRC cell line, knockout for TRIM28, that we have generated by using CRISP/cas-9 technology.

In conclusion, overall our *in vitro* and *in vivo* results bring us to consider TRIM28 as a novel regulator of cancer-related.

It is well known that TAMs largely express an M2-skewed phenotype, associated with suppression of adaptive immune functions and promotion of angiogenesis and invasion. However, due to the functional plasticity of macrophages, these cells can also express an M1 phenotype associated with anti-tumor activities[22]. Hence, 're-education' to potential anti-tumor effectors may represent a therapeutic approach that will hopefully increase the efficacy of current anti-tumor therapies. The development of TAMs-centered therapeutic strategies requires the elucidation of the molecular basis of their phenotype.

Accordingly, to study the impact of TAMs on cancer-therapy, we focus our attention on malignant pleural mesothelioma (MPM), a rare and aggressive tumor, characterized by long latency period and a strong resistance to any therapeutic strategy. MPM has been causally associated with asbestos fiber inhalation, this process activates lung macrophages to clear this exogenous material, which unfortunately is impossible to phagocytize due to its big size. Macrophages increase reactive oxygen species production and inflammatory cytokines, leading to a chronic inflammatory state able to trigger a malignant transformation of cells related[23]. In first phase there is a prevalent inflammatory M1-like TAM population, while during MPM progression M2-like TAMs support immune escape and tumor development[24–26]. *In vitro* studies have demonstrated that monocyte-derived macrophages from healthy donors conditionated by pleural effusion of MPM patients, they upregulate the expression of IL4, IL13, IL10, VEGF, TGFβ, typical M2 genes and express immunosuppressive property, down regulating the proliferation of T cells (trough the production of PGE2)[26]. Clinical studies have showed that macrophages represent the major population of inflammatory cells present in MPM, and the driving force of tumor progression, to the extent that the abundance of $CD163^+$ TAMs is correlated with poor prognosis in MPM patients. In addition, TAMs are central orchestrators of immunosuppressive TME, in particular they contribute to increase Treg proliferation[27].

Furthermore, TAMs play a crucial role in dictating the efficacy of different therapies, therefore, we decided to evaluate their impact on MPM cell responsiveness to EPZ-6438, a new epigenetic modulator that has recently entered in trial for MPM patients due to its anti-proliferative effects

on tumor cells[28]. To this purpose, we set up a 3D *in vitro* system based on spheroids of biphasic MPM cells (MSTO-211H) and human monocytes.

At first, our data indicate that MPM cells are able to attract monocytes, they selectively increased the expression of chemokine genes, particularly CCL-2, that is a major driver of TAMs accumulation in solid tumor and a significantly elevated biomarker in both pleural effusion[29] and serum of MPM patients[30,31]. Moreover, monocytes can efficiently migrate inside the MPM spheroids, where they differentiate into macrophages and acquire a TAM-like phenotype in terms of expression of M2 markers, immunosuppressive molecules, monocytes recruiting chemokines and inhibitory immune checkpoints. Overall, these results demonstrate that we have generated a reliable 3D MPM-monocytes spheroid model that recapitulates *in vitro* both monocytes recruitment in tumor, and the functional differentiation towards an immunosuppressive and pro-tumoral M2-like phenotype acquired by TAMs in the TME of MPM.

The antiproliferative activity of EPZ-6438 on MSTO-211H spheroids was confirmed by confocal analysis, that showed a significant reduction of spheroid volume and suggested the correlation with senescence induction, through p21 activation, we investigated whether EZH2 inhibition could alter the capacity of MPM spheroids to recruit monocytes.

Our results show that EPZ-6438 treatment induces an increase in mRNA levels of chemokine genes, such as CCL2, CCL5, CXCL12, MCSF and VEGF, this is particularly pronounced after 96 hours of treatment, confirming that EPZ-6438 has a significant impact on the regulation of genes encoding for chemokines and growth factors related with monocytes recruitment and maintenance. Once again suggesting that a prolonged treatment might increase TAM accumulation.

To determine the chemo-attractive activity of EPZ-6438 on monocytes recruitment in MSTO spheroids, we evaluated the effect of TAMs on MPM cell responsiveness to this treatment. As many authors have described, TAMs influence tumor growth, not only creating an immunosuppressive TME, stimulating tumor cells proliferation and survival, but also impairing the effect of antitumoral therapies.

Unfortunately, our analyses have demonstrated that this promising anti-tumor effect is completely reverted in the presence of TAMs, confirming in an *in vitro* system that the abundance of TAMs could impair antitumor treatment and favor tumor progression.

TAMs enhance proliferation and consequent tumor growth, as demonstrated by the drastic increase of spheroid volume and the significant increase of cells proliferating rate; indeed, CSFE-proliferation assay have shown that TAMs are able to induce a significant decrease in

the CSFE mean of fluorescence of MSTO-211H spheroid cells, that is inversely proportional to their ability to proliferate. Furthermore, RT-PCR analysis revealed that p21 levels in TAM co-cultures are drastically decreased even in presence of EPZ-6438 treatment. P21 is an essential factor implicated in tumor suppression, but also involved in cellular senescence[32]. Its activation triggers momentary G1 cell cycle arrest or leads to a chronic state of senescence, acting as genome guardian[33], these data confirmed TAM ability to counteract EPZ-6438 efficacy.

The strong pro-tumoral effects of TAMs, in presence of EPZ-6438, could also be exacerbated by the high number of infiltrating TAMs in EPZ-treated spheroids, as compared to control-spheroids, that contribute to completely revert the efficacy of the treatment.

Further, to demonstrate the key role exerted by TAMs in cancer progression, we evaluated in our system the ability of MSTO cancer cells to acquire a migratory phenotype.

In general agreement with our previous findings that spheroid-infiltrating monocytes acquire a pro-tumoral phenotype, MSTO-211H spheroids derived from co-cultures presented an increase of spreading cells around the spheroid, as compared to control or EPZ treated spheroids; confirming once again that the presence of TAMs is able to contrast EPZ-6438 anti-tumor effect, favoring tumor cells migration and diffusion.

Trying to dissect the molecular pathways involved in the acquisition of this migratory phenotype, we performed RT-PCR of EMT genes, this analysis revealed that in MSTO-211H spheroids, TAMs promote a selective induction of matrix metalloproteinase-9 (MMP-9), a fundamental factor for invading surrounding healthy tissues, thereby increasing cancer malignancy and decreasing survival in MPM patients; to the extent that it is considered a potential novel biomarker in mesothelioma[34,35]. Taken together, our data underline the fundamental TAMs contribution in tumor progression and diffusion and their ability to negatively affect anti-tumor therapy.

Because TAMs provide a secondary source of cytokines and chemokines, which could affect immunosuppression, tumor growth, cell survival, angiogenesis, and metastasis, we wanted to investigate possible influences of the EPZ-6438 treatment on tumor promoting activities of monocytes. We performed RT-PCR analysis to evaluate the impact of EZH2 inhibition on M2 and M1-polarized activation of monocytes and M-DM. EPZ-6438 in monocytes and MDM did not induce any relevant alterations in the expression of genes under IL-4 and IL-10 regulation. Indicating that EZH2 inhibition does not influence the polarization of human monocytes and MDM towards a cancer promoting M2 phenotype.

Therefore, in order to clarify the possible effect of EPZ-6438 on monocytes and MDM polarization, we investigated whether EZH2 inhibition could influence the capacity of macrophages to undergo M1-polarized activation, surprisingly, RT analysis revealed that EZH2 inhibition in monocytes and MDM induced a significant increase in the expression levels of typical inflammatory genes. These results suggest that EZH2 inhibition in human monocytes and MDM selectively enhanced their responsiveness to M1-polarizing signals, that could influence/increase their pro-inflammatory, pro-immunity and anti-tumor activity.

Furthermore, to better understand the impact of EZH2 inhibition on TAMs, we analyzed gene expression of monocytes derived from MSTO-211H spheroid co-cultures in presence of EPZ-6438, and we observed an increase in chemokines levels confirming EPZ's ability to induce myeloid cells recruitment and a slightly, but not relevantly, increase in typical M2 genes. Suggesting that the total effect of EPZ-6438 treatment will reasonable enhance the protumor activity of Mo-TAMs.

Immunotherapeutic strategies aim to re-program TAMs in M1 effectors have been found effective in several preclinical models of cancers and are under evaluation in clinical studies for different types of human cancers[36,37]. In order to propose this strategy also for MPM therapy, we started to investigate the cytotoxic activity of M1-polarized monocytes on different MPM cell lines, the biphasic MSTO-211H and epithelioid BR-95 MPM cells, grown in a mono-layer standard 2D conditions. Overall, our data suggest that M1 monocytes produce soluble factors able to kill both bi-phasic and epithelioid MPM cells independently of the cell subtype.

Given that our previous results have described the antiproliferative effect of M1 monocytes on 2D MPM cells, and that RT-PCR analysis of monocytes stimulated with LPS, previous pre-treatment with EPZ-6438, have revealed an increase expression of M1-inflammatory genes, we wanted to investigate if M1 monocytes could exert a cytotoxic activity, improving the anti-tumor effect of EPZ-6438, also on MSTO-211H spheroids.

Although, spheroid-cocultures treated with EPZ-6438 showed a reduction in spreading cells area as compared to control, the presence of monocytes, whether M0- or M1-polarized, completely alter their antitumoral effect.

This leads us to the conclusion that, M1-polarized monocytes do not affect MSTO-211H cell viability in a 3D system, and to confirm the complexity of spheroid as compared to monolayer cell cultures, lacking the ability to mimic many features of solid tumors. This phenomenon could be related to MSTO-211H cells ability to release factors in spheroids that protect cells inside this complex 3D system and contrast the M1 cytotoxic effect.

Furthermore, as *in vivo,* macrophages can skew their phenotype from M1 to M2, this could also happen in the complex structure: M1 monocytes, corrupted by tumor cells, could revert their cytotoxic activity and acquire pro-tumoral and immunosuppressive properties.

This result may suggest that the 3D organization better mimics the organization of a solid tumor, for its complexity could contrast and revert M1-cytotoxic activity, suggesting that either the complete depletion of TAMs or the inhibition of their recruitment to tumor site could be the better strategy to improve EPZ-6438 action, as demonstrated by Miselis and colleagues in an orthotopic murine model of diffuse malignant mesothelioma[29].

For future development, it could be very interesting to investigate the molecular circuits involved in M1-monocyte reprogramming in the complex structure of the 3D spheroids, and how this system with its structure, metabolites could interact and affect the functions of the immune cells.

Overall, our findings point out a dual activity of EPZ-6438 in MPM. Since the beneficial anti-proliferative effects of EZH2 inhibition in MPM cells are counteracted by the accumulation of pro-tumoral Mo-TAMs, strategies of macrophage depletion might enhance MPM responsiveness to EPZ-6438

Bibliography

1. Qausain, S., Srinivasan, H., Jamal, S., Nasiruddin, M. & Khan, M. K. A. Phosphorylation and acetylation of proteins as posttranslational modification: Implications in human health and associated diseases. in Molecular Nutrition: Vitamins 69–86 (Elsevier, 2019). doi:10.1016/B978-0-12-811913-6.00003-5.

2. Cheng, C.-T. KAPtain in charge of multiple missions: Emerging roles of KAP1. World Journal of Biological Chemistry 5, (2014).

3. Santoni De Sio, F. R. S. et al. KAP1 regulates gene networks controlling T-cell development and responsiveness. FASEB Journal 26, 4561–4575 (2012).

4. Santoni De Sio, F. R. et al. KAP1 regulates gene networks controlling mouse B-lymphoid cell differentiation and function. Blood 119, 4675–4685 (2012).

5.Rooney, J. W. TIF1beta functions as a coactivator for C/EBPbeta and is required for induced differentiation in the myelomonocytic cell line U937. Genes & Development 15, (2001).

6. Rakoff-Nahoum, S. & Medzhitov, R. Toll-like receptors and cancer. Nature Reviews Cancer vol. 9 57–63 (2009).

7. Green, B. D. et al. Akt1 is the principal Akt isoform regulating apoptosis in limiting cytokine concentrations. Cell Death and Differentiation 20, 1341–1349 (2013).

8. Zhou, D. et al. Macrophage polarization and function with emphasis on the evolving roles of coordinated regulation of cellular signaling pathways. Cellular Signalling vol. 26 192–197 (2014).

9.Akira, S. & Takeda, K. Toll-like receptor signalling. Nature Reviews Immunology vol. 4 499–511 (2004).

10. McNamara, C. R. & Degterev, A. Small-molecule inhibitors of the PI3K signaling network. Future Medicinal Chemistry vol. 3 549–565 (2011).

11. Fresno Vara, J. Á. et al. P13K/Akt signalling pathway and cancer. Cancer Treatment Reviews vol. 30 193–204 (2004).

12. Hu, C. et al. Roles of Kruppel-associated box (KRAB)-associated co-repressor KAP1 Ser-473 phosphorylation in DNA damage response. Journal of Biological Chemistry 287, 18937–18952 (2012).

13. Yang, Y. et al. Functional roles of p38 mitogen-activated protein kinase in macrophage-mediated inflammatory responses. Mediators of Inflammation vol. 2014 (2014).

14. An, H. et al. Involvement of ERK, p38 and NF-κB signal transduction in regulation of TLR2, TLR4 and TLR9 gene expression induced by lipopolysaccharide in mouse dendritic cells. Immunology 106, 38–45 (2002).

15. Shen, L. T.-W., Chou, H.-Y. E. & Kato, M. TIF1β is phosphorylated at serine 473 in colorectal tumor cells through p38 mitogen-activated protein kinase as an oxidative defense mechanism. Biochemical and Biophysical Research Communications 492, (2017).

16. Krischuns, T. et al. Phosphorylation of TRIM28 Enhances the Expression of IFN-β and Proinflammatory Cytokines During HPAIV Infection of Human Lung Epithelial Cells. Frontiers in Immunology 9, (2018).

17. Sio, F. R. S. et al. KAP1 regulates gene networks controlling T-cell development and responsiveness. The FASEB Journal 26, (2012).

18. Hatakeyama, S. TRIM proteins and cancer. Nature Reviews Cancer vol. 11 792–804 (2011).

19. Edin, S. et al. The Prognostic Importance of CD20+ B lymphocytes in Colorectal Cancer and the Relation to Other Immune Cell subsets. Scientific Reports 9, (2019).

20. Berntsson, J., Nodin, B., Eberhard, J., Micke, P. & Jirström, K. Prognostic impact of tumour-infiltrating B cells and plasma cells in colorectal cancer. International Journal of Cancer 139, (2016).

21. Forand, A., Dutrillaux, B. & Bernardino-Sgherri, J. γ-H2AX expression pattern in non-irradiated neonatal mouse germ cells and after low-dose γ-radiation: Relationships between chromatid breaks and DNA double-strand breaks. Biology of Reproduction 71, 643–649 (2004).

22. Sica, A. & Mantovani, A. Macrophage plasticity and polarization: in vivo veritas. Journal of Clinical Investigation 122, (2012).

23. Izzi, V. et al. Immunity and malignant mesothelioma: From mesothelial cell damage to tumor development and immune response-based therapies. Cancer Letters vol. 322 18–34 (2012).

24. Jackaman, C., Yeoh, T. L., Acuil, M. L., Gardner, J. K. & Nelson, D. J. Murine mesothelioma induces locally-proliferating IL-10+TNF-α+CD206−CX3CR1+ M3 macrophages that can be selectively depleted by chemotherapy or immunotherapy. OncoImmunology 5, (2016).

25. Burt, B. M. et al. Circulating and tumor-infiltrating myeloid cells predict survival in human pleural mesothelioma. Cancer 117, 5234–5244 (2011).

26. Lievense, L. A. et al. Pleural effusion of patients with malignant mesothelioma induces macrophage-mediated T Cell suppression. Journal of Thoracic Oncology 11, 1755–1764 (2016).

27.Hamaidia, M. et al. Inhibition of EZH2 methyltransferase decreases immunoediting of mesothelioma cells by autologous macrophages through a PD-1-dependent mechanism. JCI Insight 4, (2019).

28. Zauderer, M. G. et al. Phase 2, multicenter study of the EZH2 inhibitor tazemetostat as monotherapy in adults with relapsed or refractory (R/R) malignant mesothelioma (MM) with BAP1 inactivation. Journal of Clinical Oncology 36, 8515–8515 (2018).

29.Miselis, N. R., Wu, Z. J., van Rooijen, N. & Kane, A. B. Targeting tumor-associated macrophages in an orthotopic murine model of diffuse malignant mesothelioma. Molecular Cancer Therapeutics 7, 788–799 (2008).

30. Gueugnon, F. et al. Identification of Novel Markers for the Diagnosis of Malignant Pleural Mesothelioma. The American Journal of Pathology 178, (2011).

31. Kishimoto, T. et al. Serum levels of the chemokine CCL2 are elevated in malignant pleural mesothelioma patients. BMC Cancer 19, 1204 (2019).

32. Noda, A., Ning, Y., Venable, S. F., Pereira-Smith, O. M. & Smith, J. R. Cloning of senescent cell-derived inhibitors of dna synthesis using an expression screen. Experimental Cell Research 211, 90–98 (1994).

33. Georgakilas, A. G., Martin, O. A. & Bonner, W. M. p21: A Two-Faced Genome Guardian. Trends in Molecular Medicine 23, (2017).

34. Štrbac, D., Goričar, K., Dolžan, V. & Kovač, V. Evaluation of Matrix Metalloproteinase 9 Serum Concentration as a Biomarker in Malignant Mesothelioma. Disease Markers 2019, (2019).

35. Servais, E. L. et al. Mesothelin Overexpression Promotes Mesothelioma Cell Invasion and MMP-9 Secretion in an Orthotopic Mouse Model and in Epithelioid Pleural Mesothelioma Patients. Clinical Cancer Research 18, (2012).

36. Anfray, Ummarino, Andón & Allavena. Current Strategies to Target Tumor-Associated-Macrophages to Improve Anti-Tumor Immune Responses. Cells 9, (2019).

37. Cassetta, L. & Pollard, J. W. Targeting macrophages: Therapeutic approaches in cancer. Nature Reviews Drug Discovery vol. 17 887–904 (2018).

List of Publications

1_The Macrophages-Microbiota Interplay in Colorectal Cancer (CRC)-Related Inflammation: Prognostic and Therapeutic Significance

Silvia Mola, Chiara Pandolfo, Chiara Porta, Antonio Sica
Int J Mol Sci; 2020 Sep 18;21(18):6866. doi: 10.3390/ijms21186866

2_Myeloid-Derived Suppressor Cells: Ductile Targets in Disease

Francesca Maria Consonni, Chiara Porta, Arianna Marino, Chiara Pandolfo, Silvia Mola, Augusto Bleve, Antonio Sica
Front Immunol, 2019 May 3;10:949. doi: 10.3389/fimmu.2019.00949. eCollection 2019

3_Metabolic influence on the differentiation of suppressive myeloid cells in cancer

Chiara Porta, Arianna Marino, Francesca Maria Consonni, Augusto Bleve, Silvia Mola, Mariangela Storto, Elena Riboldi, Antonio Sica
Carcinogenesis, 2018 Sep 21;39(9):1095-1104. doi: 10.1093/carcin/bgy088

4_NAMPT: A pleiotropic modulator of monocytes and macrophages

Cristina Travelli, Giorgia Colombo, Silvia Mola, Armando Genazzani, Chiara Porta
Pharmacol Res, 2018 Sep;135:25-36. doi: 10.1016/j.phrs.2018.06.022.

1_ Inhibition of the histone methyltransferase EZH2 enhances pro-tumor monocyte recruitment in human mesothelioma spheroids

Silvia Mola, Giulia Pinton, Marco Erreni, Marco Corazzari, Marco De Andrea, Ambra A. Grolla, Veronica Martini, Laura Moro, Chiara Porta

Int J Mol Sci; **Under Review**

Acknowledgements

Un giorno qualunque, in un esperimento tra tanti, qualcuno mi ha detto: "*Ricordati, è normale, stiamo facendo RI-cerca*". Una frase all'apparenza banale, ma che in una sola parola "Ri-cerca", richiude in sé un mondo di significati. "Ricerca" vuol dire creare e disfare progetti, fare e Rifare esperimenti, ridere e piangere e a volte far le due cose insieme; pensare e fermarsi a riflettere, correre per cercare un'idea, possibilmente nuova per stare sempre al passo e se possibile farne uno in più degli altri. Ricerca però è non smettere mai di crederci, andare avanti, non piegarsi alle sconfitte e delusioni. Ricerca è crescita, imparare a conoscere i propri limiti e cercare di superarli. Ricerca è il vivere in un mondo a parte, sperando di trovare nuove soluzioni per quello reale. Ricerca non è solo una parola.

E per tutto questo non posso che ringraziare la Professoressa Chiara Porta, la mia Preziosa Tutor, che mi ha condotta in questo Mondo e supportata durante tutto questo percorso, Grazie Davvero Chiara!

Grazie al Professore Antonio Sica per i suoi importanti consigli, dettati da un'immensa esperienza!

Grazie alla Dottoressa Veronica Martini, il Suo aiuto professionale e morale è stato per me preziosissimo!

Ed infine Ringrazio tutti i mie colleghi, in particolare Francesca Consonni, Valentina Garlatti, Anna Pastò, MHD Ouis Al Kathib.

Grazie a chi mi ha teso una mano durante questa corsa accompagnadomi e anche a chi ne ha inserito gli ostacoli, forse questi ultimi sono stati utili per temprarmi.

Eh sì, come dice una delle Persone per me più Speciali: "E' ora di lasciare il nido e di Spiccare il volo!"

UNIVERSITÀ DEL PIEMONTE ORIENTALE
DOTTORATO DI RICERCA
IN CHEMISTRY & BIOLOGY

Via Duomo, 6
13100 – Vercelli (ITALY)

DECLARATION AND AUTHORISATION TO ANTIPLAGIARISM DETECTION

The undersigned .....SILVIA MOLA.....student of the Chemistry & Biology Ph.D course (XXXIII Cycle)

declares:

- to be aware that the University has adopted a web-based service to detect plagiarism through a software system called "Turnit.in",
- his/her Ph.D. thesis was submitted to Turnit.in scan and reasonably it resulted an original document, which correctly cites the literature;

acknowledges:

- his/her Ph.D. thesis can be verified by his/her Ph.D. tutor and/or Ph.D Coordinator in order to confirm its originality.

Date: 15/01/2021 Signature: Silvia Mola